



ENERGINET

Geophysical Surveys For Danish Offshore Wind 2030 - Kattegat II

Title	Geophysical and Geological Survey Report For Kattegat II
Number	BE5376H-711-02-RR
Revision	3.0

3.0	01/03/2024	For Client Review	JWA/SKA	EVA	AMO/LRO
Revision	Date	Description of Revision	Author	Checked	Approved

REVISION HISTORY

The screen version of this document is always the CONTROLLED COPY. When printed it is considered a FOR INFORMATION ONLY copy, and it is the holder's responsibility that they hold the latest valid version.

The table on this page should be used to explain the reason for the revision and what has changed since the previous revision.

Rev.	Date	Reason for revision	Changes from previous version
1.0	22/09/2023	First draft	N/A
2.0	24/11/2023	Client comments	Ref. Deliverable_Register_DOW2030_draft_WPA&C_IDW_KG_rev1
3.0	01/03/2024	Client comments	Ref. Deliverable_Register_DOW2030_draft_WPA&C_IDW_KG_rev2

TABLE OF CONTENTS

<i>Revision History</i>	2
<i>Definitions and abbreviations</i>	9
1 PURPOSE OF THE DOCUMENT	10
2 EXECUTIVE SUMMARY	11
3 INTRODUCTION AND BACKGROUND	15
3.1 Project overview	15
3.1.1 Geological site survey.....	16
3.1.2 Geophysical site survey	16
3.1.3 Area of investigation - Kattegat II.....	17
3.1.4 Existing infrastructure	18
3.2 Scope of work.....	18
3.2.1 Objectives	18
3.2.2 Line Planning	19
3.2.3 Parties Involved	22
3.3 Reference documentation	22
4 GEODETIC PARAMETERS AND TRANSFORMATIONS	24
4.1 Horizontal datum	24
4.2 Vertical reference.....	24
4.3 Time Reference	24
5 SURVEY RESOURCES	26
5.1 Survey Vessels.....	26
5.2 Equipment And Software.....	26
6 TECHNICAL QUERIES AND CHANGES TO SURVEY SCOPE	28
7 DATA PROCESSING AND INTERPRETATION METHODS	29
7.1 Multibeam echosounder.....	29
7.1.1 Data acquisition.....	29
7.1.2 MBES methodology	29
7.1.3 Backscatter methodology.....	32
7.1.4 Data quality assessment.....	33
7.1.5 Backscatter	36
7.2 Side scan sonar.....	37
7.2.1 Data acquisition.....	37
7.2.2 SSS data processing	38
7.2.3 Data quality assessment.....	44
7.3 Magnetometer	47

7.3.1	Data acquisition.....	47
7.3.2	Magnetometer data processing.....	48
7.3.3	Data quality assessment.....	51
7.3.4	Magnetometer dataset profile example.....	54
7.3.5	Magnetic residual anomaly grid.....	55
7.3.6	Magnetic analytic anomaly grid.....	56
7.4	Sub-bottom profiler.....	57
7.4.1	Data acquisition.....	57
7.4.2	Data processing.....	57
7.4.3	Data quality assessment.....	57
7.5	2D UHR seismic.....	60
7.5.1	Data acquisition.....	60
7.5.2	Data processing.....	60
7.5.3	Data quality assessment.....	61
7.6	Seabed sampling.....	61
8	RESULTS AND INTERPRETATION.....	63
8.1	Classification criteria.....	63
8.1.1	Slope classification criteria.....	63
8.2	Bathymetry.....	63
8.3	Seabed Surface Classification: Geology.....	70
8.4	Seabed Surface Classification: Morphology.....	80
8.4.1	Boulder field identification criteria.....	87
8.5	Seabed Surface Classification: Man-made features.....	87
8.5.1	Archaeological findings.....	87
8.5.2	Wrecks.....	88
8.5.3	Cables, wires and ropes.....	88
8.5.4	Pipelines.....	91
8.5.5	Debris.....	91
8.5.6	Items related to fishing activity and seabed disturbance.....	95
9	SUB-SURFACE GEOLOGY.....	96
9.1	Regional geological history.....	96
9.1.1	Pre-Quaternary Geology.....	96
9.1.2	Quaternary Geology.....	96
9.1.3	Late Glacial and Holocene.....	96
9.2	Soil Unit Interpretation.....	97
9.2.1	Shallow Geological Overview.....	97
9.2.2	Stratigraphy and general arrangement of units.....	97



9.2.3	Quaternary Deglaciation History	98
9.2.4	Shallow geological installation constraints	110
9.2.5	Sub-surface acoustic velocity model	115
10	COMPARISON BETWEEN SEABED AND SUB-SEABED FINDINGS.....	117
11	CONCLUSIONS	118
12	OVERVIEW OF THE DIGITAL DELIVERABLES	122
12.1	Geological survey	122
12.2	Geophysical survey	123
<i>REFERENCES.....</i>		<i>127</i>
APPENDIX A.	KATTEGAT II – UHR SEISMIC PROCESSING REPORT	128
APPENDIX B.	SURFICIAL GEOTECHNICAL GROUND-TRUTHING REPORT	129

LISTS OF TABLES AND FIGURES

Table 1: Abbreviations used in this document	9
Table 2: Coordinates of Kattegat II survey area	17
Table 3: Summary of Kattegat II survey area	18
Table 4: Client specifications and survey overview	21
Table 5: Reference documents	22
Table 6: Project Reports	23
Table 7: Datum parameters	24
Table 8: Projection parameters	24
Table 9: Survey vessel specifications	26
Table 10: GOV survey equipment specifications	26
Table 11: GOVI survey equipment specifications	27
Table 12: Primary software list	27
Table 13: TQ clarifications and outcomes	28
Table 14: MBES system settings	29
Table 15: MBES Client specifications	29
Table 16: Loading MBES data in Qimera	30
Table 17: MBES positioning verification	30
Table 18: MBES data de-spiking and processing	30
Table 19: MBES data quality control	30
Table 20: MBES target picking	31
Table 21: SSS system settings	38
Table 22: SSS Client specifications	38
Table 23: Importing SSS data into SonarWiz	38
Table 24: Navigation correction in SonarWiz	39
Table 25: SSS signal processing	39
Table 26: SSS infill assessment	39
Table 27: SSS contact picking	39
Table 28: SSS mosaic creation	42
Table 29: SSS seabed classification	42
Table 30: MAG system settings	47
Table 31: MAG client specifications	47
Table 32: Magnetometer navigation processing	48
Table 33: Magnetometer altitude processing	48
Table 34: Magnetometer data QC	49
Table 35: Magnetometer background calculation	49
Table 36: Magnetometer residual field calculation	49
Table 37: Magnetometer dynamic range calculation	49
Table 38: Magnetometer target picking	50
Table 39: SBP acquisition and processing methodology	57
Table 40: SBP data import and data QC	57
Table 41: UHR acquisition specifications	60
Table 42: Slope classification	63

Table 43: Geological interpretation.....	71
Table 44: Morphological interpretation	80
Table 45: Boulder field classification.....	87
Table 46: Summary of man-made objects.....	87
Table 47: Wrecks within Kattegat II survey area	88
Table 48: Shallow geological units.....	98
Table 49: Overview digital deliverables Work Package A	122
Table 50: Overview digital deliverables Work Package C.....	123
Figure 1: Project location for Kattegat II, in the Danish inner sea	15
Figure 2: Overview of Kattegat II.....	17
Figure 3: Kattegat II geological survey line plan.....	19
Figure 4: Kattegat II geophysical survey line plan	20
Figure 5: Parties involved in the project.....	22
Figure 6: General MBES data processing workflow.....	32
Figure 7: TVU coverage map.....	34
Figure 8: THU coverage map	35
Figure 9: Backscatter data across the Kattegat II survey area	36
Figure 10: Example of stripe effect on the backscatter mosaic in Kattegat II.....	37
Figure 11: Automated boulder detection progress.....	41
Figure 12: Automatic correct boulder detection vs false positive boulder detection	42
Figure 13: SSS data processing workflow	43
Figure 14: SSS coverage map.....	44
Figure 15: Pycnocline and effect on the SSS dataset.....	45
Figure 16: Pycnocline effect on the outer range of the SSS data (left) and trimmed-cleaned SSS data after Far field transparency function in SonarWiz (right)	46
Figure 17: SSS data example KG_II_B02_SSS_GO5_0319 (MMO ID 413)	47
Figure 18: Magnetometer processing workflow	51
Figure 19: Data example within the Kattegat II area B04 (line 1424 _- 5376_C_KG_GO5_L661V_- _MAG) with red profile showing the raw data and the green profile representing the filtered, de-spiked data.....	52
Figure 20: Data example within the Kattegat II area B04 (line 1537 _- 5376_C_KG_GO5_1632V_- _MAG) where the blue profile and green profile are corresponding to the raw altitude values and the filtered altitude values, respectively.....	52
Figure 21: Data example showing comparison between the raw and filtered altitude values	52
Figure 22: Data example in B02 (line 1262 _- 5376_C_KG_GO5_L041V_- _MAG).....	53
Figure 23: Data example from line 1542 _- 5376_C_KG_GO5_1623V_- _MAG (green profile: residual signal; blue profile: total magnetic field).....	53
Figure 24: Data example of a signal strength profile (line 1542 _- 5376_C_KG_GO5_1623V_- _MAG)	53
Figure 25: MAG profile example, line 5376_C_KG_GO5_L702V, crossing a wreck	54
Figure 26: MAG residual anomaly grid across the survey site	55
Figure 27: MAG analytic anomaly grid across the survey site.....	56
Figure 28: SBP data example in the Kattegat II site.....	58
Figure 29: SBP data examples.....	59

Figure 30: UHR data example within the Kattegat II site	61
Figure 31: Proposed surficial geotechnical ground-truthing sampling locations within Kattegat II area	62
Figure 32: Bathymetry across Kattegat II area	64
Figure 33: Bathymetry profiles based on selected line plan segments in the north of the survey area	65
Figure 34: Detailed overview of bathymetry in the north of the survey area	66
Figure 35: Slope map of the north of the survey area	68
Figure 36: Bathymetry and slope map of a boulder field in the northeastern part of the survey area.....	69
Figure 37: Wentworth Scale – classifying sediment particles	73
Figure 38: EMODNET Folk substrate classification	74
Figure 39: Seabed surface geology classification	75
Figure 40: Seabed surface classification: Seabed geology across the northern/north-eastern section of Kattegat II	77
Figure 41: Seabed surface classification: Seabed geology across central section of Kattegat II.....	78
Figure 42: Seabed surface classification: Seabed geology across southern section of Kattegat II	79
Figure 43: Seabed morphology classification	82
Figure 44: Seabed morphology classification: Morphology across northern section of Kattegat II	84
Figure 45: Seabed morphology classification: Morphology across central section of Kattegat II	85
Figure 46: Seabed morphology classification: Morphology across southern section of Kattegat II	86
Figure 47: Overview of wreck.....	88
Figure 48: Overview of linear MMO found within the survey site.....	89
Figure 49: Possible linear objects (MMO ID 742 & 747)	90
Figure 50: Possible soft rope (MMO ID 32) which appears to be attached to a debris item (MMO ID 33) at top, and possible rope/wire/cable fragment (MMO ID 401) at bottom	91
Figure 51: Possible anchors MMO ID 413 and 613	92
Figure 52: Cluster of metallic objects (MMO IDs 21, 22 and 24).....	93
Figure 53: Overview of debris items within the survey site	94
Figure 54: Geological schematic overview and general arrangement of seismic units	98
Figure 55: SBP data example, line X10 (location presented in Figure 58), Holocene deposits, mounded ...	100
Figure 56: SBP data example, line X13 (location presented in Figure 58), Holocene deposits, thin.....	100
Figure 57: SBP data example, line X24 (location presented in Figure 55).....	101
Figure 58: Thickness and distribution of Holocene deposits.....	102
Figure 59: UHR data example, line X20 (location presented in Figure 58), downlapping Unit II	103
Figure 60: UHR data example, line X16A (location presented in Figure 58), downlapping Unit II.....	104
Figure 61: Thickness and distribution of Unit II Late Glacial Deposits	105
Figure 62: Thickness and distribution of Unit III Glacial Deposits	107
Figure 63: UHR data example, line L025 (location shown in Figure 62), Unit III, till	108
Figure 64: UHR data example, line X13 (location presented in Figure 62), Unit III, till	108
Figure 65: Depth BSB to H30 (Bedrock).....	109
Figure 66: SBP data example, line X004, Holocene deposits (Holocene unit), rare point diffraction.....	110
Figure 67: Boulder Factor, Quaternary.....	112
Figure 68: Depth BSB, Gas	114
Figure 69: SBP data example, line L077 (location presented in Figure 68), gas in Unit II	115
Figure 70: UHR data example, line X17C (location presented in Figure 68), gas in Unit II.....	115

DEFINITIONS AND ABBREVIATIONS

Throughout this document the abbreviations are listed in Table 1. Where abbreviations used in this document are not included in this list, it may be assumed that they are either equipment brand names or company names.

Table 1: Abbreviations used in this document

Abbreviation	Definition	Abbreviation	Definition
2D	Two Dimensional	KG II	Kattegat II site
3D	Three Dimensional	MBES	Multibeam Echosounder
AS	Analytical Signal	mE	Metres East
BSB	Below Seabed	mN	Metres North
BSL	Below Sea Level	MRU	Motion Reference Unit
CPT	Cone Penetration Test	MSL	Mean Sea Level
dB	Decibel	NMEA	National Maritime Electronics Association
DGNSS	Differential Global Navigation Satellite System	nT	Nanotesla
DTM	Digital Terrain Model	QC	Quality Control
ECR	Export Cable Route	RES	Residual Magnetic Field
EGN	Empirical Gain Normalisation	SBP	Sub-Bottom Profiler
EPSG	European Petroleum Survey Group	SEGY	Society of Exploration Geophysicists Y format
ETRF2000	European Terrestrial Reference Frame 2000	SIMOPS	Simultaneous Operations
ETRS89	European Terrestrial Reference System 1989	SP	Shot Point
FMGT	Fledermaus Geocoder Toolbox	SSS	Side Scan Sonar
GIS	Geographic Information System	SVP	Sound Velocity Profile
GOIV	Geo Ocean IV	THU	Total Horizontal Uncertainty
GOV	Geo Ocean V	TPU	Total Propagated Uncertainty
GRS80	Geodetic Reference System 1980	TVU	Total Vertical Uncertainty
Hz	Hertz	TWT	Two Way Time
IHO	International Hydrographic Organisation	UHR	Ultra-High Resolution
INS	Inertial Navigation System	USBL	Ultra-Short Baseline
IOGP	International Association of Oil and Gas Producers	UTM	Universal Transverse Mercator
ITRF	International Terrestrial Reference Frame	UXO	Unexploded Ordnance
ka BP	kilo annum [thousand years] Before Present	ZDA	NMEA-0813 Date Time Message String (UTC, day, month, year, and local time zone offset)



1 PURPOSE OF THE DOCUMENT

This report focuses on the geological and geophysical surveys, detailing the geophysical and geological results for the Kattegat II survey site. This report will detail the findings from the five sensors used to investigate the Kattegat II area, giving a detailed overview of the survey site, as well as listing any hazards that are likely to affect the scope or objectives of the survey, or potential later installation works.

2 EXECUTIVE SUMMARY

Kattegat II			
Survey dates	Geological survey	Start	07/04/2023
		End	14/04/2023
	Geophysical survey	Start	28/01/2023
		End	10/03/2023
Sensors	Multibeam Echo Sounder (MBES), Side Scan Sonar (SSS), Magnetometer (MAG), Sub-Bottom Profiler (SBP), 2D Ultra-High Resolution seismic (2D UHR)		
Coordinate system	Datum	European Terrestrial Reference System 1989 (ETRS89)	
	Projection	UTM Zone 32 N (EPSG: 25832)	
Bathymetry			
Depth	15.5 m MSL – 48.6 m MSL		
Site topography	<p>A meandering, NE-SW orientated, 750 – 1650 m wide channel feature crosses much of the site. Depths within the channel range from approximately 23.0 m MSL to depths of up to 48.6 m MSL, near 640875 mE, 6249495 mN. Within the northern part of the channel, the seabed is very uneven, with a series of narrower channels separated by narrow ridges of sediments, which stand up to 9.0 m shallower than the localised surrounding seabed.</p> <p>To the south-east of the major channel feature, seabed levels are generally relatively flat, mainly ranging from 19.0 m MSL to 24.0 m MSL. The only exception to this is a broad area of seabed in the central, eastern section of the site, where seabed levels are almost completely flat, lying between 17.0 m and 18.0 m MSL.</p> <p>A smaller, associated channel feature spurs off towards the west, in the northern section of the site. This feature runs approximately east to west and is between 1000 m and 1400 m wide, with depths of up to 29.0 m MSL.</p>		
Slope angles	<p>Localised slope gradients of between 5.0° and 20.0° are present along the northern and southern slopes of this channel. Maximum side slopes of up to 3.0° are present within the smaller channel feature.</p> <p>The highest slope values (very steep slopes; >15°) are associated with seabed features such as boulders, and on the sides of the broad channel, ridges and smaller elevated features.</p>		
Seabed surface: Geology			
<p>The seabed sediments across much of the northern/north-eastern and southern sections of the site comprise a series of large, irregular outcrops of till/Diamicton, partially covered by large, irregular areas of sands and muddy sands (silty, clayey sands), with finer grained, muddy sands (silty/clayey sands) becoming more prevalent towards the south and west. Muddy sand is predominant in Kattegat II. A curved area of outcropping Quaternary clay and silt is present within the eastern section of the meandering channel feature, which runs across much of the northern section of the site.</p> <p>The seabed across the central, western section of the site comprises an expanse of muddy sands (silty/clayey sands), with occasional, irregular areas of sands and/or areas of gravels and coarse sands. Smaller, less extensive areas of Till/Diamicton are also present in the southern/south-western section of the site, together with several small areas of sands and a larger, irregular area of gravels and coarse sands.</p>			

Kattegat II	
Seabed surface: Morphology	
<p>A 750 – 1650 m wide, NE-SW orientated channel feature crosses much of the site. In the northern section, the channel is deep, becoming shallower in the southern section. The channel is bounded to the north-west and south-east, by frequent boulder fields, with extensive trawl scarring also noted. Some localised areas of indistinct bedforms are present.</p> <p>Alternating zones of low to medium reflectivity are present, centred within a small part of the channel and more extensively in the southern section of the site. These are clearly visible in the MBES data, where they show positive relief, generally less than 1 m, with a tentative NW -SE direction. They may be interpreted as bedforms, possibly related to channel bottom currents. The surficial sediment is ‘Muddy sand’ in the extended southern area and ‘Gravel and coarse sand’ in the smaller northern part.</p> <p>Four seabed scour patterns are present in the northern and eastern parts of the site. They are possibly related to fishing activities. Seabed scars are also present, mainly in the north-western and central parts of the site. These scars are orientated in SW-NE, NW-SE and SW-NE directions. The most extended one is found in the north-western part of the site, crossing more than half of the area, with a length of approximately 9000 m.</p> <p>In the northern part of the site, three elongated areas of alternating low to medium reflectivity are noted, over a sandy substrate, near or within the Till/diamicton sediment. They have approximately 0.1 m difference in elevation and are predominately of SW-NE orientation. They are possible bedforms.</p>	
Seabed surface: Man-made features and site-specific hazards	
Wrecks	1
Metallic objects	569
Anchors	2
Other contacts	401
Rope	10
Cables	0
Pipelines	0
Sub-seabed soil units	
Unit I	Holocene deposits
Unit II	Late Glacial deposits
Unit III	Glacial deposits
Unit IV	Bedrock (likely Cretaceous Chalk, and/or Jurassic clastics)
2D UHRS: Geology	
<p>The geological foundation zone extends to ~70 m below seabed, with the rocks and sediments interpreted with reference to the supplied GEUS desk study. There is generally a good correlation between the shallow geology imaged in this project’s sub-seabed data and the desk study. In general, the area has a glacial to post-glacial sequence of relatively recent sediments (Units I, II and III), overlying much older bedrock. The recent sediments are generally 40-50 m thick, although locally, are interpreted to be much thicker.</p> <p>Holocene unit (Unit I) comprises Holocene deposits, namely a post-glacial silty, sandy CLAY, which is less than 1.5 m thick over much of the site. Unit 1 includes a veneer of sandier seabed sediments. The Holocene sediments are widely distributed over the study area, but are very thin or absent (unmapped) over the centre/north of the area and in the far south, where till is close to seabed. Small pockets of Holocene sediments may occur in these areas and a <0.2 m thick seabed veneer may still be present.</p> <p>The Holocene sediments are thickest over a south-west to north-east trending, ~1 km wide zone, crossing the area. Here, these deposits partially infill a channel, which is still apparent at the seabed. The thickness</p>	

Kattegat II

of these deposits increases to 9.5 m and is generally over 3 m thick. The sediments are best developed on the eastern side of the axis of the channel. In the south of the area, the Holocene sediments on the east flank of the channel are quite mounded. The channel may have originated during the late glacial/glaciomarine period, but is located over a broad low in the bedrock. Here, some of the bedded deposits included within Unit II (the Late Glacial division) may correspond with the earliest Holocene sediments.

The base Holocene is mapped as horizon H05. Where the Holocene is thin, H05 is interpreted to be a mild erosion surface, where thickness variations are due to relief at this surface and a degree of mounding at the seabed. The H05 erosion surface may be related to the final regression of the area ~10 000 years ago, when sea level dropped, potentially allowing storm erosion of the contemporary seabed.

The Holocene unit (Unit I) has seismic characteristics indicating that it is extremely soft/weak. There were instances of seabed equipment sinking into these sediments during geotechnical work. There are also very occasional bright spots, which may possibly be organic material or, more likely, dropstones melted out of floating icebergs.

The Late Glacial deposits of **Unit II** are very complex, due to the area's range of environmental conditions during the Late Weichselian and earliest Holocene. Some intervals show laminations, indicative of clays and silts, others may represent sandy beach-type deposits. The unit is mapped with horizon H20 at its base. This generally marks the top of deposits that show clear signs of ice contact - true glacial deposits.

In the extreme south, and over many parts of the central and northern regions of the area, the Unit II glaciomarine sediments pinch out over ridges and highs, comprised of the subcropping Unit III tills. As a result, the distribution pattern of Unit II is fragmentary and complex and closely linked to the morphology at the top till surface.

Unit III (glacial deposits) occur throughout the entire study area. Unit III is interpreted to be a till, deposited in association with the last major ice advance over the area, approximately 22 000 years ago. The till forms a relatively thick blanket over the site, with variations due to bedrock highs, patterns of primary deposition and possible erosion at the later onset of glaciomarine conditions. Unit III is typically 25 to 40 m thick, but can range locally from 2 m to 90 m. The GEUS desk study provides an explanation for this and shows that the area is at a confluence of ice marginal ridges, which have amalgamated to generate a great volume of tills.

The till of Unit III is at, or close to, outcrop over the southern 5 km of the area and over a significant proportion of the central and northern parts of the site, to the west of the seabed channel.

Unit III is generally a glacial till, which has been subjected to direct ice contact. The ice-contact facies may comprise a clay-prone diamicton, which is likely to contain subordinate silt, sand, gravel, cobbles and boulders, and will be overconsolidated. Consolidation levels may vary significantly over short distances. Seismically, the ice contact facies are structureless, with a very irregular upper surface, which probably forms a series of ridges. Unit III might be further sub-divided, possibly separating the ice contact facies from the ice-marginal glaciomarine packages.

The GEUS desk study shows that the Grenå-Helsingborg Fault runs west-north-west to east-south-east through the centre of the Kattegat II site. Bedrock faults are not so well imaged, though they are almost certainly present. These ancient faults were reactivated during the Jurassic/Cretaceous and, in this area, generated subsidence.

The desk study indicates that the bedrock (**Unit IV**) will likely comprise Cretaceous carbonates and/or Jurassic clastics. The top of the bedrock is generally 30-50 m below seabed (BSB), exceeding 60 m over

Kattegat II

small parts of the centre of the site. The latter may be related to displacements on the Grenå-Helsingborg Fault.

The upper surface of the bedrock is a truncation surface, with an angular unconformity between the Mesozoic rocks and their much younger overburden.

The presence of gas and cobbles and/or boulders may constrain installation. The Holocene unit (Unit I) and II sediments contain diffuse gas, while numerous cobbles and boulders may be present within Unit III.

3 INTRODUCTION AND BACKGROUND

3.1 PROJECT OVERVIEW

Following a decision in the Danish Parliament in 2022, Denmark is on the path to establish offshore energy infrastructure in the Danish inner sea (Kattegat) to connect further offshore wind energy to the Danish mainland. The regional locations of the project are shown in Figure 1.

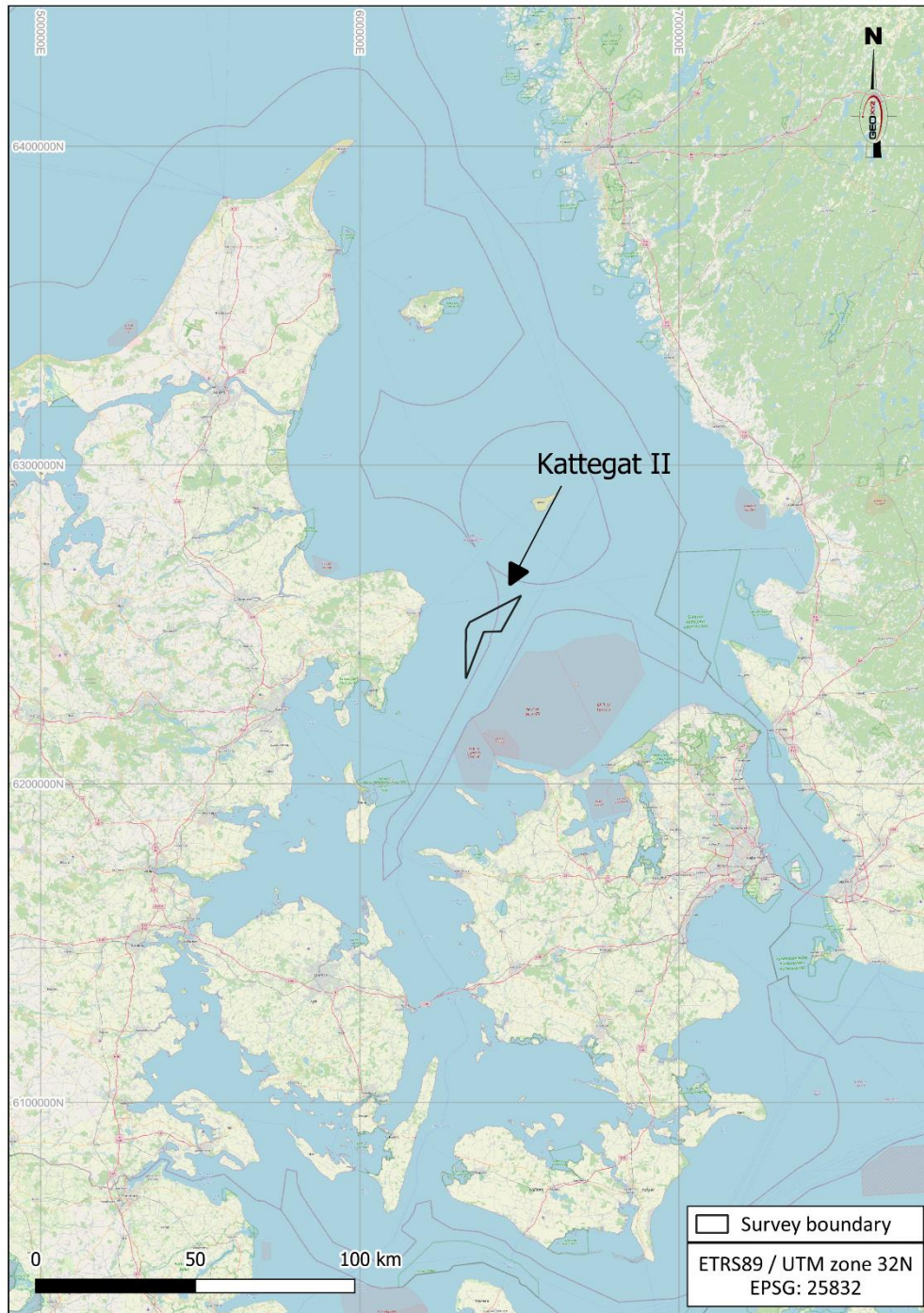


Figure 1: Project location for Kattegat II, in the Danish inner sea

The offshore elements of the project comprise the following main parts:

- An offshore windfarm in Kattegat (Kattegat II)
- Offshore platforms for substations
- Export cable between the offshore wind farm and the Danish mainland

The Danish Energy Agency has instructed the Client to initiate site investigations, environmental and metocean studies for the abovementioned main project elements.

The Client has awarded GEOxyz a contract for a geophysical survey of the Kattegat and Danish Baltic Sea project components, denoted in Figure 1.

The scope of the project includes the following work packages:

- Work Package A – Geological site survey
- Work Package C – Geophysical site survey

The scope of Work Package A and C includes the following:

3.1.1 Geological site survey

A geophysical site survey comprising Multi Beam Echo Sounder (MBES) including backscatter, Sub Bottom Profiler (SBP) and 2D UHR seismic system is to be performed to map the subsurface geological soil layers. Bathymetry should be mapped along the survey lines, as should the shallow geology.

The functional requirements of this work package are to:

- Map all major geological layers and structures to at least 100 m below seabed.
- Locate structural complexities or geohazards within the shallow geological succession such as faulting, accumulations of shallow gas, buried channels, soft sediments, hard sediments, mobile sediments etc.

3.1.2 Geophysical site survey

A full coverage geophysical site survey comprising MBES including backscatter, SSS, magnetometer, and SBP to map the bathymetry, static and dynamic elements of the seabed surface, and the subsurface geological soil layers to at least 10 m below the seabed. Grab sampling is also required to support the interpretation of the seabed surface geology.

The functional requirements of this work package are to carry out a detailed mapping of the seabed surface to provide:

- Accurate bathymetric data and charts in the surveyed areas
- The morphology and natural features of the seabed surface such as megaripples, sandwaves, boulders, outcropping geology, seaweed and reefs
- Possible man-made features such as wrecks, debris, fishing gear, trawl marks, anchor scars and objects of potential archaeological interest
- Identification of features of potential conservation interest including but not limited to; sandbanks, gravel reef, cobble reef, rocky reef and biogenic reef structures.

Mapping of the upper part of the seabed subsurface is required to a sufficient level of detail to:

- Locate structural complexities or geohazards within the shallow geological succession such as faulting, accumulations of shallow gas, buried channels, soft sediments, hard sediments, high boulder density estimation, mobile sediments etc.

3.1.3 Area of investigation - Kattegat II

The Kattegat II survey site is located in the Kattegat Region off the eastern coast of Denmark (Figure 2). A summary of coordinates and the site extents are displayed in Figure 2 and Table 3.

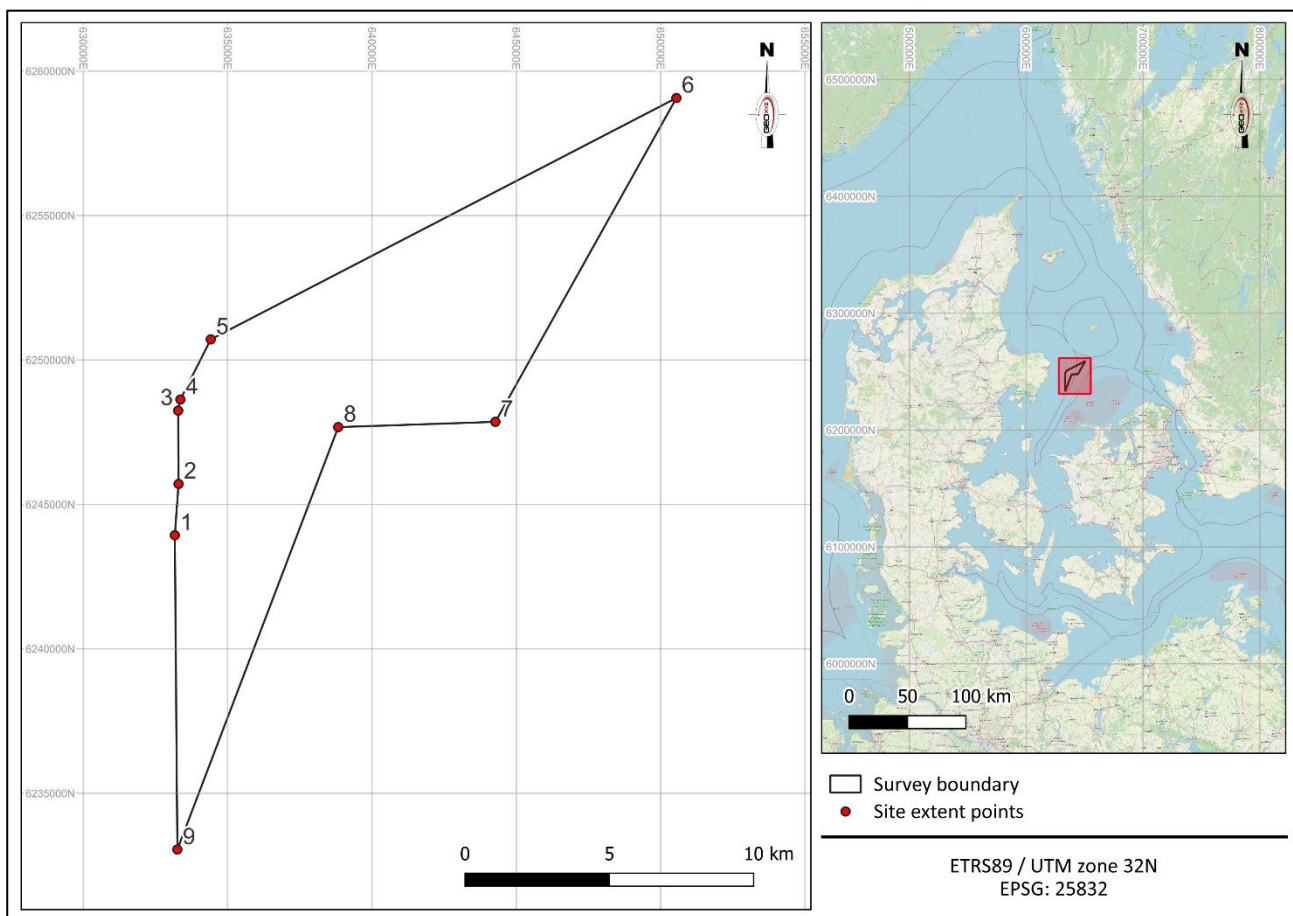


Figure 2: Overview of Kattegat II

Table 2: Coordinates of Kattegat II survey area

Point ID	Easting EUREF89 Zone 32N (m)	Northing EUREF89 Zone 32N (m)	Longitude EUREF89	Latitude EUREF89
1	633170	6243935	11° 09.200' E	56° 19.284' N
2	633299	6245712	11° 09.379' E	56° 20.239' N
3	633285	6248250	11° 09.443' E	56° 21.607' N
4	633363	6248635	11° 09.530' E	56° 21.813' N
5	634414	6250716	11° 10.614' E	56° 22.916' N
6	650544	6259071	11° 26.561' E	56° 27.125' N

Point ID	Easting EUREF89 Zone 32N (m)	Northing EUREF89 Zone 32N (m)	Longitude EUREF89	Latitude EUREF89
7	644273	6247861	11° 20.091' E	56° 21.204' N
8	638829	6247677	11° 14.804' E	56° 21.203' N
9	633257	6233058	11° 08.956' E	56° 13.424' N

Table 3: Summary of Kattegat II survey area

Site	Region	Survey Area Extent (km ²)
Kattegat II	Kattegat	123

3.1.4 Existing infrastructure

No existing infrastructure was found crossing the Kattegat II survey site.

3.2 SCOPE OF WORK

The scope for the geological and geophysical surveys was undertaken across two vessels, Geo Ocean V and Geo Ocean VI. The vessels were mobilised at the end of 2022 and the surveys were undertaken in 2023 for all sites. The surveys achieved full coverage in the areas of investigation and mapped the bathymetry, the static and dynamic elements of the seabed surface, and the sub-surface geological soil layers to at least 100 m below seabed.

3.2.1 Objectives

The results of the survey will be used as basis for:

- Initial marine archaeological site assessment.
- Planning of environmental investigations.
- Planning of initial geotechnical investigations.
- Decision of foundation concept and preliminary foundation design.
- Assessment of installation conditions for foundations and inter-array cables.
- Site information enclosed the tender for the offshore wind farm concession.

To accomplish these aims GEOxyz:

- Acquired high resolution bathymetric data to ascertain water depth and changes in topography across the sites using multibeam echosounder (MBES) data.
- Acquired high frequency (900 kHz) side scan sonar (SSS) data to identify seabed objects and features.
- Acquired low frequency (300 kHz) side scan sonar (SSS) data to distinguish seabed sediments.
- Acquired magnetometer data to identify magnetometer anomalies relating to cables, pipelines and other ferrous objects, on and below the seabed.
- Acquired high-resolution and 2D ultra high-resolution seismic data, in order to locate structural complexities or geohazards within the shallow geological succession, such as faulting, accumulations of shallow gas, buried channels, soft sediments, hard sediments, mobile sediments, high boulder density estimation, etc.

3.2.2 Line Planning

For the geological survey, the survey lines comprised of main lines were spaced at 250 m, and cross lines were spaced every 1000 m. Survey lines that were shorter than four km were extended outside the survey area to obtain this minimum length. Orientation of survey lines were determined to acquire main lines predominantly along the long axis of the site where this is apparent. Figure 3 shows a schematic diagram of the line plan for the geological survey.

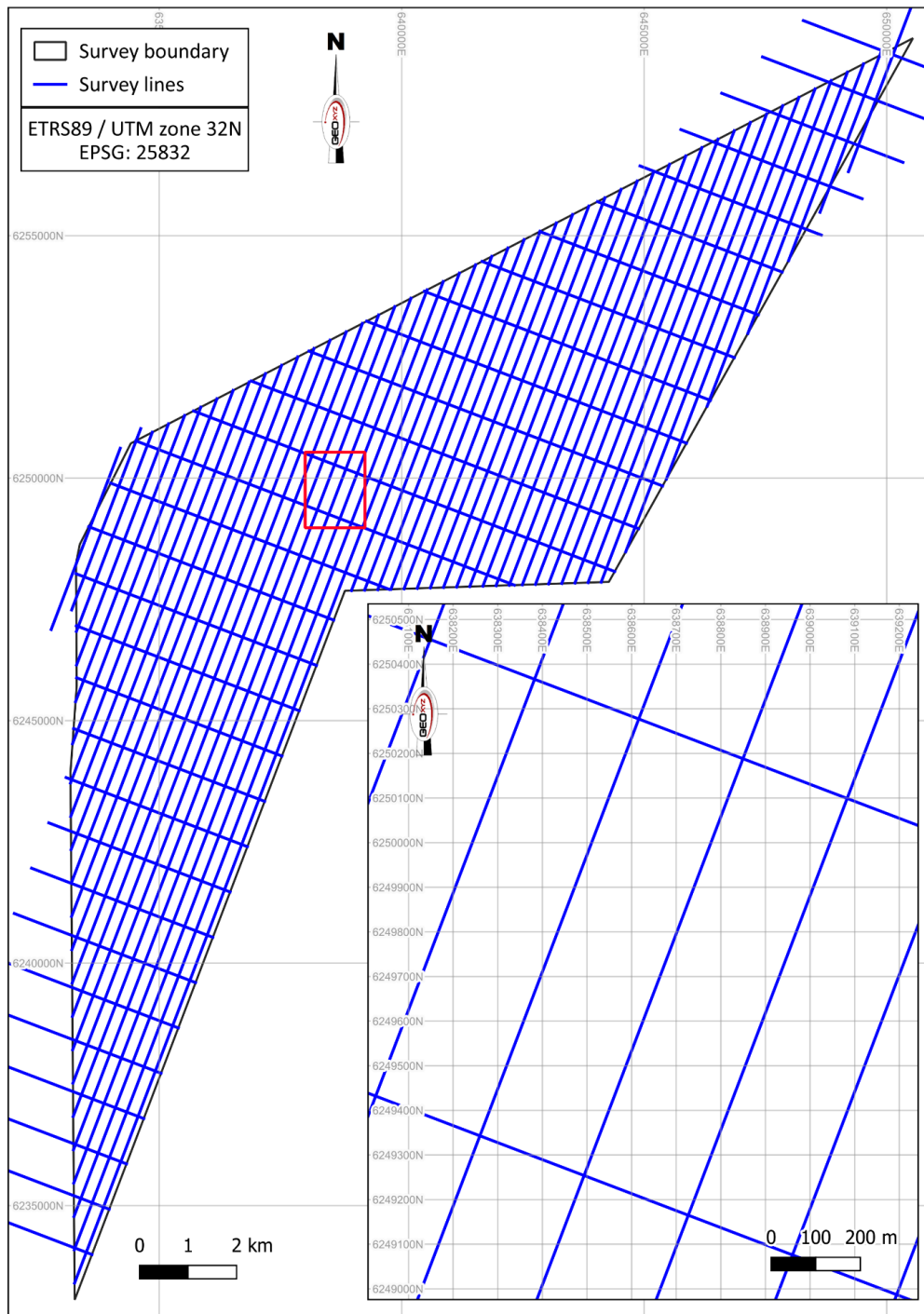


Figure 3: Kattegat II geological survey line plan

For the geophysical survey, the survey lines were spaced at 62.5 m apart, oriented predominantly along the long axis of the site where this is apparent.

Figure 4, below, shows a schematic diagram of the line plan for the geophysical survey.

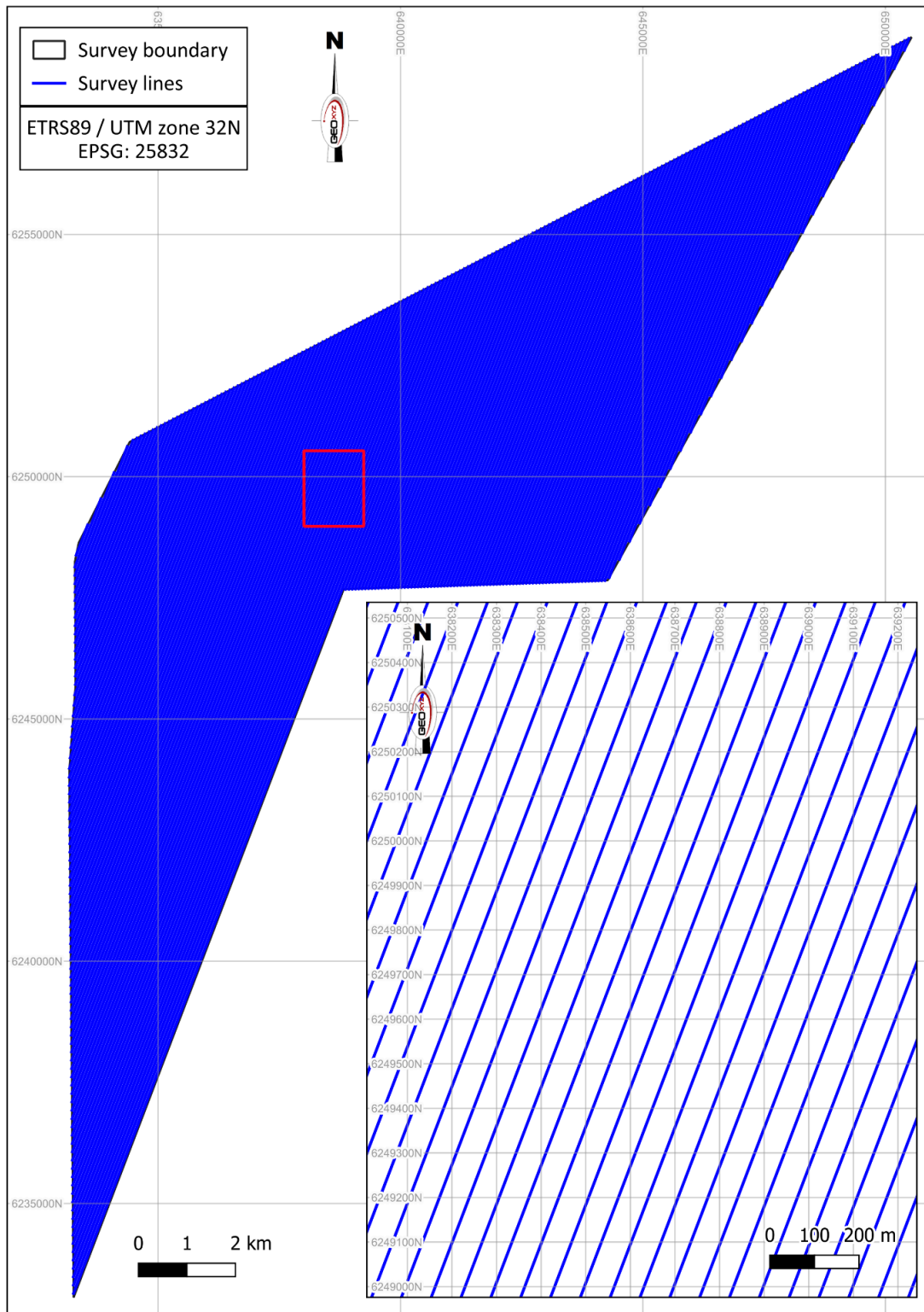


Figure 4: Kattegat II geophysical survey line plan

The client specification and survey overview are detailed in Table 4.

Table 4: Client specifications and survey overview

Equipment	Specification	Survey Requirement
Vessels	Multi-vessel operations	Geo Ocean V (GOV) and Geo Ocean VI (GOVI)
Line Planning	Main Lines mag box survey	Spaced at 250 m
	Cross Lines geological survey	Spaced at 1000 m
	Main Lines geophysical survey	Spaced at 62.5 m
	Cross Line geophysical survey	none
MBES Bathymetry/ Backscatter	Data density	16 hits/m ² on 99 % of site
	Standard Deviation	0.20 m on 95 % of the site
	MBES Mode	Equidistant
	Gridded	0.25 m cell size
	Coverage	100 %
Side Scan Sonar	Resolution sufficient for detecting seabed object/features	0.5 m (length, width and height)
	Towing altitude	8 - 12 % of range (optimised for data quality)
	Positional accuracy	± 2 m (using vessel course-over-ground and USBL)
	Operating mode	High Definition Mode
	Range	70 m
	Coverage	200 %
Magnetometer	Seabed altitude	≤ 3.0 m
	Measurement sensitivity	0.02 nT
	Sampling frequency	≥ 10 Hz
	Noise level	≤ 2 nT
	Coverage (in areas of operation)	100 %
Sub-Bottom Profiler	Penetration	10 m
	Vertical resolution	0.3 m
	System	Innomar SES 2000 or similar
2D Ultra High Resolution	Fundamental frequency	Between 1 and 3 kHz
	Vertical resolution	0.3 m to 40 m depth; 0.5 m to 100 m depth ²
	Minimum Penetration	100 m
	Fire rate	2 pulses/second
	Feather angle	<12° during 95 % of the shots
	Streamer depth	As per last PEP rev 1.4: 1.0 m ± 0.5 m (although primarily determined by weather and data quality)
	Other acquisition parameters (dropped channels, noise threshold etc)	Source depth: 0.4 m ± 0.1 m. Noise thresholds: <ul style="list-style-type: none"> - Random noise: 7 µB (10 µB near/far traces & depth controller locations. - Coherent Noise ahead/astern: 15 µB. - Coherent noise abeam: 5µB. Dropped bad shots threshold: No dead channels in the near 6 channels and a maximum of 2 non-consecutive dead channels from channel 6 to the far channel. Dropped/bad channels threshold: ≤ 2 channels.

Equipment	Specification	Survey Requirement
	Variable energy levels	Between 100 and 1000 Joules
	System	A suitable multi-channel and multi-element hydrophone streamer with depth control plus depth measurement for continuous monitoring and recording of streamer depth

3.2.3 Parties Involved

The parties involved in the project are represented by the organogram given in Figure 5.

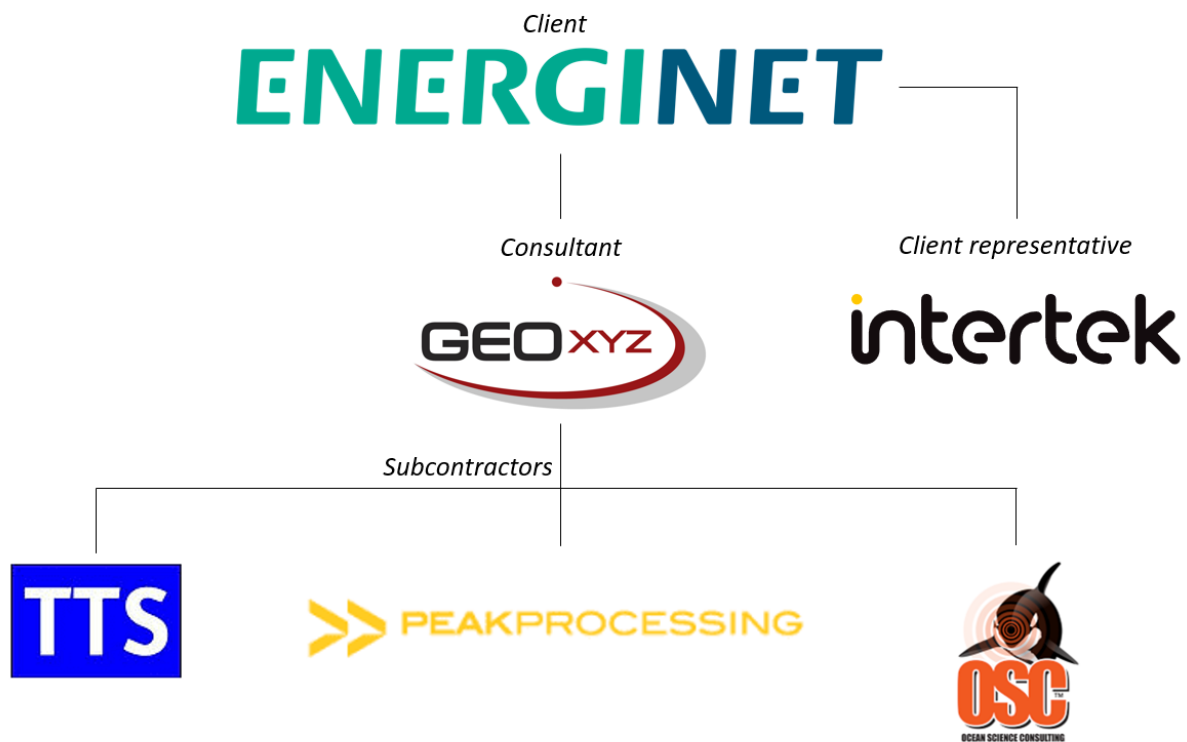


Figure 5: Parties involved in the project

3.3 REFERENCE DOCUMENTATION

Key project documentation from the Client is listed in Table 5.

Table 5: Reference documents

Ref.	Document Number	Title	Owner
1.	22/02940-1	Scope of Services	Client
2.	22/02940-2	Scope of Services – Enclosure 1 – Technical Requirements	Client
3.	22/02940-5	Scope of Services – Enclosure 2 – Standards of Deliverables	Client
4.	22/02940-3	Scope of Services – Enclosure 3 – HSE Requirements	Client
5.	22/02940-4	Scope of Services – Enclosure 4 – Quality Management Requirements	Client
6.	16/19566-2	Requirements to TSG	Client

Ref.	Document Number	Title	Owner
7.		TQ system (Energinet SharePoint site)	Client

Details on the conducted calibrations prior to the start of the survey and the operational aspects of the survey, including resources, event logs, etc., can be found in the Mobilisation and Calibration Report and the Operations Report, respectively. Information on the methodology and workflow on the datasets are outlined in the Processing Report. This report presents the interpreted results of the geophysical and geological datasets of the survey for the Kattegat II site.

Table 6 lists all the reports delivered as part of this survey, with this report highlighted in **bold**.

Table 6: Project Reports

Ref.	Report Document Number	Title	Type of Report
8	BE5376H-711-MCR-01	Mobilisation and Calibration Report Geo Ocean V	Mobilisation and Calibration Report
9	BE5376H-771-MCR-02	Mobilisation and Calibration Report Geo Ocean VI	Mobilisation and Calibration Report
10	BE5376H-711-OR-01	Operations Report geological survey	Operations Report
11	BE5376H-711-OR-03	Operations Report geophysical survey	Operations Report
12	BE5376H-771-02-RR-2.0	Kattegat II Geophysical Report – Geological and Geophysical Survey	Results Report

4 GEODETIC PARAMETERS AND TRANSFORMATIONS

4.1 HORIZONTAL DATUM

The datum parameters for the survey are described in Table 7 and the projection parameters are given in Table 8.

Table 7: Datum parameters

Parameter	Details
Name	European Terrestrial Reference System 1989 (ETRS89)
EPSG Datum Code	6258
EPSG Coordinate Reference System	4258
Spheroid	GRS80
EPSG Ellipsoid Code	7019
Semi-Major Axis	6378137.000
Semi-Minor Axis	6356752.314140
Flattening	1/298.2572221010
Eccentricity Squared	0.00669428002290

Table 8: Projection parameters

Parameter	Details
EPSG Coordinate Reference Code	25832
EPSG Map Projection Code	16032
Projection	UTM
UTM Zone	32N
Central Meridian	9° East
Latitude of Origin	0°
False Easting	500000.00 m
False Northing	0.00 m
Scale Factor at Central Meridian	0.9996
Units	Metres

4.2 VERTICAL REFERENCE

The vertical datum for the project is Mean Sea Level (MSL) as defined by the Technical University of Denmark geoid model DTU21MSL. Height data was acquired relative to the ellipsoid and reduced to the project vertical datum. All reported depths in the current report are related to DTU21MSL.

4.3 TIME REFERENCE

The time frame set up in all survey systems on board the vessel as well as the reported time in any official form and document is provide in Coordinated universal time (UTC).



Online displays, overlays and logbooks are annotated in UTC as well as the daily progress report (DPR) and the Daily Processing Progress report (DPPR).

The synchronisation of the survey system is controlled by the ZDA NMEA time and date and the pulse per second (PPS) issued by the primary positioning system.

5 SURVEY RESOURCES

5.1 SURVEY VESSELS

For the geological and geophysical surveys, the survey vessels Geo Ocean V (GOV) and Geo Ocean VI (GOVI) were utilised to complete the work across the four sites. Both vessels are 54 m long and equipped to perform a range of subsea surveys in the offshore renewables, and oil and gas industries. Additionally, they can both operate 24 hours/day and can remain at sea for up to four weeks. The specifications of GOV and GOVI are summarised in Table 9.

Table 9: Survey vessel specifications

Feature	Geo Ocean V	Geo Ocean VI
Owner:	GEOxyz	GEOxyz
Flag:	Luxembourg	Luxembourg
Length:	53.8 m	53.8 m
Width:	13.0 m	13.0 m
Draught:	4.0 – 4.8 m	4.8 m
Speed:	10 knots (cruising)	11 knots (cruising)
Main Propulsion:	Hybrid propulsion CP-propeller	Hybrid propulsion CP-propeller
Endurance:	28 days	28 days
Accommodation:	24	24
Positioning:	DGPS, HiPaP351 USBL	DGPS, HiPaP352P USBL NAVIS NavDP 4000
A-Frame:	10t Stern	13t Stern
Image of the vessel		

5.2 EQUIPMENT AND SOFTWARE

Details on the survey equipment used for this project onboard the GOV and GOVI are listed in Table 10 and Table 11, respectively.

Table 10: GOV survey equipment specifications

System	Manufacturer – Model	Equipment Specifications
GNSS	Trimble BX992 & BD982 (2x G4 corrections)	RTK: < 0.05 m; DGNSS: <0.10 m
INS (motion, heading)	IXBlue Octans V SBG Apogee Navsight	H: 0.1°; R&P: 0.01°; Heave: 5 cm H: 0.01°, R&P: 0.03°, Heave: 5 cm
SVP	Valeport Swift	0.02 m/s

System	Manufacturer – Model	Equipment Specifications
MBES	Kongsberg EM2040 Dual Rx, Dual ping	Freq: 200 – 400 kHz Focus: 0.4° x 0.7° at 400 kHz
USBL	Kongsberg HiPAP 351P	0.02 m range detection accuracy or < 0.3% of slant range
Magnetometer	Geometrics G882	Accuracy: < 2 nT throughout range. Freq: up to 40 Hz
SSS	2x Edgetech 4200 (300/600 kHz)	Horizontal beamwidth: 0.5° @ 300 kHz, 0.26° @ 600 kHz Resolution Across Track: 3 cm @ 300 kHz, 1.5 cm @ 600 kHz
SBP	Innomar SES-2000 Medium	2-22 kHz 1-5 cm resolution

Table 11: GOVI survey equipment specifications

System	Manufacturer – Model	Equipment Specifications
GNSS	2x Trimble BX992 (1 x XP2 and 1 x G4 corrections)	RTK: < 0.05 m; DGNS: <0.10 m
INS (motion, heading)	IXBlue Hydrins SBG Apogee Navsight	H: 0.01°; R&P: 0.01°; Heave: 5cm H: 0.01°, R&P: 0.03°, Heave: 5cm
SVP	Valeport Swift	0.02 m/s
MBES	Kongsberg EM2040 MKII Dual head, Dual swath	Freq: 200 – 400 kHz Focus: 0.4° x 0.7° at 400 kHz
USBL	Kongsberg HiPAP 352P	0.02 m range detection accuracy or < 0.3% of slant range
Magnetometer	Geometrics G882	Accuracy: < 2 nT throughout range. Freq: up to 40 Hz
SSS	2x Edgetech 4200 (300/600 kHz)	Horizontal beamwidth: 0.5° @ 300 kHz, 0.26° @ 600 kHz Resolution Across Track: 3 cm @ 300 kHz, 1.5 cm @ 600 kHz
SBP	Innomar SES-2000 Medium	2-22 kHz 1-5 cm resolution

The primary software that was used to acquire and process the data is listed in Table 12.

Table 12: Primary software list

Type	Software	Related equipment
Acquisition	QPS QINSY	Navigation, MBES, GNSS, SSS, MAG
	Edgetech Discover	SSS Edgetech
	Innomar SESwin	SBP
Processing	Beamworx Autoclean	MBES
	QPS Qimera	MBES
	QPS FMGT	Backscatter
	SonarWiz	SSS
	Oasis Montaj	MAG
	Kingdom or Silas	SBP
	ProMax	2D UHR (processing)
	Kingdom	2D UHR (Interpretation)
	QGIS / AutoChart / ArcGIS	SSS, MBES, MAG, SBP

6 TECHNICAL QUERIES AND CHANGES TO SURVEY SCOPE

Geological, oceanographic, and technical site limitations resulted in necessary adjustments to the survey scope. These survey scope adjustments were made as Technical Queries (TQs) and were checked and validated by the Energinet (Client) and by GEOxyz. Table 13 outlines the project specific TQs related to the geological and geophysical surveys; below the table, their implications for the survey are outlined.

Table 13: TQ clarifications and outcomes

TQ ID	Subject	Conclusion
TQ - 004	SBP Interpretation	Where homogeneous geology is interpreted on SBP lines of the geophysical survey, interpretations are performed on every 2nd line
TQ - 009	Boulder Field Criteria geophysical survey	Picking criteria within in boulder fields targets: Boulders ≥ 2 m in any direction & "Non-geological contacts" ≥ 0.5 m in any direction
TQ - 010	SSS nadir coverage	SSS Coverage of 200% acquired at entire site, except area affected by pycnocline effects

7 DATA PROCESSING AND INTERPRETATION METHODS

7.1 MULTIBEAM ECHOSOUNDER

7.1.1 Data acquisition

The system settings and Client specifications for the project are listed in Table 14 and Table 15, respectively.

Table 14: MBES system settings

Kongsberg EM2040 (DH/DSW)	Head 1 port	Head 2 stbd
Survey speed	Average 4 knots	
Frequency	400 kHz	400 kHz
Bottom sampling	High Density Dual Swath (1024 beams)	
Range	50 m	
Power	Maximum	
Pulse length	Auto	
Patch test roll	<i>TX -0.205°, RX -40.005°</i>	<i>TX -0.270°, RX 42.530°</i>
Patch test pitch	<i>TX 0.340°, RX 0.340°</i>	<i>TX 0.242°, RX 0.242°</i>
Patch test heading	<i>TX -2.238°, RX 177.762°</i>	<i>TX -2.345°, RX 177.655°</i>
Sector width	80°	80°
Ping rate	25 Hz – 30 Hz (maximum)	

Table 15: MBES Client specifications

Item	Specification
Data density	16 hits/m ² at 99 % of the site.
Standard Deviation	0.20 m on 95 % of the site.
MBES Mode	Equidistant
Grid	0.25 m cell size
Coverage	100 %

In TQ 008- MBES, it was requested and agreed to increase the MBES SD limit to 0.25 on 95 % of the site and to modify the hit count specifications to the following: A minimum of 99 % of site will show a hit count of at least 16 hits/m.

7.1.2 MBES methodology

The objective of the MBES processing workflow was to create a final digital terrain model (DTM) that provided the most realistic representation of the seabed.

The processing workflow is comprised of four general steps, which are summarized in the tables below:

Table 16: Loading MBES data in Qimera

Step 1	Load MBES data into Qimera
Set Up Project	Load in RAW multibeam files (*.db) as recorded by QINSy in a new project Grid cell size 0.25 m * 0.25 m
QC of coverage	Check completeness of data by cross-referencing the imported files with the Survey Log

Table 17: MBES positioning verification

Step 2	Positioning
All verification during the Positioning control was performed by checking the data with the 95% confidence option	
SVP correction	Applying the last SVP done into the data set
Overall statistics	Run Standard Deviation statistics. The standard deviation must be < 0.25 m
Verify horizontal positioning and Total Horizontal Uncertainty (THU)	Create a dynamic surface at 0.20 m. A .xyz file with THU values can be exported or a static surface can be created with THU values in it. The surface needs to be updated and a new export can be done (for the 24 hours QA deliverables)
Verify vertical positioning and Total Vertical Uncertainty (TVU)	Create a dynamic surface at 0.20 m. A xyz with TVU values can be exported or a static surface can be created with TVU values in it. The surface needs to be updated and a new export can be done (for the 24 hours QA deliverables)
FAU export	FAU files export to finalise the processing in BeamWorx Autoclean processing software (separate export per head)

Table 18: MBES data de-spiking and processing

Step 3	Data de-spiking
Quality assessment and data correction/filtering	Refraction and vertical mismatch issues due to pycnocline to be assessed and filtered when possible. Outer ranges to be trimmed when data cannot be properly filtered.
Manual De-spiking	Remove remaining substantial spikes manually using the 2D and 3D views. Correct where necessary
Filter De-spiking	Filters applied to de-spike the data
Coverage reassessment (SD and Hit count)	Coverage and specifications reassessment after processing

Table 19: MBES data quality control

Step 4	Quality Control
Shallowest/Deepest Areas	Special attention is needed for these areas to verify all spikes are removed.
Check for steps in data	Change plan view to the mean depth colour data to verify no steps are present in the data.
Statistics Control	Final statistics exports per block/area to track and save the final specifications.

Table 20: MBES target picking

Step 5	MBES target picking
Target picking	Targets picked manually in Qimera from the grid

The MBES data was initially brought into QPS processing software Qimera, to check that the coverage and density requirements were achieved before any further steps were taken. It was confirmed that a post-processed navigation solution was not necessary, as the dynamic PPP applied online provided the vertical and horizontal accuracy necessary for the survey. THU and TVU values were checked and confirmed to be within the specifications defined for the dataset. The DTU21MSL vertical model applied in Qinsy online was confirmed to properly reduce the ellipsoidal heights to the project vertical datum. Subsequently, in Qimera, the bathymetry data for each data file is merged to create a dynamic surface, to review the standard deviation and sounding density results.

After this preliminary check and after confirmation that the data was within the project specifications, the process of removing outlying soundings, refraction and SVP corrections, as well as the refined cleaning routine, was performed.

The last step of processing was carried out in Autoclean, as it has been proven that, if no further processing was needed in the data coming from Qinsy (post processing, computation recalculation, misalignments adjustments...), the Beamworx software manages high amounts of MBES data more quickly, which made the cleaning process more efficient and faster. In addition, it allows a more detailed statistical analysis to be performed at the end of the processing process.

Finally, MBES target picking was carried out after processing using the automatic tool in BeamWorx Autoclean software. Targets were detected based on a reference grid, which automatically measures the targets in Length x Width x Height. The detection process is fully automated and based on input parameters. These parameters could change per area depending on data quality, target numbers, size, and seabed complexity, but always in accordance with the specification of the project relative to minimum size and their interpretation as per TSG requirement. Detection and accuracy are greatly dependent on data quality. Artefacts such as thermocline, vertical alignment and complex morphology could impact the detectability of potential targets.

After running the detection process, a manual QC was conducted and any amendment were applied if needed e.g. false positives are removed, false negatives are added, and target dimensions were adjusted manually if required. The automated routine combined with a manual QC gave this output a reliable result.

Finally, a target correlation was done with the SSS and MAG contacts, and a final QC was done to ensure consistency on the target classification across the sites.

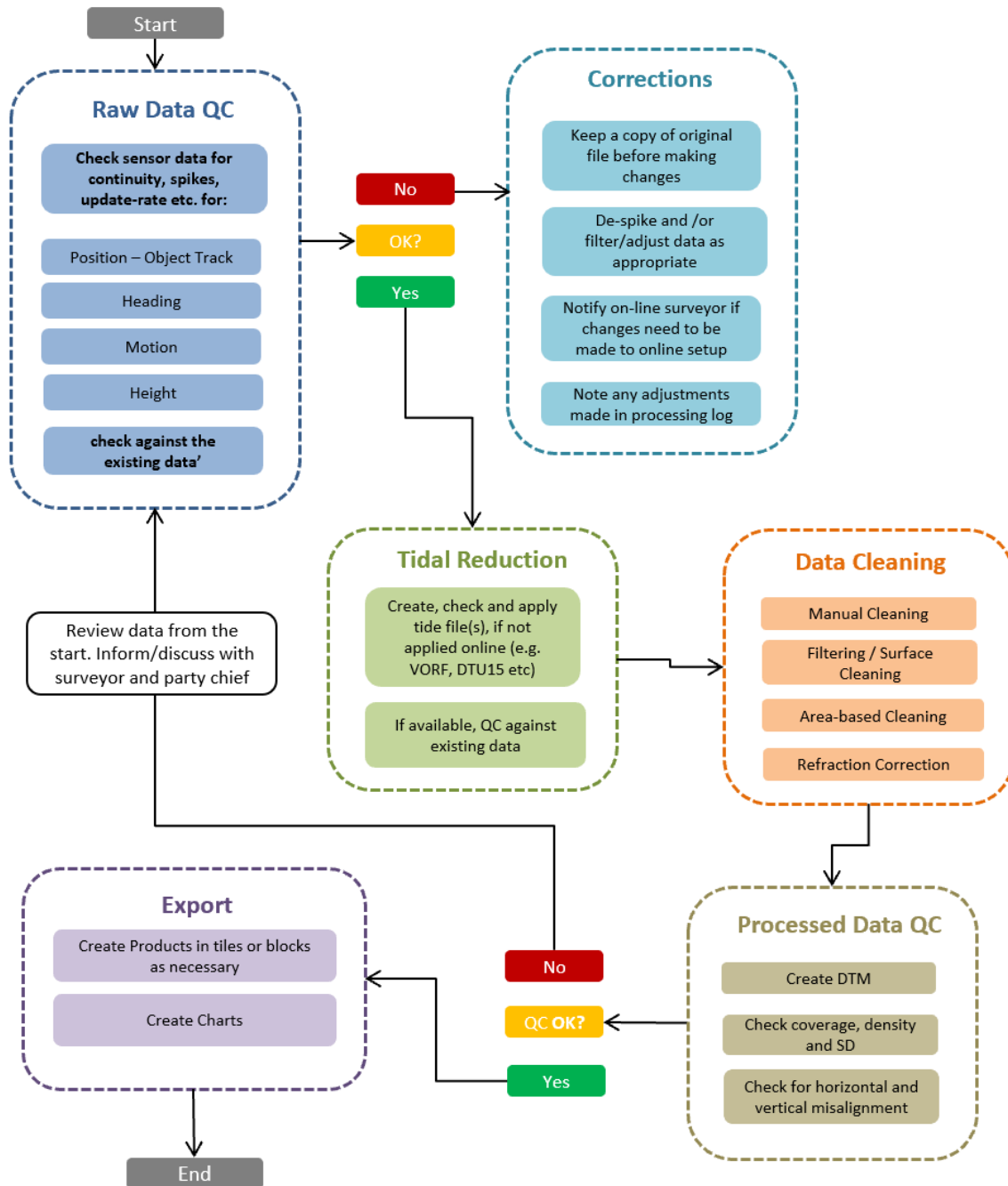


Figure 6: General MBES data processing workflow

7.1.3 Backscatter methodology

The backscatter data were processed and exported, using QPS Fledermaus GeoCoder Toolbox (FMGT) software.

Backscatter processing was carried out on the fully cleaned and processed MBES data files, from previous steps in the Qimera software. Combined GSF (both heads exported in the same file) were exported and then imported in FMGT along with a MBES reference surface.

The gain was modified to normalize the intensity over the survey area. It was also optimized to enhance changes in seabed sediment composition and morphological features on the seafloor.

Data from both vessels (GOIV and GOV) were processed in the same FMGT block projects to optimize the blending of overlapping data from the two vessels.

7.1.4 Data quality assessment

IHO Standards for Hydrographic Surveys define a maximum THU value of 2 m for a First Order Survey, and a 100 % of the THU values for Kattegat II are below this limit. In case of TVU, the maximum limit is defined by a relation between the uncertainty that varies with the depth and the uncertainty not dependent of the depth. For Kattegat II, a theoretical mean TVU max calculated for the site is 0.65 m, being all TVU values below this theoretical limit. The TVU and THU values must be understood as an interval of \pm the stated value. The TVU coverage map for Kattegat II is displayed in Figure 7. The THU coverage map for Kattegat II is displayed in Figure 8.

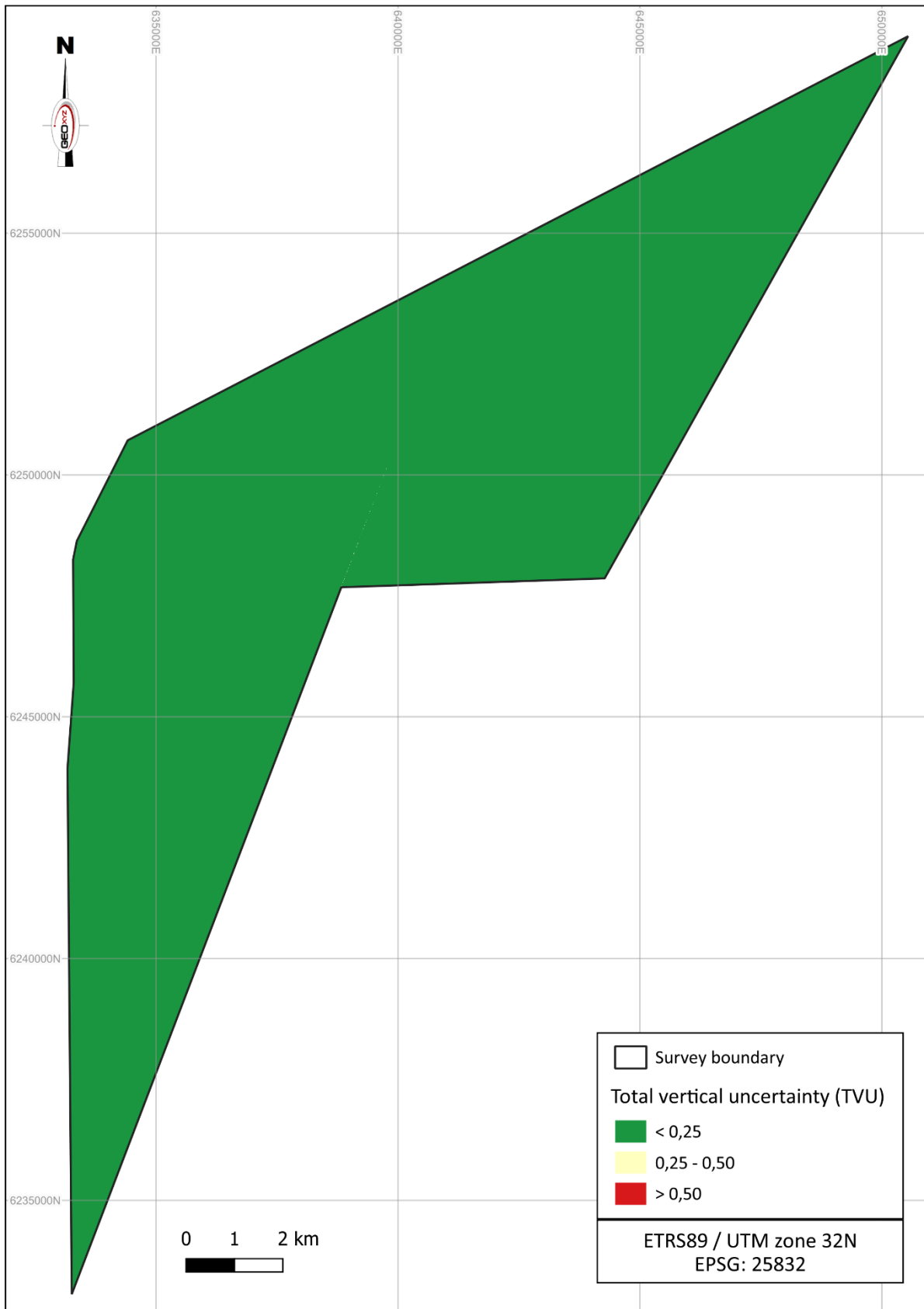


Figure 7: TVU coverage map

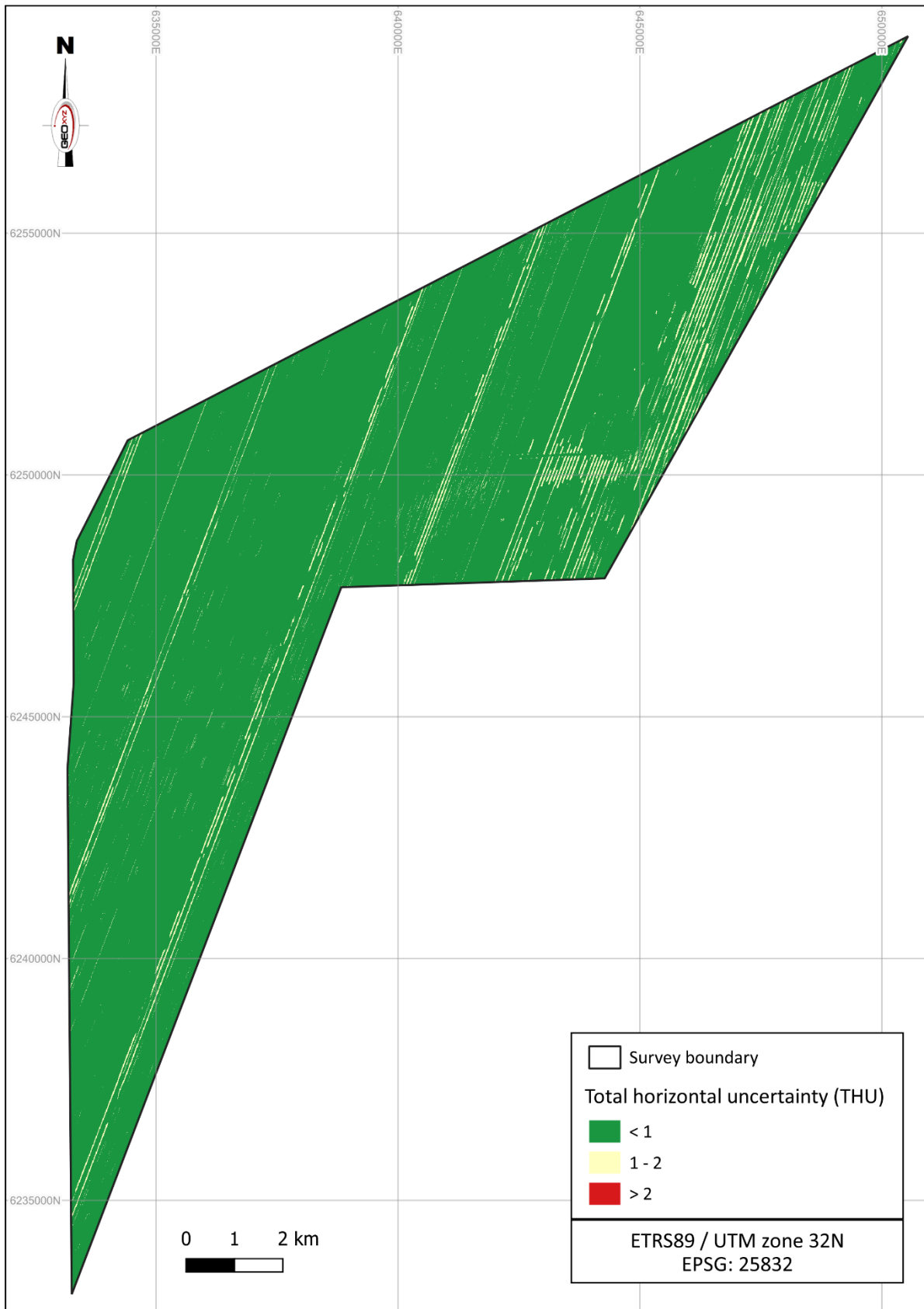


Figure 8: THU coverage map

7.1.5 Backscatter

The quality of the final processed backscatter was assessed in GIS software (QGIS and Global Mapper) after combining all processed blocks in one gridded surface as 1 m resolution backscatter mosaic (Figure 9).

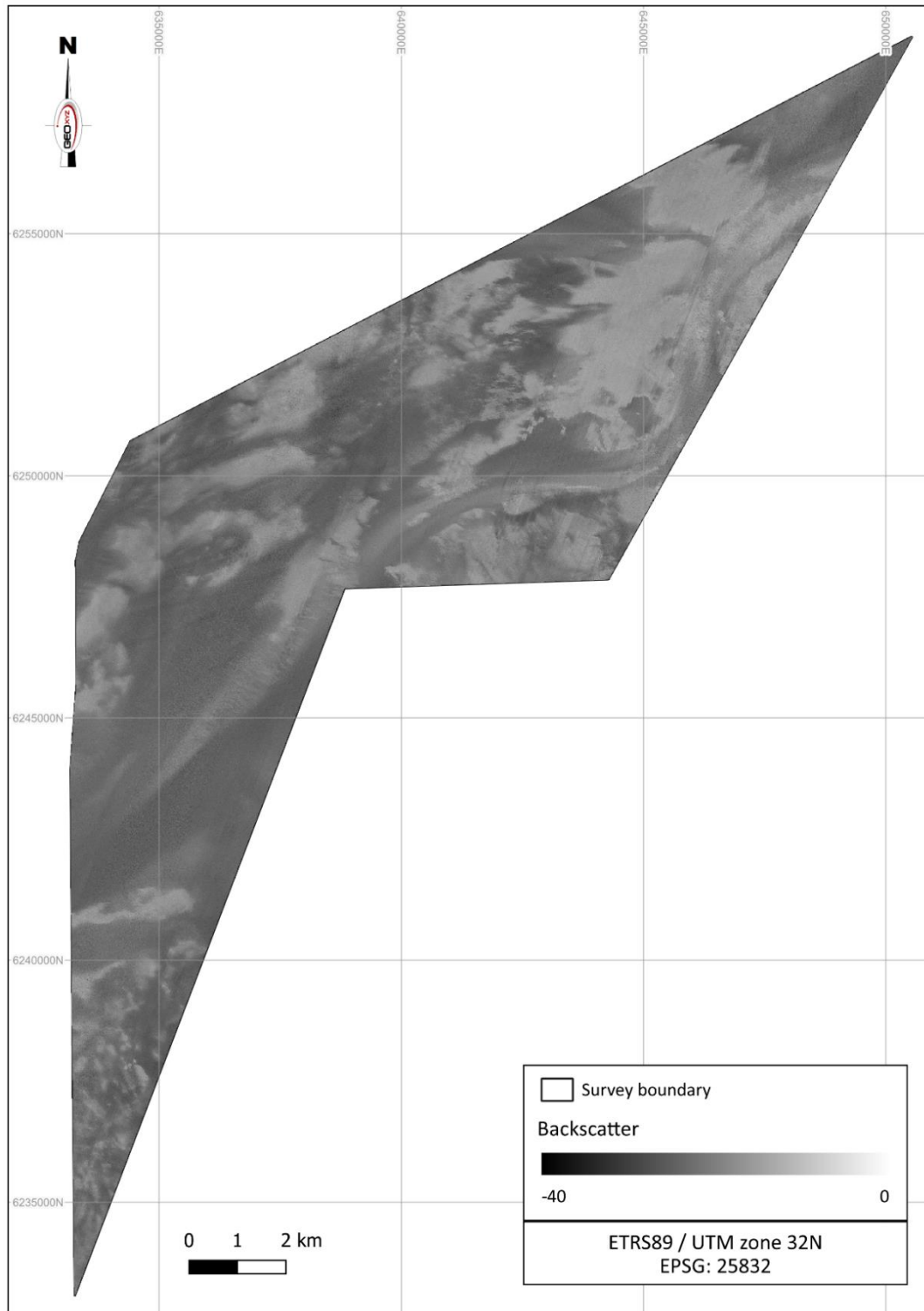


Figure 9: Backscatter data across the Kattegat II survey area

The aim of processing the backscatter data was to achieve a homogeneous colour scale between the survey blocks. The colour scale was normalised between blocks. This step was necessary, as it is not possible to process the entire survey area into a single mosaic due to the size of the dataset and the resolution specifications.

The backscatter mosaic assessment indicated that the boundaries between different sediment types were differentiated and therefore the results were fit for purpose.

Some artefacts are present which mostly manifest as stripes aligned with the survey line direction (Figure 10). These artefacts also appear to be exacerbated during periods of poor weather. The MBES acquisition setup was preferential to the backscatter one.

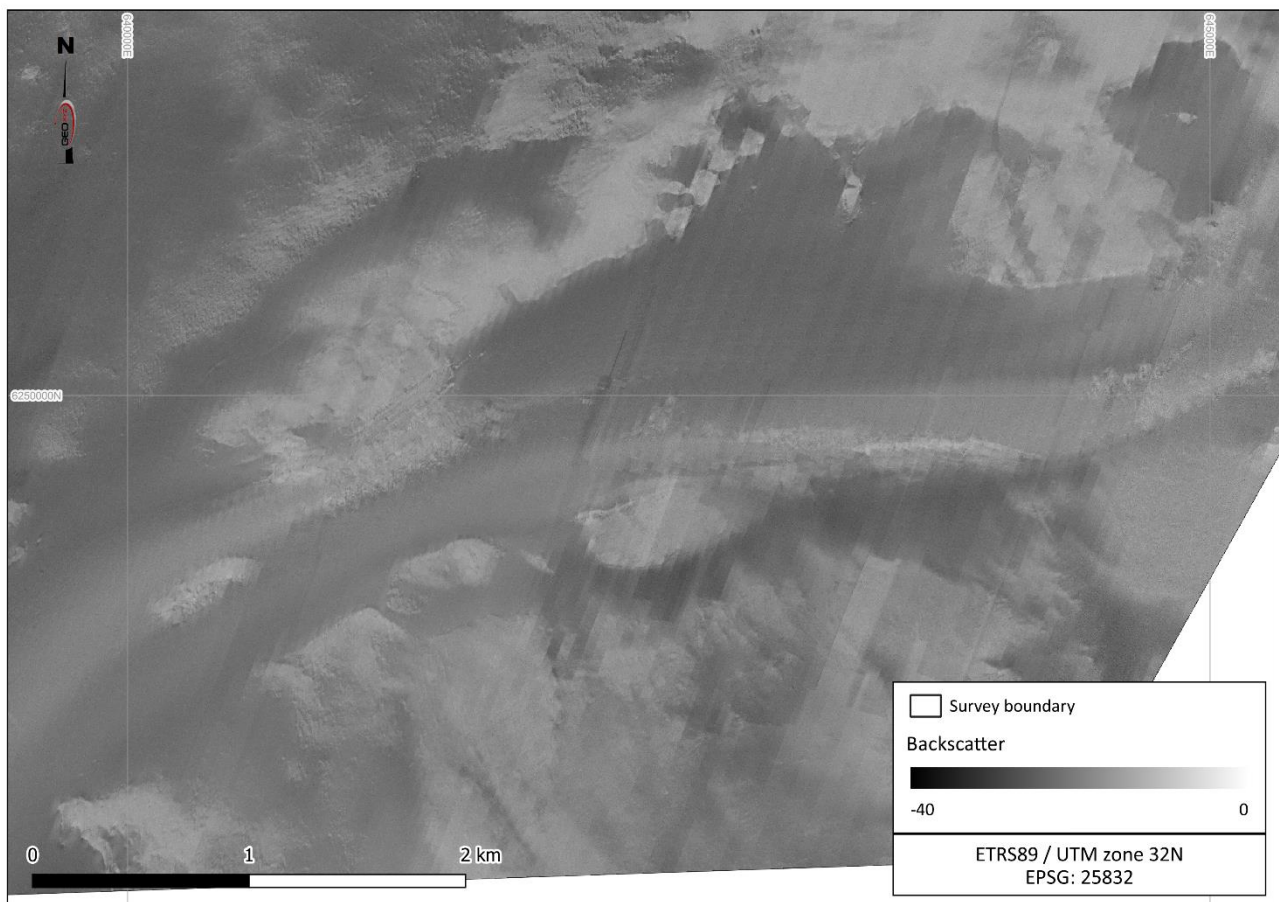


Figure 10: Example of stripe effect on the backscatter mosaic in Kattegat II

Despite the presence of these artefacts, the backscatter data is of sufficient quality to derive sediment boundaries and aid the interpretation of the SSS dataset.

7.2 SIDE SCAN SONAR

7.2.1 Data acquisition

The SSS system settings and Client specifications are listed in Table 21 and Table 22, respectively.

Table 21: SSS system settings

Edgetech 4200 300/600 kHz	
Survey speed	Average 4 knots
Positioning	HiPAP 351 USBL
Mean fish altitude	Between 4.5 - 5 m
Trigger	High Frequency = Master
TVG / Gain	Recording RAW (*.jsf)
Range	HF = 70 m / LF = 70 m
Mode	High Definition Mode

Table 22: SSS Client specifications

Item	Specification	Achieved during survey
Resolution sufficient for detecting seabed feature/object	0.5 m (length, width and height)	< 0.5 m (length, width and height)
Towing altitude	8 - 12 % of range (optimised for data quality)	10 % of range
Positional accuracy	± 2 m (using vessel course-over-ground and USBL)	± 2 m (using vessel course-over-ground and USBL)
Operating mode	High Definition Mode	High Definition Mode
Range	70 m	70 m
Coverage	200 %*	200% except under nadir: coverage 100%

* SSS coverage adjusted to 100% for nadirs, due to thermocline/pycnocline effects. Also, coverage in some places was accepted to be only 100%.

During the geophysical survey operations, a dual SSS configuration was employed to increase coverage and help mitigate the potential effects of pycnocline interference. This comprised each SSS being towed on separate winches, with a longitudinal offset (nominally of approximately 20 m). A depressor was employed on one of the SSS fish, to ensure both fish were flown at similar, consistent altitudes within the water column.

7.2.2 SSS data processing

Side Scan Sonar (SSS) data were processed and interpreted using Chesapeake SonarWiz software. The SSS processing steps are outlined in Table 23 to Table 29. Figure 11 outlines the SSS processing workflow used for the project.

Table 23: Importing SSS data into SonarWiz

Step 1	Importing data: overview of the acquired lines
Set Up Project	The raw sonar files (*.jsf) had corrected navigation applied, using the SonarWiz NavInjectorPro utility, before being imported into Chesapeake SonarWiz software. The navigation data was de-spiked and exported from QINSy validator, to provide a smoothed position, with a bearing to towpoint heading solution. The processed sonar files (*.jsf) were imported into the SonarWiz project with the appropriate file type

Step 1	Importing data: overview of the acquired lines
	<p>specific settings, as those were determined during the mobilization and calibration tests.</p> <p>A smoothing filter of 100 pings was applied during import. Once the parameters were agreed and checked with the Employer's Offshore Supervisor, they were used for the remainder of the dataset.</p>
Bottom track	Using the automatic bottom tracking feature, SSS data were bottom tracked, line by line, and then, if needed, bottom track was manually adjusted.

Table 24: Navigation correction in SonarWiz

Step 2	Navigation correction
Check position	The SSS data were checked for positional accuracy against the MBES data, by locating clearly distinguishable features and contacts in both datasets and comparing their positions. If needed, the navigation data were re-processed and re-exported from Qinsy as new navigation files (x, y, heading) and injected into the SSS data, using the SonarWiz NavInjectorPro utility. After that, positional accuracy was checked again.
Navigation	<p>The towfish heading source was set to the fish heading to tow point. Using the SonarWiz ZEdit utility, navigation spikes were corrected and the positional accuracy was checked.</p> <p>The towfish heading was QC'd for small data jumps or artifact "vortex" effects.</p>

Table 25: SSS signal processing

Step 3	Signal processing
EGN (Empirical Gain Normalization)	An EGN (Empirical Gain Normalization) table was calculated and applied to the data, creating a normalised gain, both along track and across track.
TVG (Time Variable Gain)	If the EGN table applied to the data did not have the desired effect, an Auto TVG was used.

Table 26: SSS infill assessment

Step 4	SSS infill assessment
Manual check for gaps	Manual check for data gaps, overlap and data loss during QC/QA.
Check for pycnocline interference	Quality control check for pycnocline interference towards swath edges. Affected areas were marked for infill and re-run if required.
SonarWiz coverage	Checked for 200 % coverage (100 % nadir coverage for pycnocline- thermocline affected data), using SonarWiz Coverage report.

Table 27: SSS contact picking

Step 5	SSS target picking
Target picking	<p>Must include:</p> <ul style="list-style-type: none"> H-L-W measurements Description of the target Confidence level <p>The interpretation of contacts was performed in SonarWiz digitizing mode, in accordance with the specifications. Contacts were digitized alongside MBES data and confidence level was updated accordingly. Wrecks and cables were correlated to relevant databases.</p>

Step 5	SSS target picking
Criteria of object detection	Minimum of 0.5 m (height, width or length) Object is identified as deviation from natural seabed forms The object is verified in wing line side scan image Position is verified with MBES data Man-made objects or very clear objects (even if only detected on one line only) Contact classification criteria defined with the Reporting Coordinator and sent to the Data Coordinator onshore.
Image picture	Colour grey inverted
Confidence level (Low, Medium, High)	Every contact has a confidence level attributed to it based on its detection in: <ul style="list-style-type: none"> • 1 SSS line -> Low, • 2 or more SSS lines -> Medium • 1 or more SSS lines and MBES data -> High
Boulder fields	Boulder field areas were outlined in SonarWiz map view whereas waterfall view was also used where needed. The boulder zone defining criteria are: <ul style="list-style-type: none"> • < 40 boulders: Not a boulder zone • 40 – 80 boulders: Boulder zone type 1: Intermediate boulder density • > 80 boulders: Boulder zone type 2: High boulder density • No minimum size requirement, all covered boulders count towards the minimum boulder amount to determine boulder zones The digitized polygons have been edited in QGIS and re-imported in SonarWiz. No manual target picking was performed within the boulder field polygons and a machine learning automatic picking algorithm was used instead. The results were confirmed to be representative and correct. Man-made objects have been manually picked within the boulder field areas

SSS contact picking was performed using two different methodologies related to the presence or not of boulder fields in the area.

Outside boulder fields:

Contacts were manually picked in the waterfall display in the Sonarwiz project, and measured for length (largest dimension of object), width (perpendicular to length) and height of the target.

Piking targets was in accordance with the specification of the project relative to minimum size and their interpretation as per TSG requirement. All contacts from 0.5 m were picked. Once all SSS targets were picked, they were correlated with MBES and MAG contacts.

Several QC steps are performed during the manual target picking and interpretation, and a final QC by the Lead Geo is done to ensure consistency on the target classification across the sites.

Inside boulder fields:

Automatic boulder picking was performed using an algorithm to analyse contacts from raster analysis. This methodology runs different scripts that detect and isolate the crucial components of reflections and shadows from the SSS data, which are fundamental for the representation, identification and measurement of boulders/targets.

Inside the mapped boulder fields, picking targets was in accordance with the specification of the project relative to minimum size and their interpretation as per TSG requirement. All contacts from 2 m and all MMO/debris were picked.

The detection process (Figure 11) was performed on each individual SSS line, and for each target the automated detection yielded a polygon that outlines the reflection and a line that outlines the shadow. When requested to identify the same target from several SSS lines, a specifically developed tool compared target position and dimension on different lines and created average values for one representative target. This task was especially challenging inside high-density boulder fields where target reflection varied between the lines and shadows overlaps between contacts.

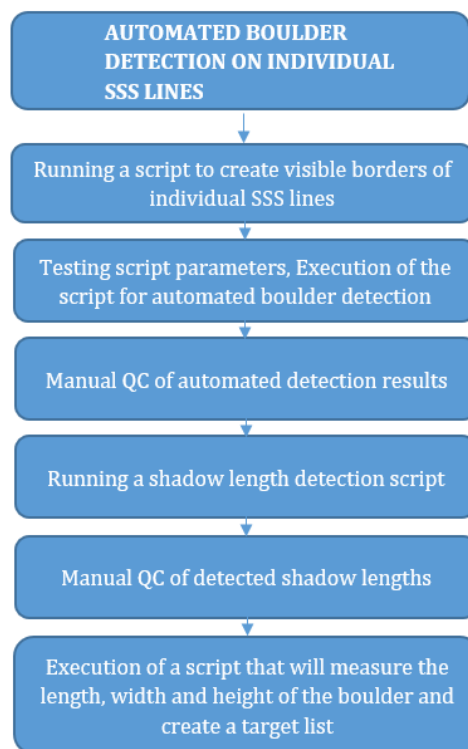


Figure 11: Automated boulder detection progress

A QC process was manually performed by a processor to check whether the detection results correspond to the real target by size and location, making adjustments if necessary to avoid false positive target detections (Figure 12). Manual quality control enabled the processor to ensure accurate and reliable detection results, adjust the results where needed, and improve the overall quality of the detection process.

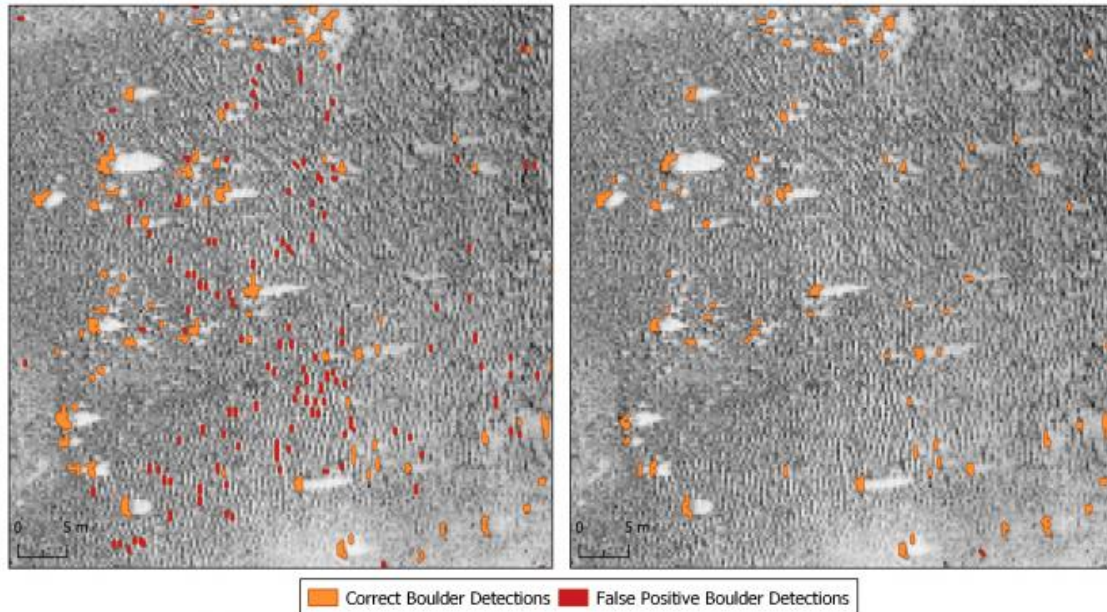


Figure 12: Automatic correct boulder detection vs false positive boulder detection

Once the algorithm was run and the QC was finished, a SSS boulder shapefile was exported and correlated with the MBES and MAG contacts. A final QC by the Lead Geo was done to assure the correct definition of contact.

The accuracy of this tool’s detection varies between 90 % and 95 %, depending on the morphology of the seabed and the data quality.

Table 28: SSS mosaic creation

Step 6	SSS mosaic creation (HF and LF)
Adjust SSS line drawing order	SSS lines drawing order was adjusted to optimize the exported seabed image
Line grouping	Lines were grouped in: Approved, Rejected, Trials or Other
EGN and gain check	Final QC of EGN and gains was performed. If required, new EGNs and gains were recalculated and reapplied.
Inter file gap check	Data was checked for small inter-file gaps. SonarWiz inter-file gap tool was used when required.
Range check	Range was adjusted for optimized quality without compromising the 200 % data coverage.
Mosaic export	SSS mosaics were exported using the standardised project tile size and arrangement.

Table 29: SSS seabed classification

Step 7	Seabed classification
Seabed features	Seabed features have been created and QC’d using the exported SSS LF mosaics. SSS HF mosaics and the MBES exports were also taken into account.
Seabed Geology	The SSS LF and HF mosaics, as well as the MBES data and the SBP contours were used in order to outline the sediment differences, as those are represented by the

Step 7	Seabed classification
	reflectivity changes mainly on the SSS mosaics. Grab samples were the most useful for editing and confirming the outlined sediment boundaries

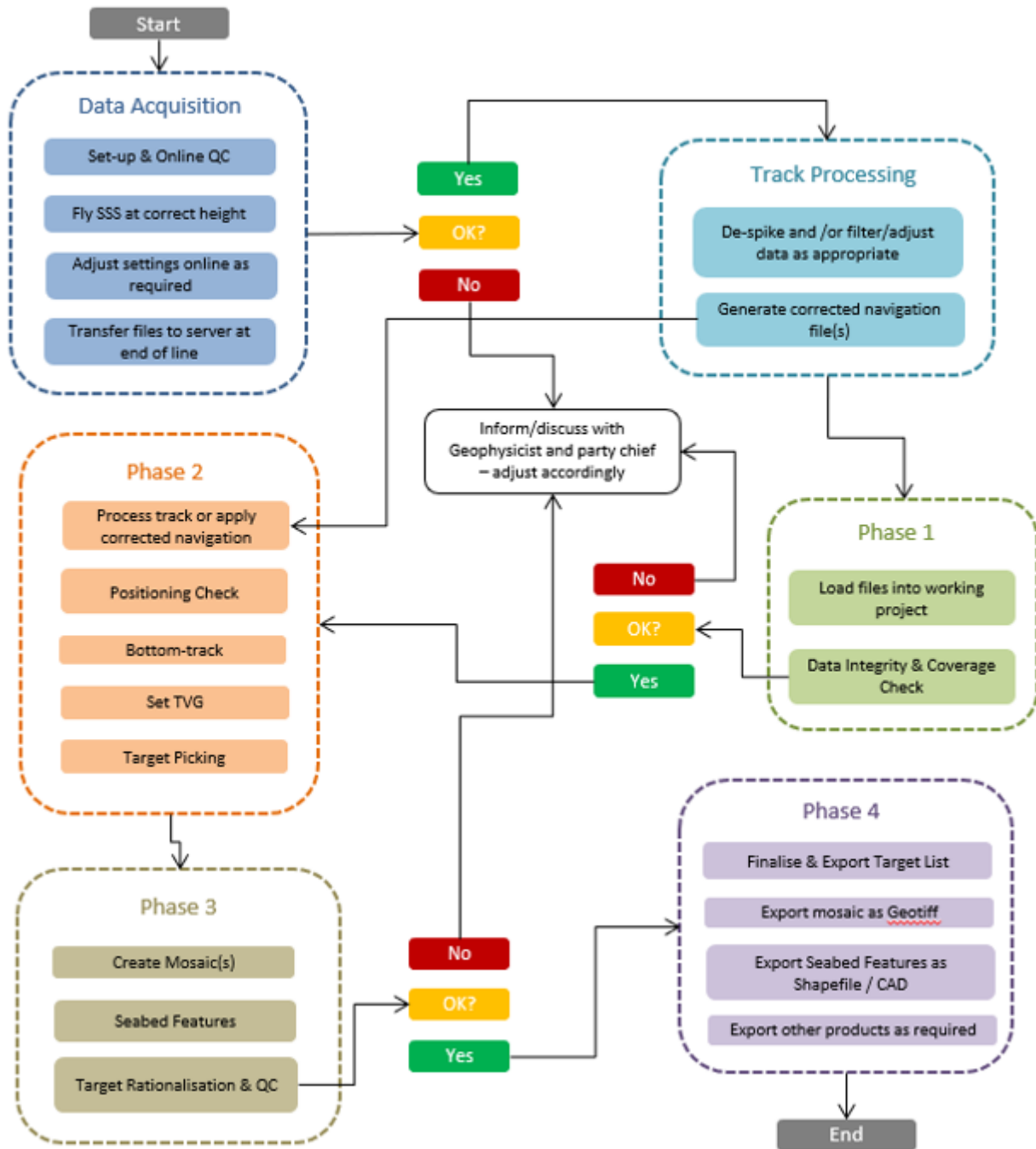


Figure 13: SSS data processing workflow

7.2.3 Data quality assessment

Overall, the SSS data quality was monitored throughout the survey and was of high quality, achieving Client specifications (Table 22).

The SSS coverage across the Kattegat II site is displayed in Figure 12. The requirement for 200 % SSS coverage was reduced to 100 %, due to the effect of the pycnocline on the SSS dataset.

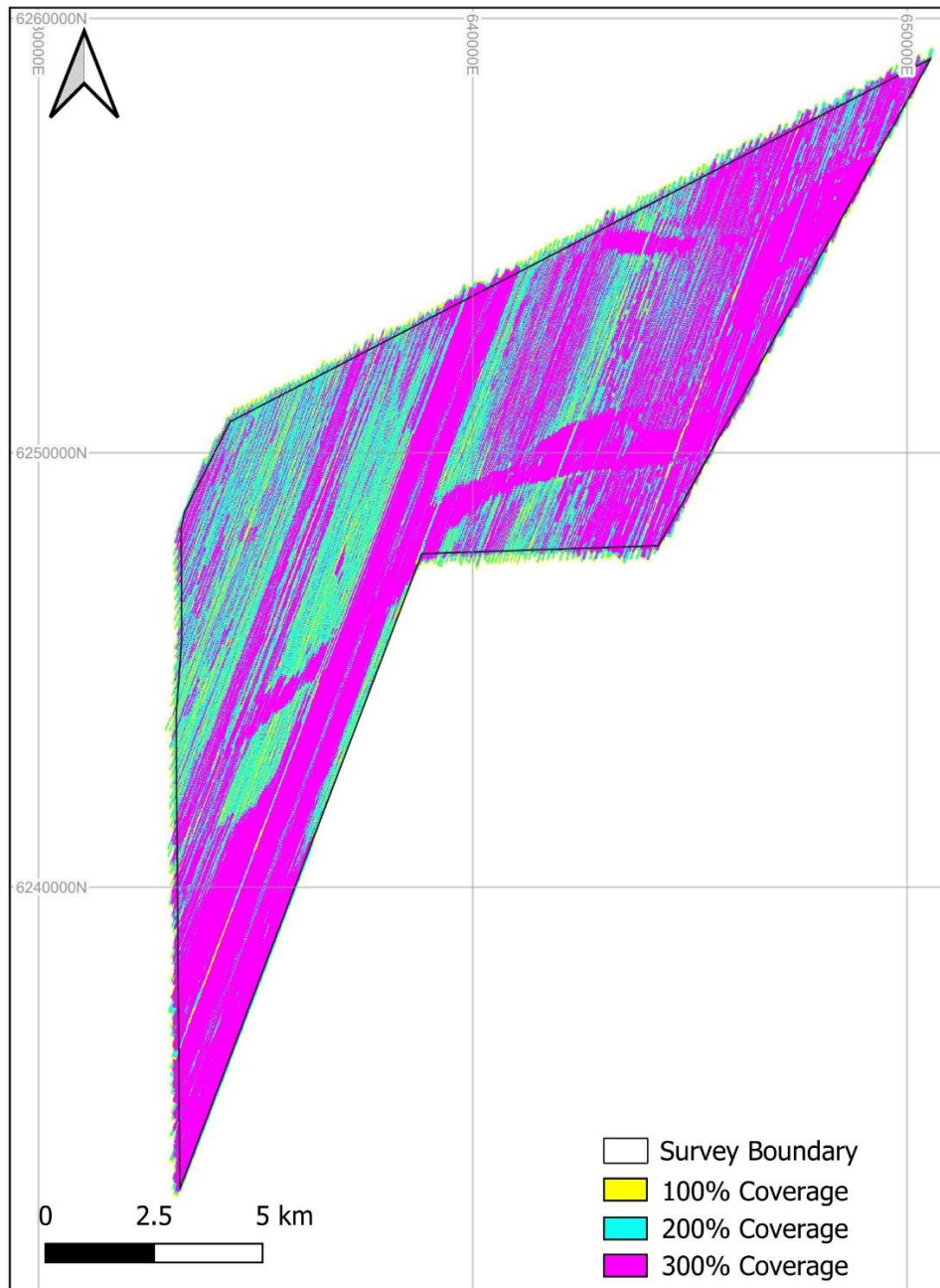


Figure 14: SSS coverage map

Kattegat II was slightly affected by the pycnocline and generally 200 % coverage was achieved across the site, resulting in no infill being required. In various places within the survey blocks, SSS coverage was reduced from 200 % to 100 %, due to severe pycnocline effects.

The pycnocline resulted in marginal/bad data in the outer range of the SSS lines (Figure 15). The affected parts have been removed during processing and good quality data has been used for mosaic exports and target picking (Figure 16).

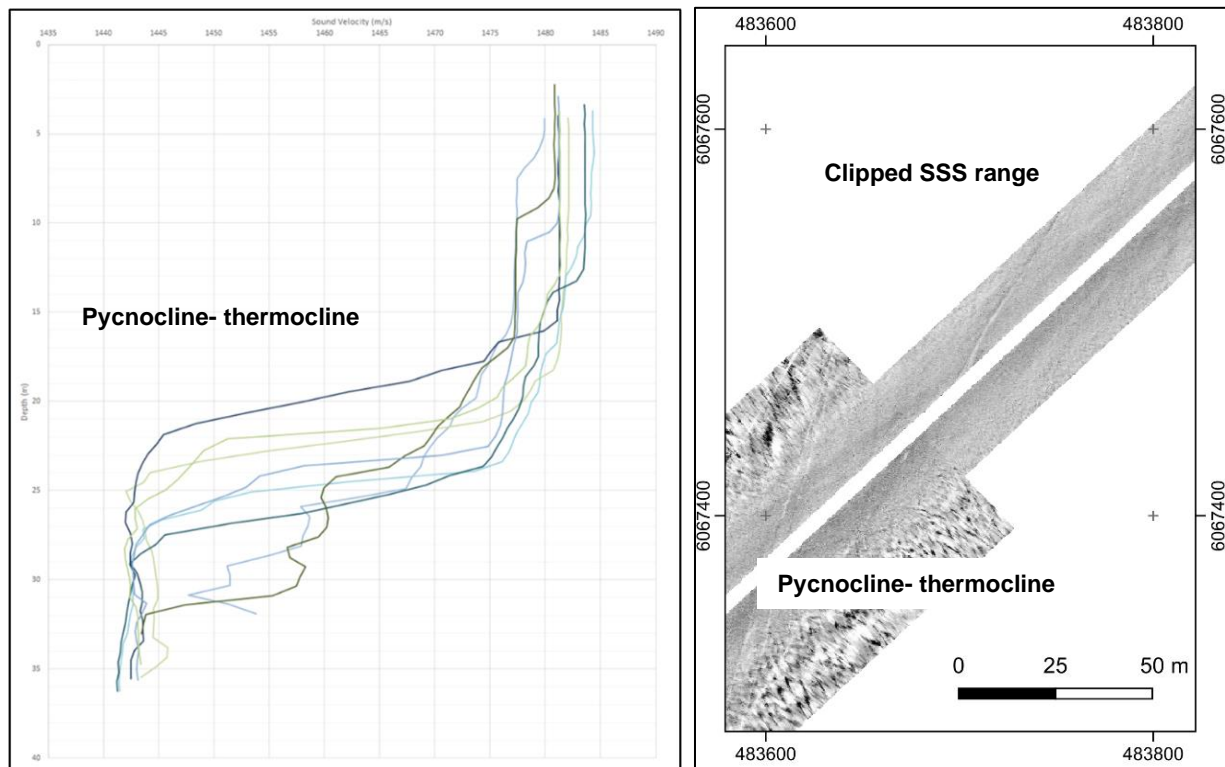


Figure 15: Pycnocline and effect on the SSS dataset

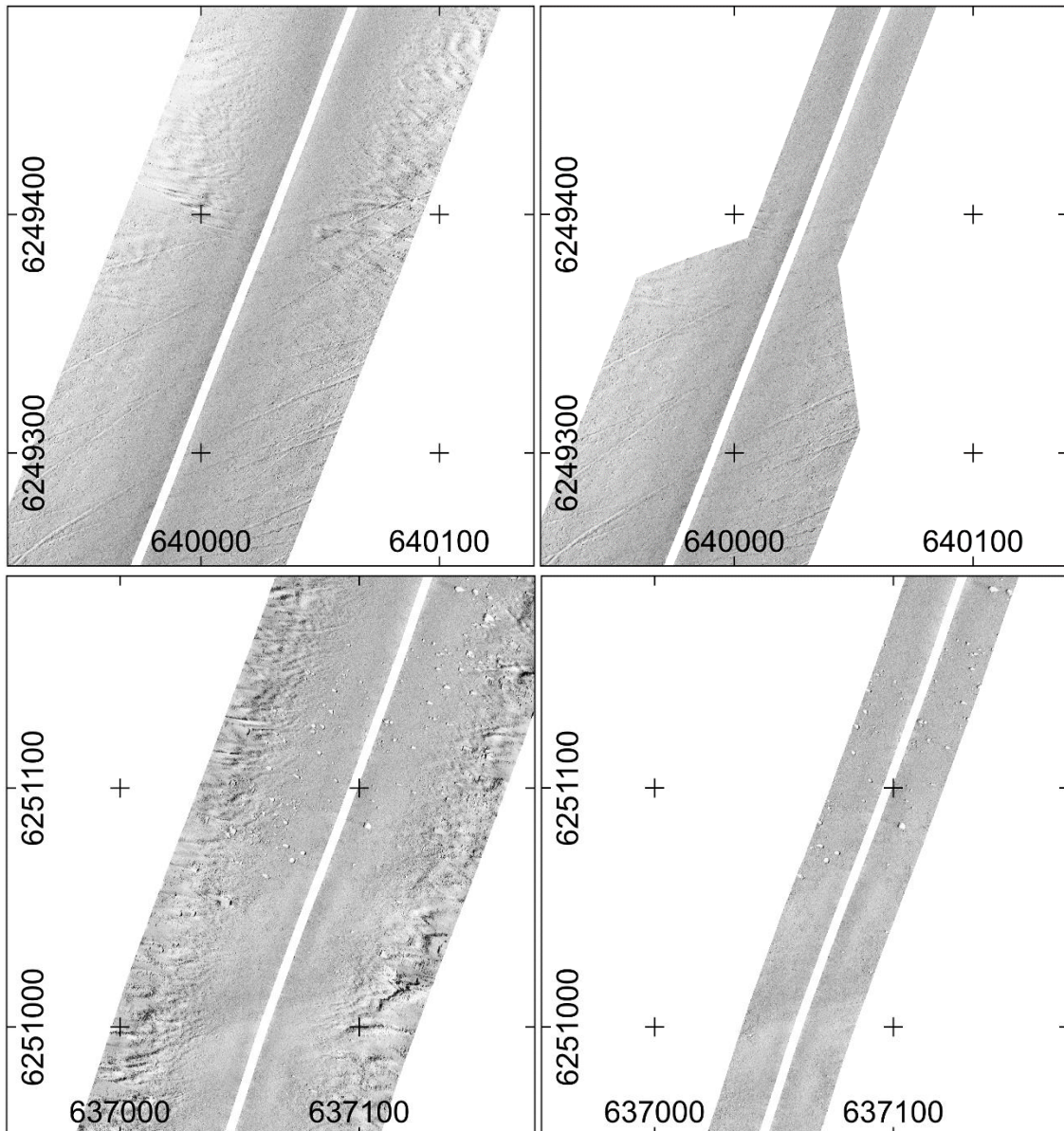


Figure 16: Pycnocline effect on the outer range of the SSS data (left) and trimmed-cleaned SSS data after Far field transparency function in SonarWiz (right)

An example of good SSS data quality is presented in Figure 17. The anchor details are clearly presented with good image definition.

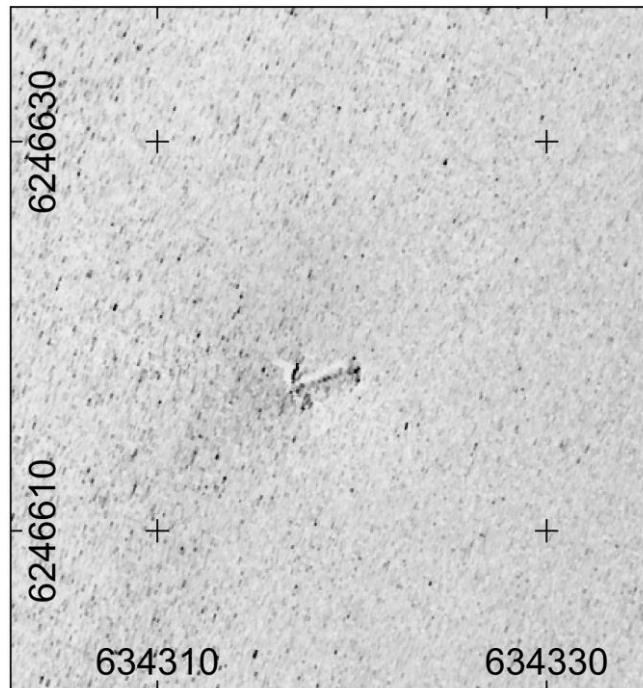


Figure 17: SSS data example KG_II_B02_SSS_GO5_0319 (MMO ID 413)

7.3 MAGNETOMETER

7.3.1 Data acquisition

The MAG system settings and Client specifications are listed in Table 30 and Table 31, respectively.

Table 30: MAG system settings

Geometrics G882	
Survey speed	Average 4 knots
Positioning	HiPAP 351 USBL
Fish altitude	2 to 3 m
Frequency	10 Hz

Table 31: MAG client specifications

Item	Client Specification	Achieved by survey
Seabed altitude	≤ 5 m	≤ 5 m
Measurement sensitivity	0.01 nT	0.01 nT
Sampling frequency	1-20 Hz (selectable)	10 Hz
Noise level	≤ 2 nT	≤ 2 nT

The magnetometer was towed behind the SSS in a “piggyback” configuration. The magnetometer data was collected, together with all analogue data, as a single pass.

7.3.2 Magnetometer data processing

The magnetometer data were processed using GeoSoft Oasis Montaj. The magnetometer processing steps used for the project are outlined in Table 32 to Table 38.

Table 32: Magnetometer navigation processing

Step 1	Magnetometer navigation processing
Backup of "CMP_Easting" and "CMP_Northing"	The raw easting and northing for the common mid-point (CMP), (<i>CMP_Easting</i> and <i>CMP_Northing</i>) of the Eiva Scan Fish were copied; all subsequent navigation processing were performed upon these copies.
De-spiking	Data windowed for survey site Non-linear filter applied, with a fiducial width of 5 (and tolerance of 1.5 m). The filter was used to remove small spikes present in the data.
Interpolation	Interpolation of the gaps created by removing the navigation spikes. This was done using a linear interpolation, for gaps over six fiducials (one more than the de-spike length).
Back up of smoothed navigation	The smoothed/interpolated/de-spiked data were backed up
Projection	Project projection is set
Distance	Calculates the total distance along the track for each fiducial.
Distance Separation	The distance between each fiducial is calculated. This was done by applying a convolution filter to the distance. The settings were -1, 1, 0. The results were written to the <i>Dist_QC</i> channel. This helped to monitor the frequency (10 Hz) of the magnetometer, it helped to spot any "freezes" in the data acquisition. It was compared to the magnetometer signal. Any large jumps in distance separation could have caused a spurious anomaly or missed data.
Comparison	The raw navigation, de-spiked navigation, smoothed navigation, the distance separation and magnetometer signal had their profile plotted together within Oasis Montaj. This allowed the quality control (QC) of the navigation and its processing. The database view plots these profiles against each other.

Table 33: Magnetometer altitude processing

Step 2	Magnetometer altitude processing
De-spiking	The raw altitude of each magnetometer was de-spiked. The filter stripped out any data spike that is above 10 m (or the value of the altitude cut-off defined during the EVT). This was done within Oasis Montaj using channel tools and channel mathematics.
Interpolation	The interpolation restored the gaps created by removing the altitude spikes. This was done using a linear interpolation, for gaps over ten fiducials (approximately 2 m).
Smoothing filters	A set of filter (low pass and B-spline) was applied to the de-spiked/interpolated altitudes to produce a smooth, more realistic values for altitude.
Alt cut-off	Clipped any data above 4 m and below 1.5 m
Clip X and Y with Alt masked	Clipped the position according to the altitude cut-off

Step 2	Magnetometer altitude processing
Copy Mask of interpolated altitudes to Easting and Northings	Not done at this step
Comparison	The raw altitudes, de-spiked, smoothed altitudes, averaged altitudes and smoothed average altitudes, the distance separation and magnetometer signal had their profile plotted together within Oasis Montaj. This allowed QC of the altitude and the processing.

Table 34: Magnetometer data QC

Step 3	Magnetometer data QC
De-spiking	A de-spiking filter was applied to the total magnetic TMF values.
Non-linear filtering	A non-linear filter was applied to attenuate any noise present in the data.
B-spline smoothing	A "B Spline" filter was applied to the non-linear filter. This helped to make the signal to appear more realistic (smooth).
Removal of data with poor magnetic signal	Any data with a magnetic signal strength below 200 was removed.
Copy Mask of interpolated TMF values and poor magnetic signal to Easting and Northings	The stripped magnetic data is used to mask the eastings and northings. The data gaps that are present in the interpolated TMI values were reintroduced by using these TMI values to mask the eastings and northings. This is done because original gaps may have been reduced due by the previous smoothing filters.
Comparison	All the processing steps for the TMI are plotted along with the magnetometer signal for QC.

Table 35: Magnetometer background calculation

Step 4	Magnetometer background calculation
Background	To obtain the background magnetometer signal, a series of non-linear filters were applied. These were as per GeoXYZ's procedures. An additional geological filter was produced by using a variation of filter parameters to attenuate magnetic anomalies.
B-Spline	A "B Spline" filter was applied to the final non-linear filters to smooth the result.
Compare	The final data were compared with the raw data to identify over or under filtering of the data.

Table 36: Magnetometer residual field calculation

Step 5	Magnetometer residual field calculation
Residual (Anomalies)	Filtered magnetometer data minus the background signal (anomaly and geology).
Residual (Geology)	An additional geological residual field was also calculated using an additional non-linear filter set.
Gridding	Data were gridded using Minimum Curvature with a Cell Size of 0.5 m and a blanking distance of 6 m. Coverage assessment for infills were based in dynamic coverage analysis.

Table 37: Magnetometer dynamic range calculation

Step 6	Magnetometer dynamic range calculation
Detection ranges	Detection ranges were calculated from a pre-survey equipment evaluation test (EVT)

Step 6	Magnetometer dynamic range calculation
Coverage plot	Coverage plots were created through use of proportional symbols within Oasis Montaj rather than blanking data to various distances. Dynamic coverage calculation: $C0 = 2 * (\sqrt{X.X^2 - (C1 + 1.5)^2})$ C0 = Dynamic Coverage X.X = Detection range depending on altimeter values. C1 = altitude 2 = the burial depth
Final grid blanking distance	Caution was required when selecting the final blanking distance, to ensure that the edge of survey results were not exaggerated.

Table 38: Magnetometer target picking

Step 7	Magnetometer target picking
Analytic Signal	AS grids were produced using a 0.5 m cell size, blanking distance set at 6 m.
Target picking	Anomalies greater than 5 nT peak to peak were picked. The background removal was checked to be optimal for target picking and the pick-to-pick measures are correct. Residual field was checked against total field to help determine anomalies.
De-duplication of targets	Compare targets with Altitude and Residual and TMI profiles. Targets were de-duplicated as required.
Target List	Magnetometer target list was compiled, as per client requirements

The general magnetometer processing workflow used in the project is outlined in Figure 18.

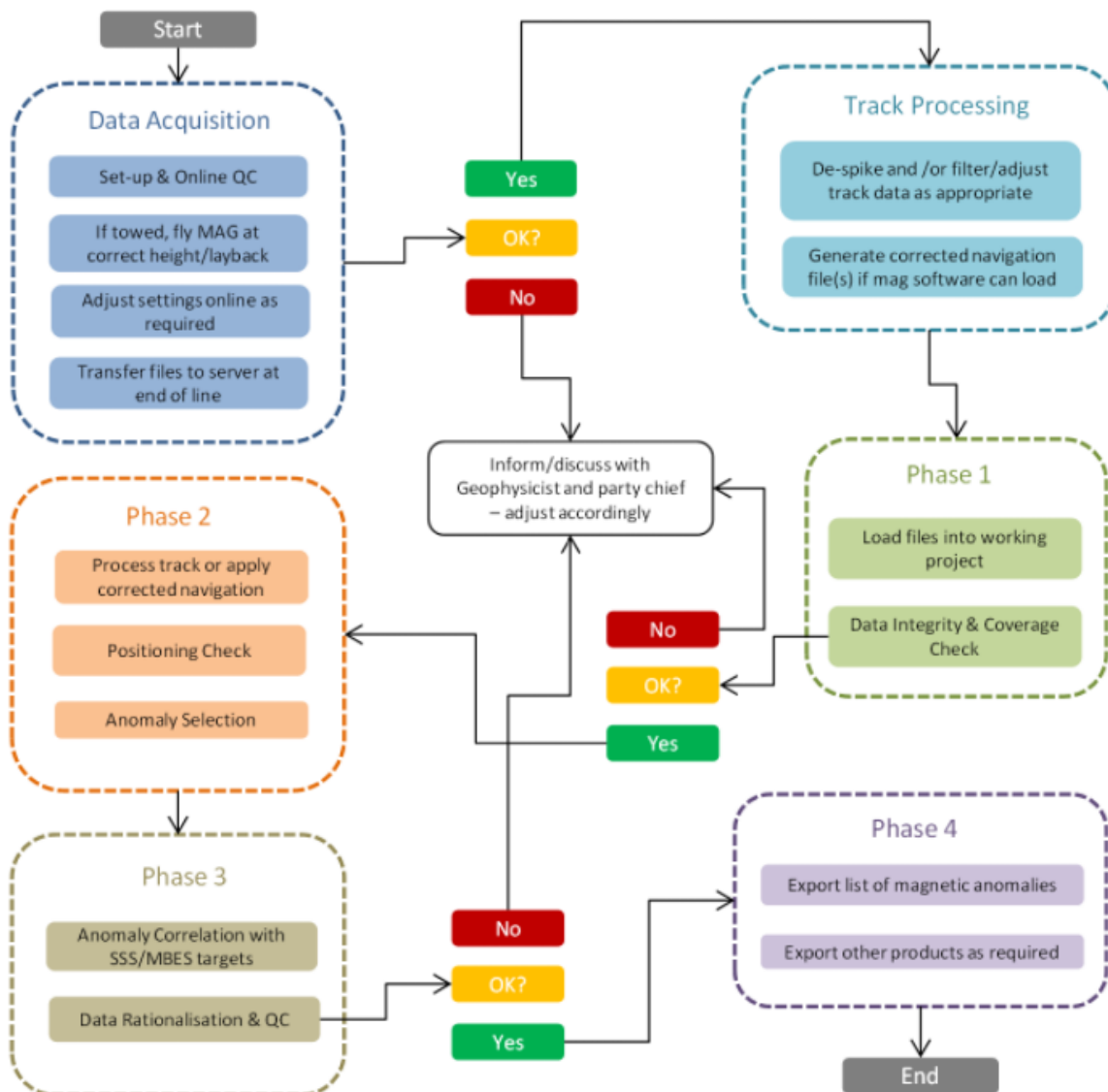


Figure 18: Magnetometer processing workflow

7.3.3 Data quality assessment

In general, data quality is good and meets the project requirements. A comparison between raw and filtered and smoothed altitude values is presented in Figure 19.

Spikes occur within the data of the total magnetic field (Figure 17). Spikes are overall more frequent for the altitude channel. Figure 18 presents an example of the comparison between raw and filtered and smoothed altitude values.

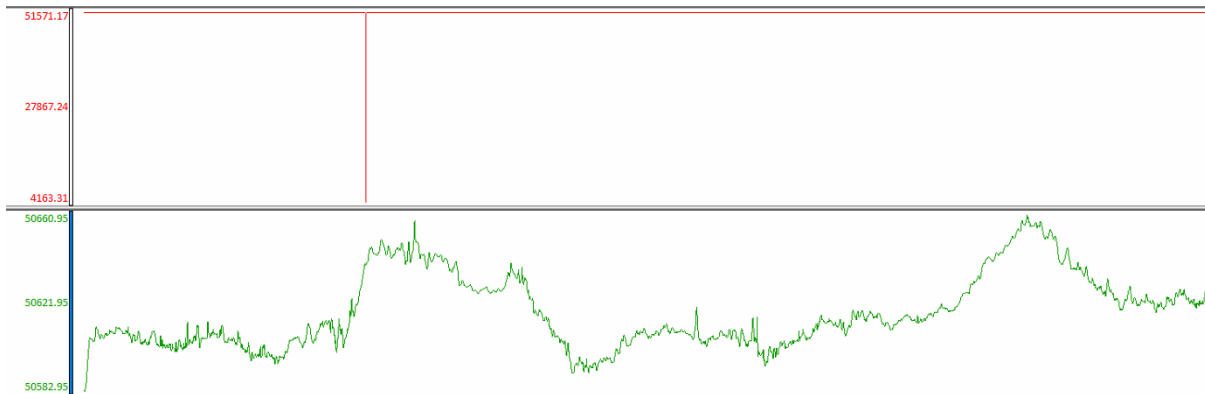


Figure 19: Data example within the Kattegat II area B04 (line 1424_- 5376_C_KG_GO5_L661V_-_MAG) with red profile showing the raw data and the green profile representing the filtered, de-spiked data

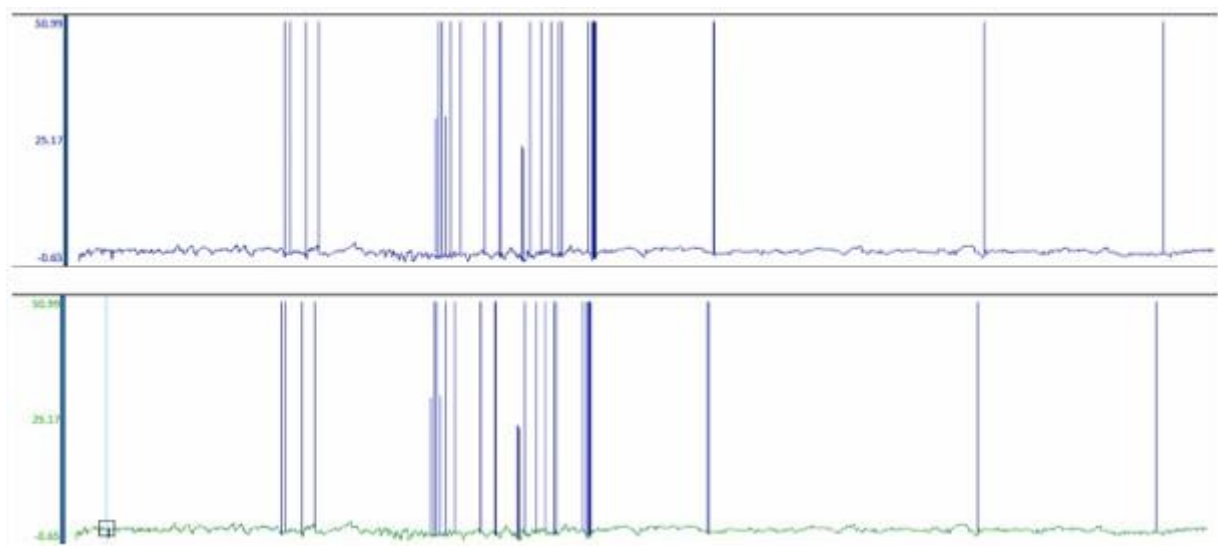


Figure 20: Data example within the Kattegat II area B04 (line 1537_- 5376_C_KG_GO5_1632V_-_MAG) where the blue profile and green profile are corresponding to the raw altitude values and the filtered altitude values, respectively

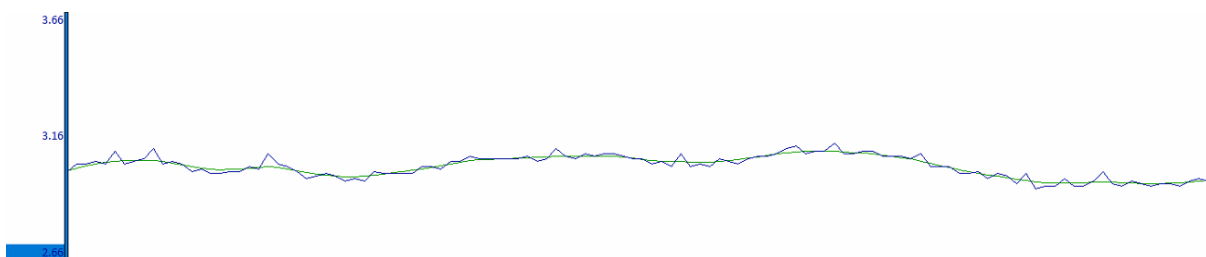


Figure 21: Data example showing comparison between the raw and filtered altitude values

A non-linear filter was used for de-spiking and smoothing was achieved using the B-Spline filter. Further processing then continued on the filtered data.

Easting and northing coordinates were de-spiked and smoothed as well. Figure 19 presents a data example showing smoothed easting and northing coordinates where no jumps or gaps are present. However, only few jumps or spikes were present in navigation. Where gaps were present due to navigation drop out, interpolation to 20 m was performed. Infill or replayed lines were included in the data to solve any jumps in navigation.



Figure 22: Data example in B02 (line 1262_-_5376_C_KG_GO5_L041V_-_MAG)

Based on final Easting and Northing coordinates residual was generated as well. An example is shown in Figure 20. The Residual was generated from the measured total magnetic field and calculated background. The background field was calculated using a series of non-linear filters. Based on this calculation, anomalies were highlighted.

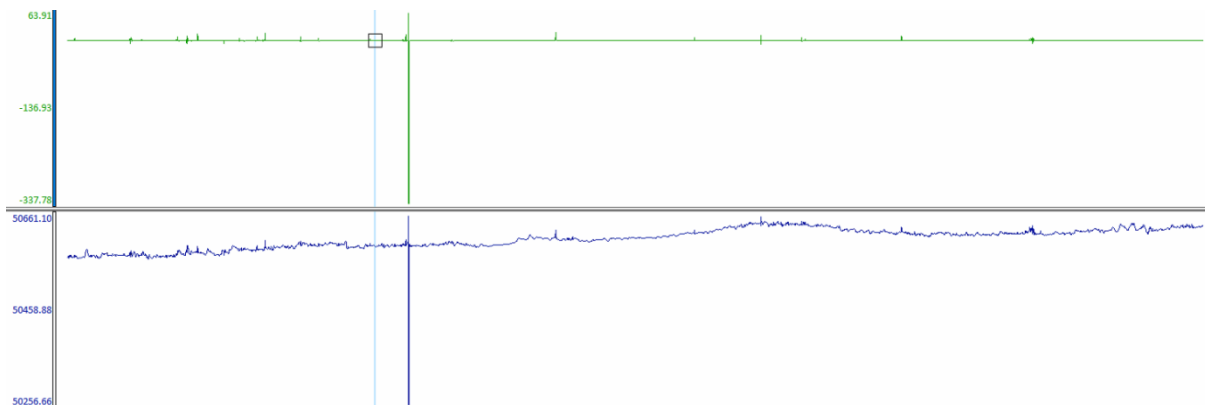


Figure 23: Data example from line 1542_-_5376_C_KG_GO5_1623V_-_MAG (green profile: residual signal; blue profile: total magnetic field)

Signal strength values were mostly above 1000 (Figure 21). Short drop out in signal strength values were present, yet, these were under acceptable values.

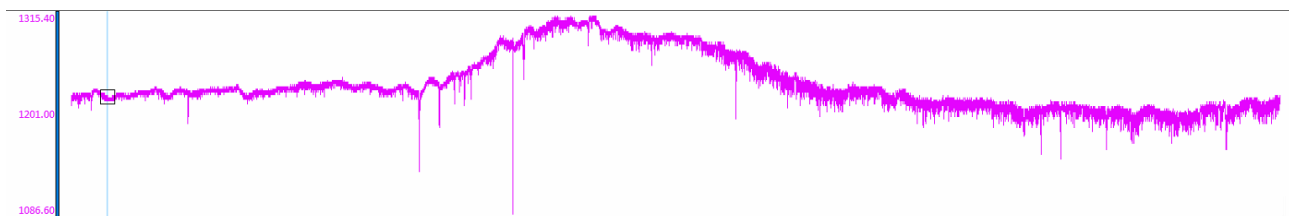


Figure 24: Data example of a signal strength profile (line 1542_-_5376_C_KG_GO5_1623V_-_MAG)

7.3.4 Magnetometer dataset profile example

An example profile for the MAG dataset, crossing the wreck in B07 (Target KT_B07_MAG_G06_0006) is presented in Figure 22 below:

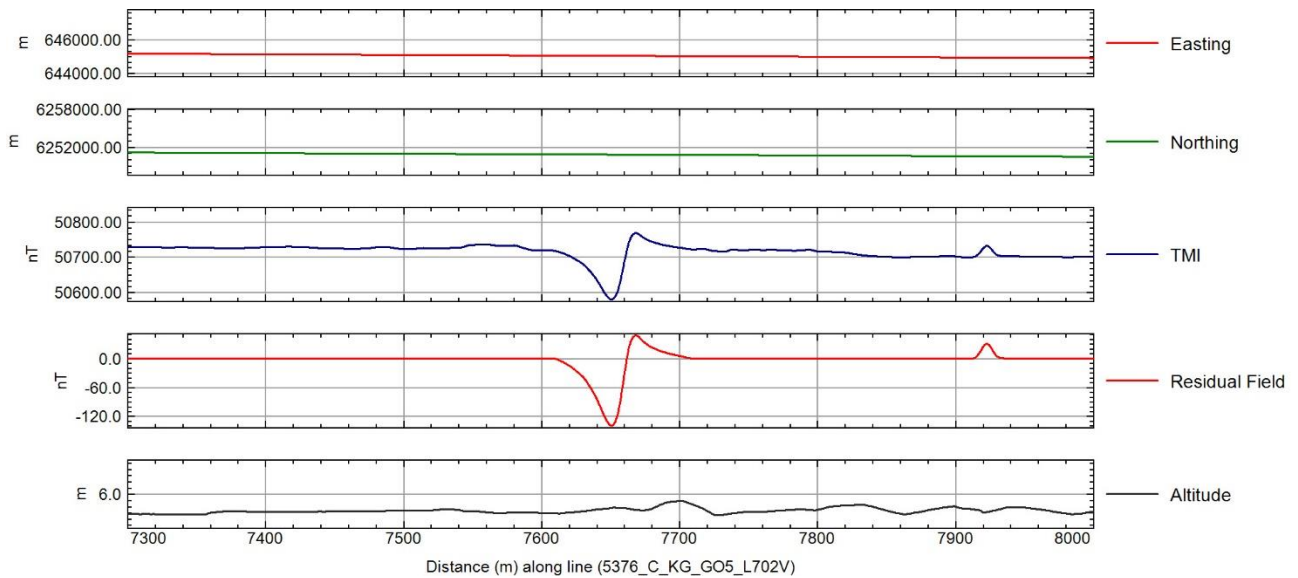


Figure 25: MAG profile example, line 5376_C_KG_G05_L702V, crossing a wreck

7.3.5 Magnetic residual anomaly grid

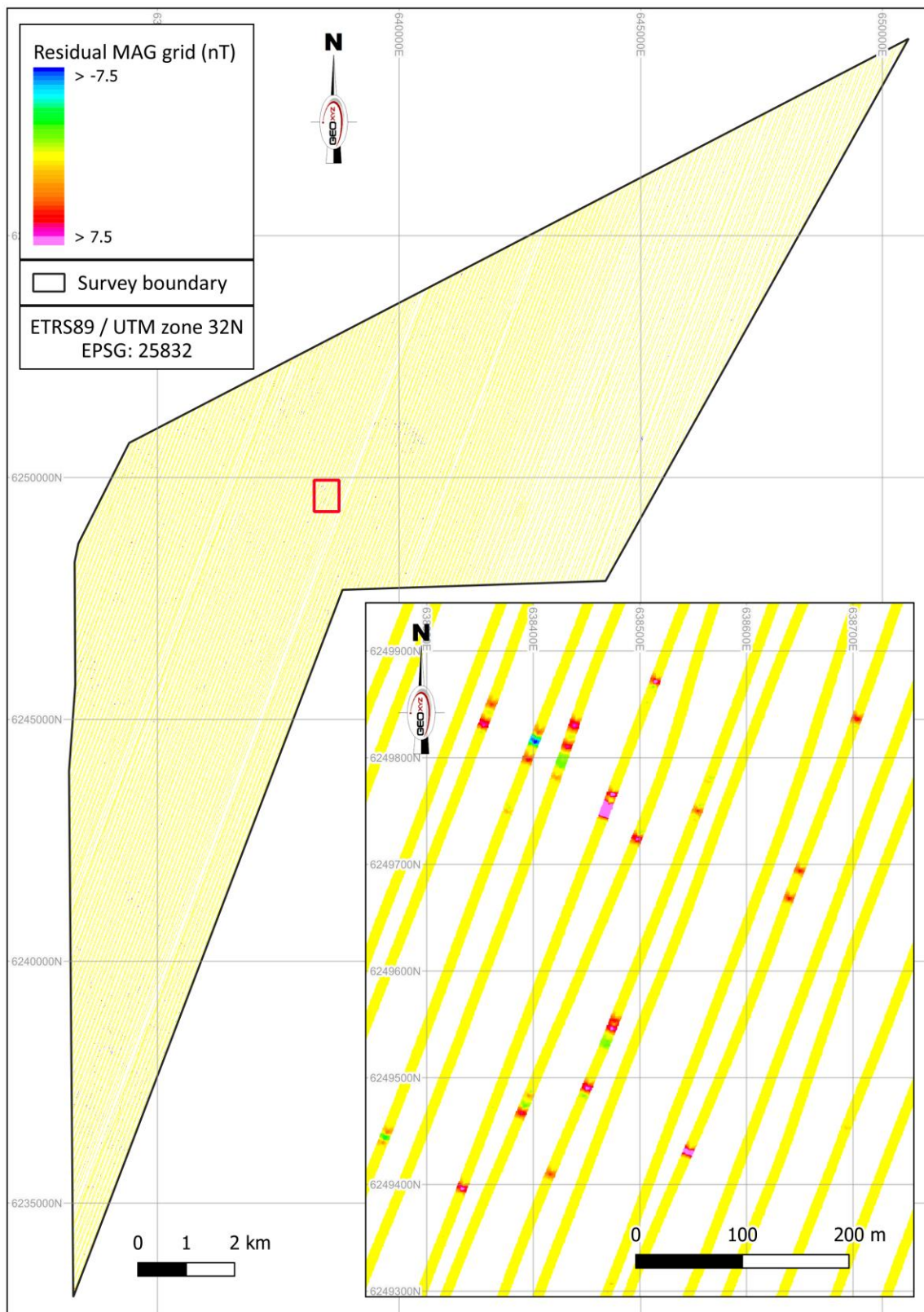


Figure 26: MAG residual anomaly grid across the survey site

7.3.6 Magnetic analytic anomaly grid

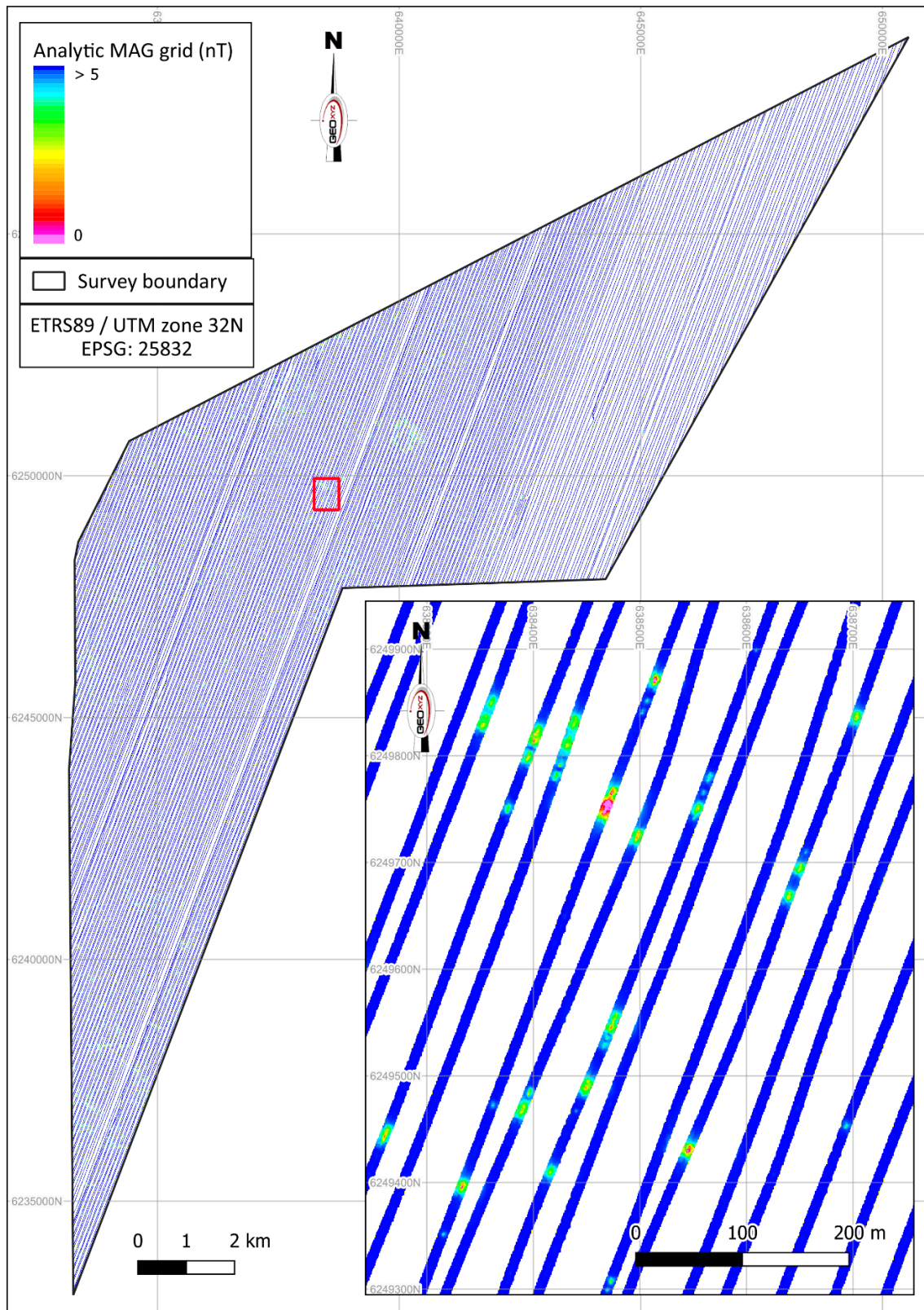


Figure 27: MAG analytic anomaly grid across the survey site

7.4 SUB-BOTTOM PROFILER

7.4.1 Data acquisition

Both vessels were mobilised with the Innomar SES-2000 Medium. The SBP system was recorded with the Innomar software and data tidally corrected using reduced GNSS height data recorded during acquisition. The client requirements for the SBP survey are outlined in Table 39.

Table 39: SBP acquisition and processing methodology

Item	Specification
Penetration	10 m
Vertical resolution	0.3 m
System	Innomar SES 2000 Standard

7.4.2 Data processing

Sub-bottom profiler (SBP) data were acquired using an Innomar SES 2000 Standard System and recorded using SESWIN recording software. SBP data processing and data QC was performed using Innomar ISE, Innomar SES Convert and Stema Silas software.

The main SBP processing steps used for the QC are outlined in Table 40.

Table 40: SBP data import and data QC

Steps	SBP data import and QC
Import of SEGYS	Import SEGY Tide file applied
Data Quality	Lines checked for: No empty pings Correct bottom detection No motion influence No noise in the data No artefacts in data Good reflector visibility Good penetration (5 m)
Position check	Lines checked for: Data coverage Verification of the absolute height by importing the MBES grid (no manual offset is accepted, after tide/heave correction applied online)

7.4.3 Data quality assessment

In terms of data quality/utility, the general standard is very good. In general, good imaging of the shallow geology is produced. The vertical resolution allows separation of surfaces ~0.15 m apart.

The picked horizons were gridded to 5 m lateral resolution using the IHS Kingdom Flex Gridding algorithm default settings. The final project datum depth grids were created from thickness horizons, which were then added to the MBES bathymetry. This was to remove the effect of any static miss-ties and to provide the best

gridded surface possible. Sub-bottom data and interpretations were depth converted using a velocity of 1600 m/s.

An SBP data example for the Kattegat II site, showing penetration to approximately 15 m Below Seabed (BSB) and clear differentiation between the units is presented in Figure 25 below.

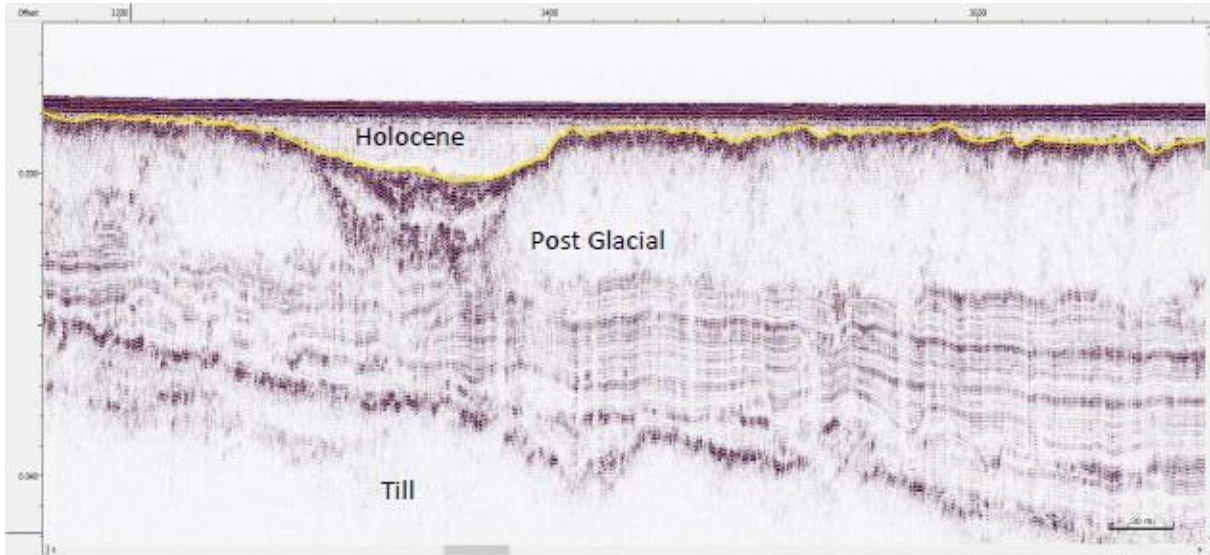


Figure 28: SBP data example in the Kattegat II site

The high resolution and narrow beam angle make the sensor worse for boulder detection as the qualities of the instrument all results in reduced diffractions. The SBP data do show evidence for boulders at the seabed where there is till at, or close to, outcrop. However, sub seabed evidence is ambiguous but there are probably boulders present (Figure 26).

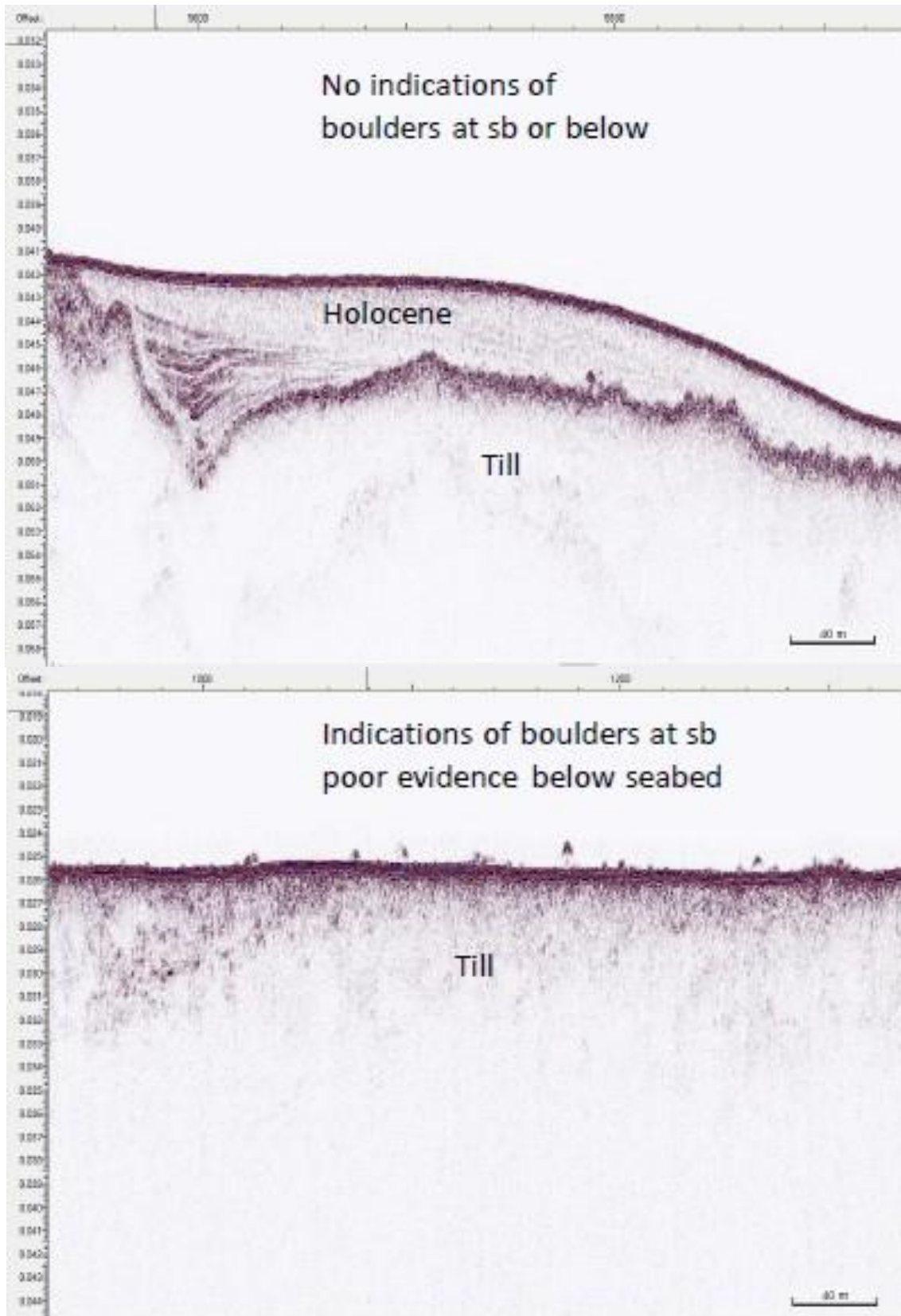


Figure 29: SBP data examples

In order to assess the frequency of sub-seabed boulder distribution (up to a depth of 10 m BSB), a stratigraphic approach was adapted based on careful calibration of the likelihood of boulders in each unit (the Holocene, the post-glacial, and till units). The Holocene unit only shows very rare indications of boulders and was factored as 1. The post-glacial unit, which shows slightly more numerous indications was factored as 3. Finally, till shows much more numerous boulder indications and was factored as 8. Eventually, the thickness of each unit in metres was multiplied by the boulder factor to obtain the likelihood of boulders.

The depth grids show some very minor artefacts (<0.2 m) related to busts between adjacent lines. These artefacts are primarily caused by the high density of survey lines and slight variations in horizon picking between these lines.

The depth grids show some very minor artefacts (<0.2 m) related to busts between adjacent lines. These artefacts are primarily caused by the high density of survey lines and slight variations in horizon picking between these lines.

7.5 2D UHR SEISMIC

7.5.1 Data acquisition

The client requirements for the UHR seismic survey are outlined in Table 41. A horizontal tow configuration (with the head and tail at 1 m water depth) was employed. This configuration was tested during the verification phase at the start of the project and adjusted to determine the optimal consideration to vertical resolution and weather dependency of survey operations. Sparker and streamer components were towed inline to optimise launch and recovery activities and line turns.

Table 41: UHR acquisition specifications

Item	Client specification
Fundamental frequency	Between 1 and 3 kHz
Vertical resolution	0.3 m at seabed (weather dependant)
Minimum Penetration	100 m
Fire rate	2 pulses/second
Feather angle	<12° during 95 % of the shots
Variable energy levels	Between 100 and 1000 Joules
System	A suitable multi-channel and multi-element hydrophone streamer, with depth control, plus depth measurement for continuous monitoring and recording of streamer depth

7.5.2 Data processing

A horizontal tow configuration (with the head and tail at 1 m water depth) was employed. This configuration was tested during the verification phase at the start of the project and adjusted to determine the optimal consideration to vertical resolution and weather dependency of survey operations. Sparker and streamer components were towed inline to optimise launch and recovery activities and line turns. The processing workflow applied to the datasets for Kattegat II is outlined in detail within APPENDIX A.

7.5.3 Data quality assessment

The multichannel seismic data are of good quality and resolve primary reflections to greater than 100 m below seabed. There are minor variations in signal phase in some of the lines and occasional missed shots. These faults have a negligible effect on interpretation. The most significant imaging problem is related to the shallow gas, which is distributed over a large proportion of the northern and central parts of the area. This blanks out the signal and gives rise to reverberations at the period between the seabed and the gas. The latter is not due to an error in processing or acquisition, but is due to the physical properties of the gas and the geophysical limitations of a pressure wave. A $7\mu\text{B}$ threshold became applicable, after a 20Hz low-cut filter was applied at the QC stage.

The data allow separate mapping of reflections ~ 0.5 m apart. The data were depth converted using stacking velocities and a time grid of the top bedrock. The interpretation was depth converted using a velocity of 1600 m/s to Unit II (Late Glacial), 1800 m/s was applied to Unit III (Glacial).

A UHR data example is presented in Figure 27.

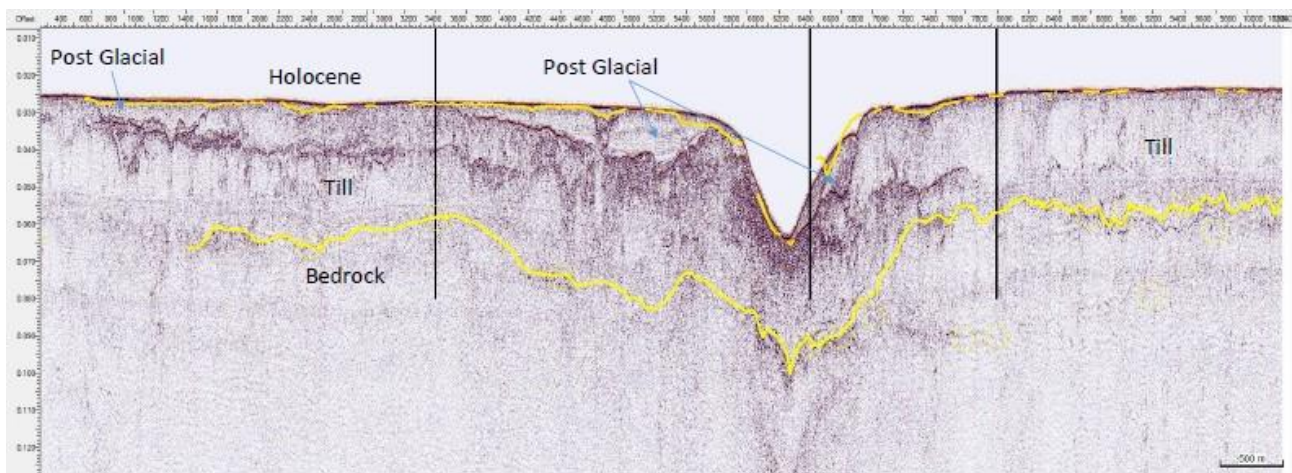


Figure 30: UHR data example within the Kattegat II site

7.6 SEABED SAMPLING

The geotechnical ground-truthing phase of the survey was conducted, in order to provide initial surface sediment classifications and establish baseline physico-chemical parameters at specific locations across the site.

A total of forty sampling stations were proposed by the onboard senior Marine Environmental Scientist and grab samples were collected at each of these stations. Samples were successfully acquired at thirty-eight of the proposed forty stations. Samples could not be acquired at stations KG_II_14 and KG_II_34, due to coarse sediment conditions. Samples acquired at station KG_II_025 were obtained from an attempt with a recovery volume of $<40\%$; however, this were deemed to be of sufficient volume and of representative sediment type, to justify retainment for analysis. A full suite of physico-chemical samples (PC1 and PC2) were obtained at all of the other stations.

One full suite of physico-chemical samples was acquired at each of the stations, using a 0.1 m^2 dual van Veen grab sampler or a 0.1 m^2 mini Hamon grab.

A basic suite of Physico-Chemical (PC) samples, comprising a single primary (PC1) and single secondary (PC2) were acquired at each location. Particle Size Analysis (PSA), Total Organic Matter (TOM) and Carbonate Content (CC) components were sub-sampled ex-situ once sent to the benthic laboratory. PSA1, TOM1 and CC1 were subsampled from the primary (PC) sample and PSA2, TOM2 and CC" were extracted from the secondary (PC2) sample, as required.

Any conspicuous benthic macrofauna and species of potential conservation value were noted.

Figure 28 below indicates the proposed grab sampling positions across the Kattegat II site.

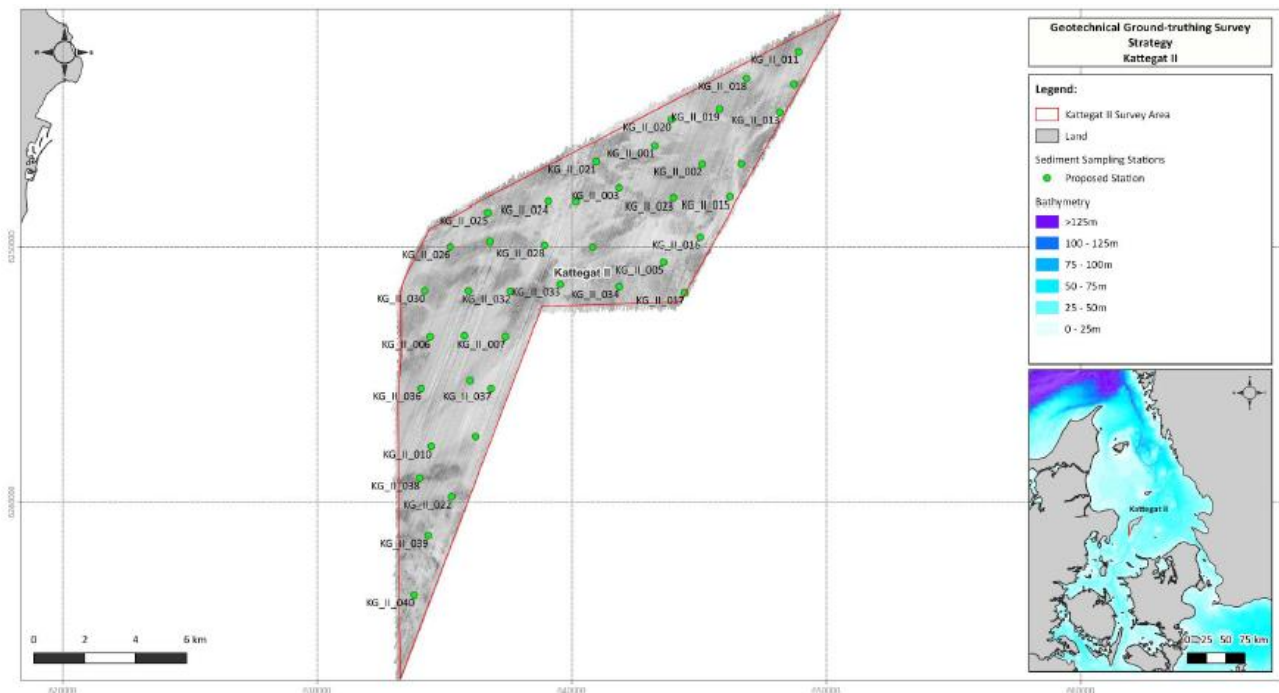


Figure 31: Proposed surficial geotechnical ground-truthing sampling locations within Kattegat II area

The full results of the geotechnical ground-truthing at the Kattegat II site can be found in APPENDIX B of this report: *Danish Offshore Wind Lot 1, Kattegat II: Surficial Geotechnical Ground-Truthing Data Report, prepared on behalf of GEOxyz, by Ocean Sciences Consulting (OSC).*

8 RESULTS AND INTERPRETATION

8.1 CLASSIFICATION CRITERIA

8.1.1 Slope classification criteria

Seabed gradient has been classified as per Table 42 below.

Table 42: Slope classification

Classification	Slope
Very Gentle	< 1°
Gentle	1° - 5°
Moderate	5° - 10°
Steep	10° - 15°
Very Steep	> 15°

8.2 BATHYMETRY

Seabed levels across the Kattegat II site range from a minimum of 15.5 m MSL, in the central, eastern of the site near 643930 mE, 6248470 mN, to a maximum of 48.6 m MSL near 640875 mE, 6249495 mN, within the central section of a meandering, 750 – 1650 m wide channel feature, which runs from north-east to south-west across much of the area.

An overview of the bathymetry within the Kattegat survey area is shown in Figure 32; bathymetry profiles for several line plan segments in the northern part of the area are shown in Figure 30; and a detailed bathymetric overview of the northern part of the survey area, especially the wide channel feature, is shown in Figure 31.

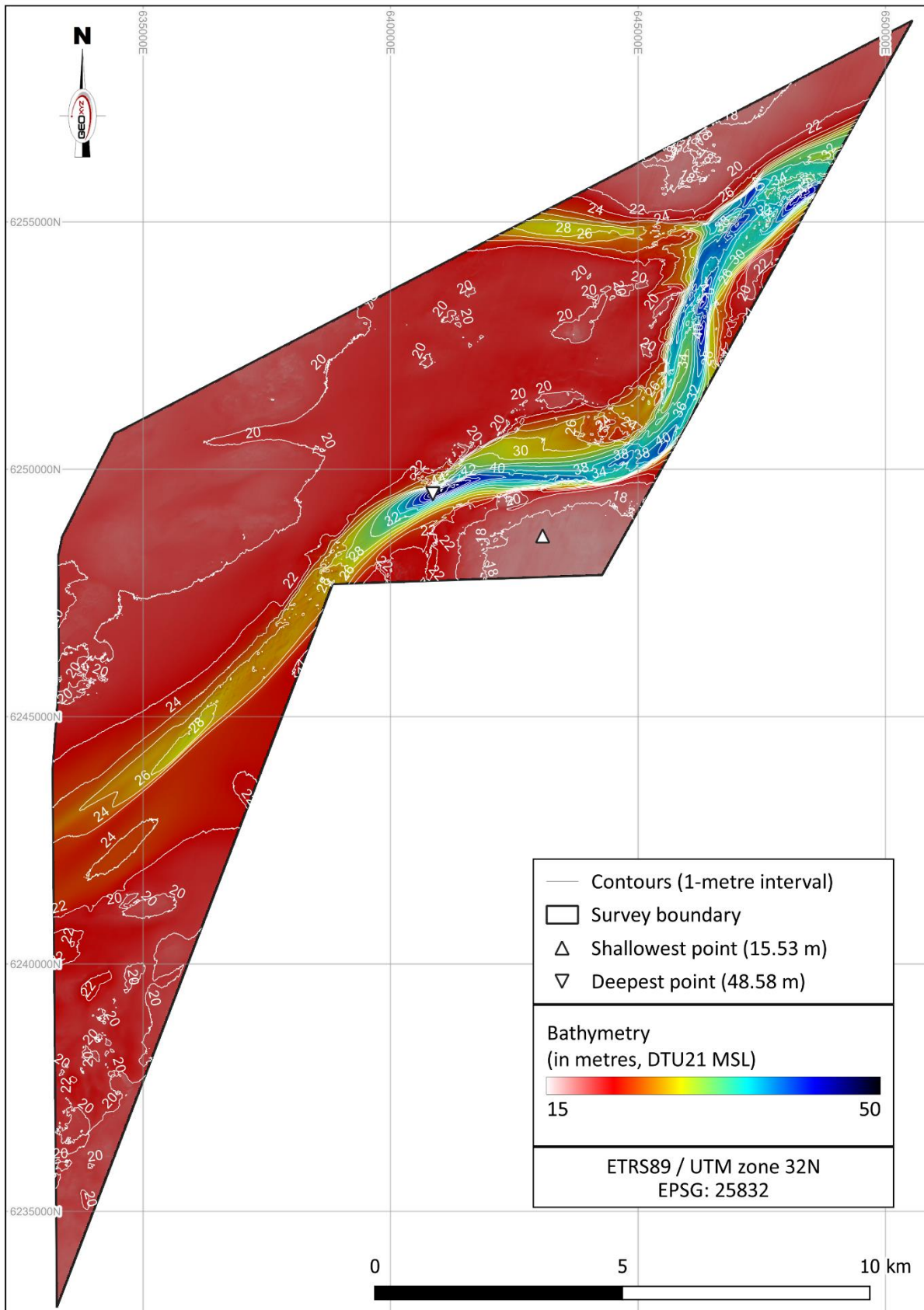


Figure 32: Bathymetry across Kattegat II area

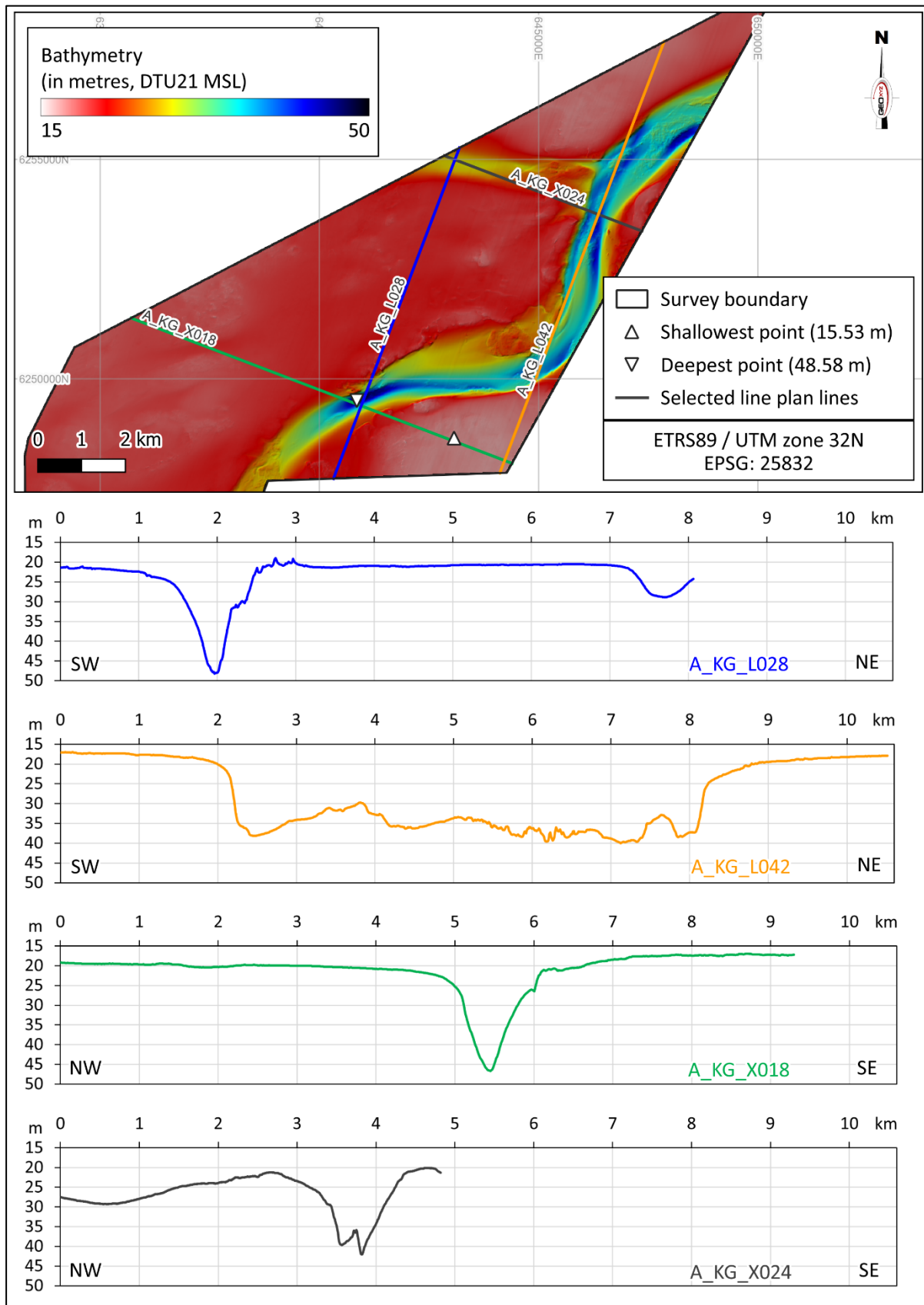


Figure 33: Bathymetry profiles based on selected line plan segments in the north of the survey area

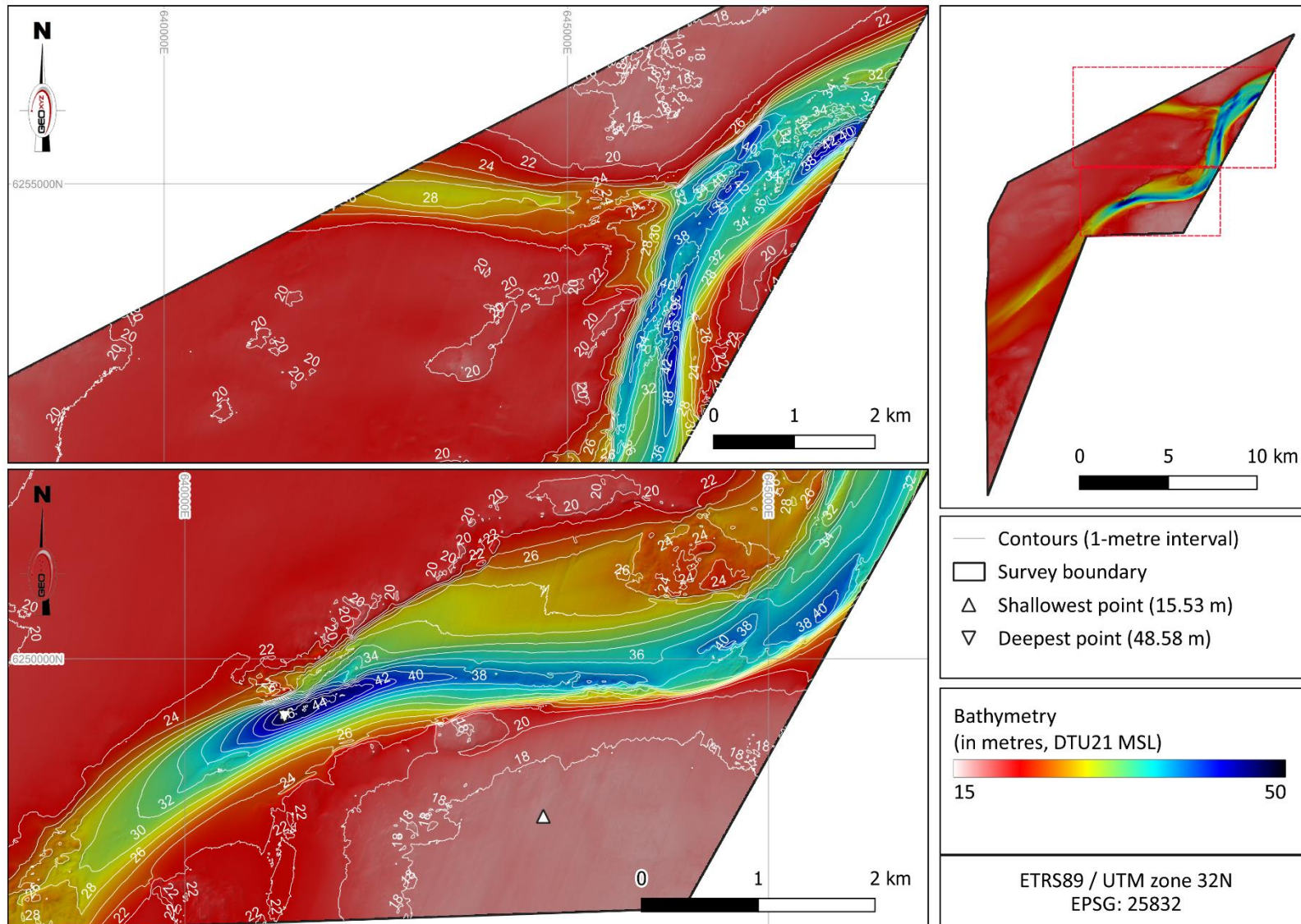


Figure 34: Detailed overview of bathymetry in the north of the survey area

A meandering, 750 – 1650 m wide channel feature crosses much of the site, approximately delineated by the 23.0 m MSL contours (Figure 33 and Figure 31). This feature runs approximately north-east to south-west. Seabed levels within this channel feature range from approximately 23.0 m MSL to depths of up to 48.6 m MSL, near 640875 mE, 6249495 mN, within the central, northern section of the Kattegat II site.

Steep side slopes, with localised slope gradients of between 5.0° and 20.0°, are present along the northern and southern slopes of this channel feature (Figure 35). Within the northern part of the channel, the seabed is very uneven, with a series of narrower channels separated by narrow ridges of sediments, which stand up to 9.0 m shallower than the localised surrounding seabed.

A smaller, associated channel feature spurs off towards the west, in the northern section of the site (first and fourth profile in Figure 33 and top chartlet in Figure 31). This feature runs approximately east to west and is between 1000 m and 1400 m wide, with depths up to 29.0 m MSL. Maximum side slopes of up to 3.0° are present.

Elsewhere across the site, to the north-west of the major channel feature, seabed levels are relatively flat, lying between 19.0 m MSL and 22.0 m MSL.

To the south-east of the major channel feature, seabed levels are generally relatively flat, mainly ranging from 19.0 m MSL to 24.0 m MSL. The only exception to this is a broad area of seabed in the central, eastern section of the site, where seabed levels are almost completely flat, lying between 17.0 m and 18.0 m MSL (bottom chartlet in Figure 31).

The highest slope values (very steep slopes; >15°) are associated with seabed features such as boulders (Figure 36) and on the sides of the broad channel, ridges and smaller elevated features (as seen on various locations shown in Figure 35).

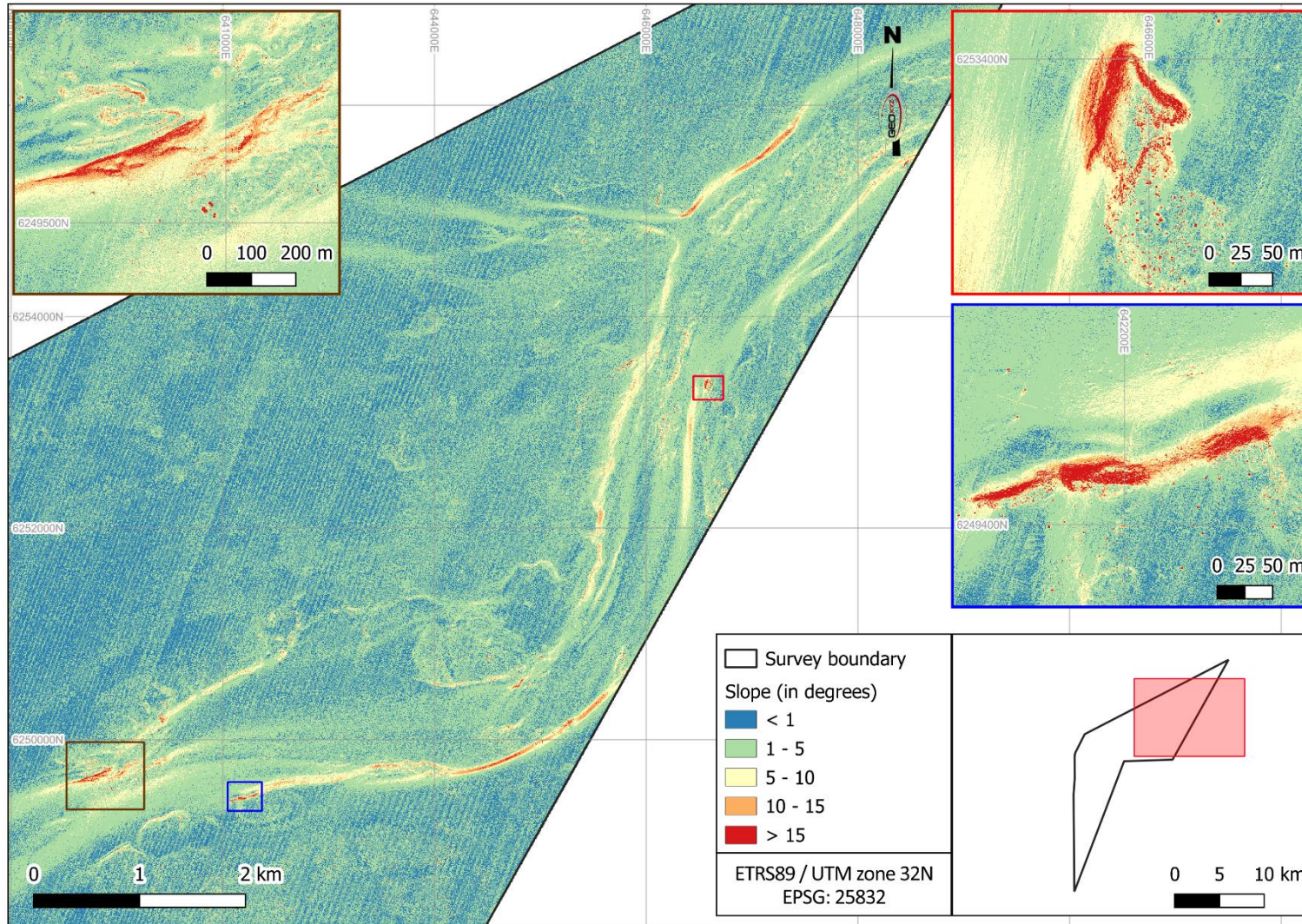


Figure 35: Slope map of the north of the survey area

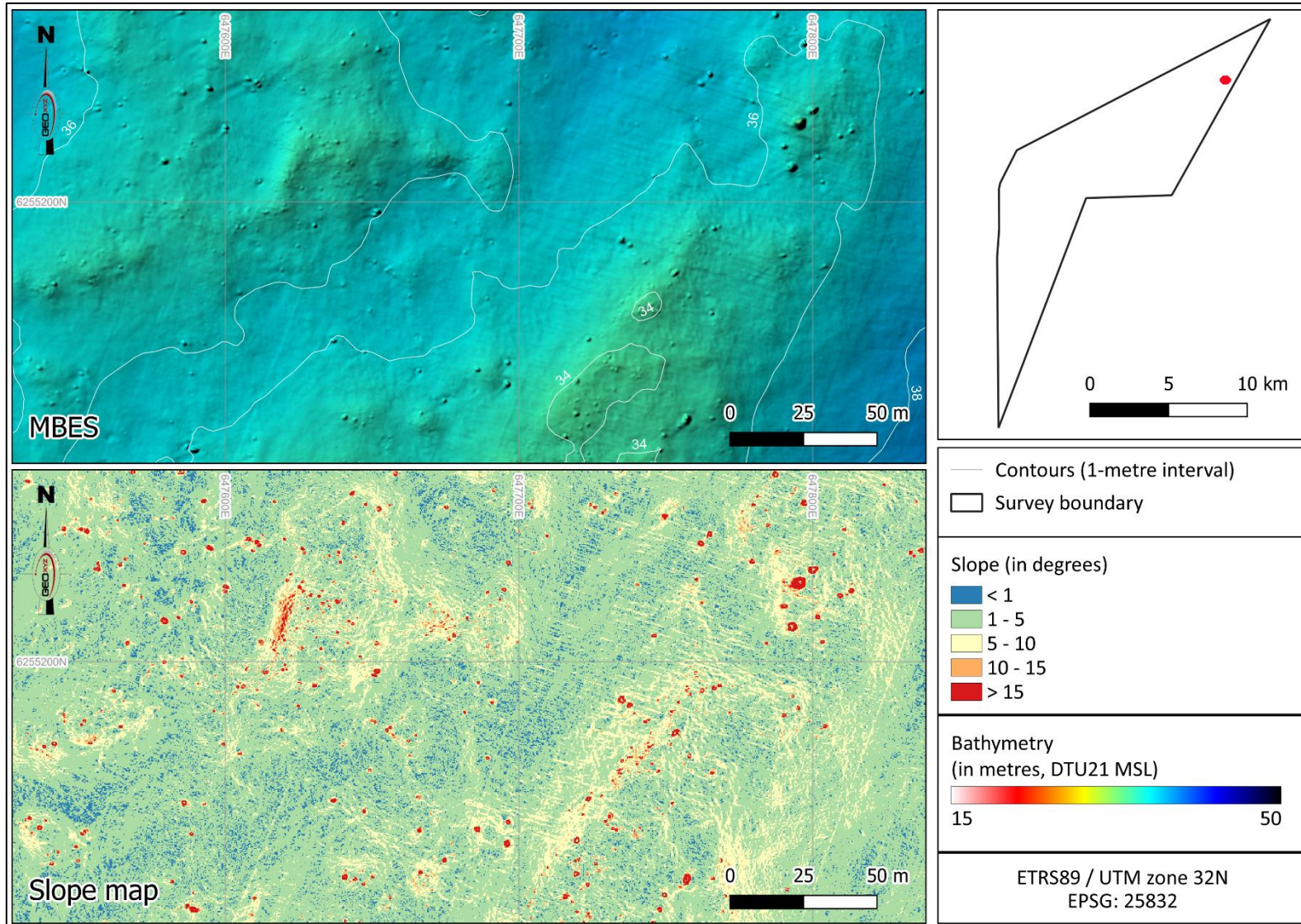
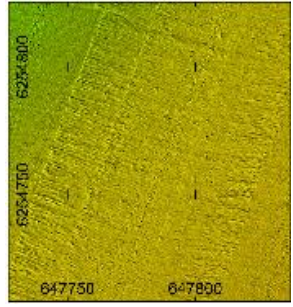
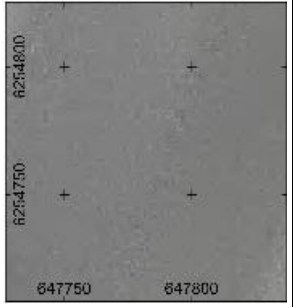
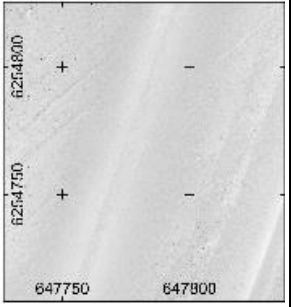
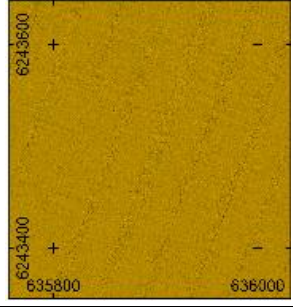
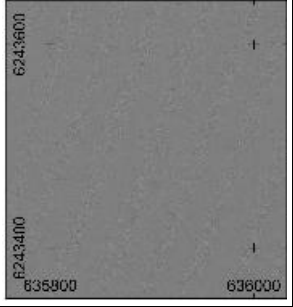
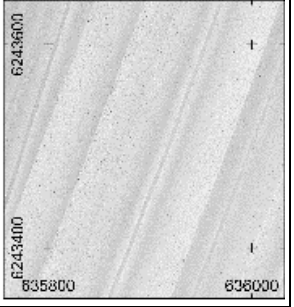
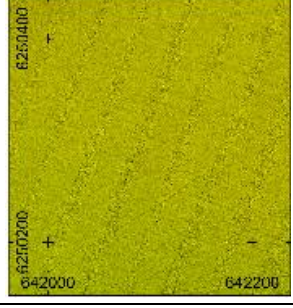
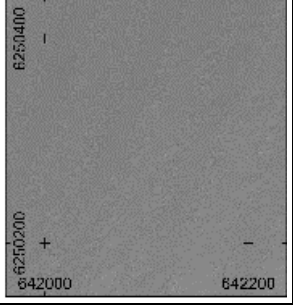
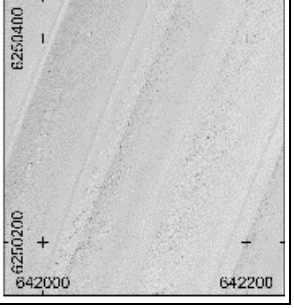


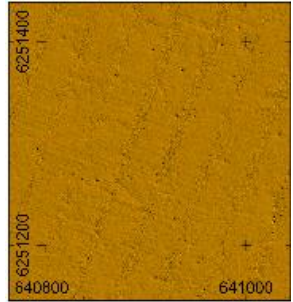
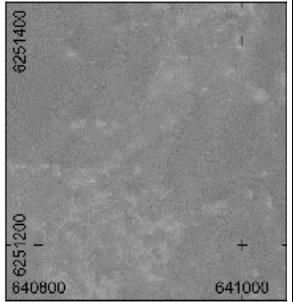
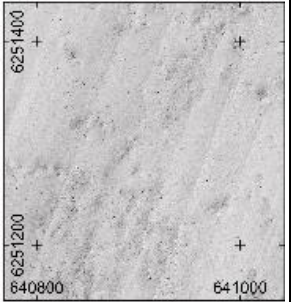
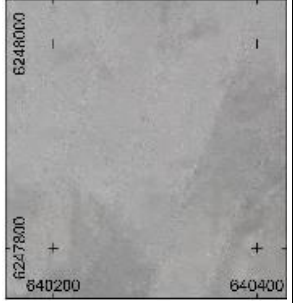
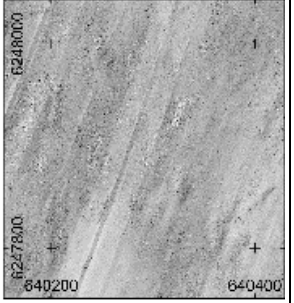
Figure 36: Bathymetry and slope map of a boulder field in the northeastern part of the survey area

8.3 SEABED SURFACE CLASSIFICATION: GEOLOGY

The seabed geology for the Kattegat II site was evaluated from the interpretation of the low and high frequency SSS data, the backscatter imagery and the MBES dataset. Data analysis and classification was performed using the seabed acoustic characteristics, such as reflectivity and backscatter strength, as well as the seafloor relief and the overall pattern. During the interpretation of the backscatter data, higher reflectivity areas – higher intensity sonar returns (darker grey to black colours) have been related to relatively coarse-grained sediments and lower reflectivity areas – lower intensity sonar returns were related to relatively fine-grained sediments (Table 43). GEUS terminology was used to define the identified seafloor sediment across the Kattegat II site.

Table 43: Geological interpretation

Geological interpretation	Colour and code	Sediment interpretation	Acoustic Description (Backscatter)	MBES image	Backscatter image	LF SSS image
Mud and sandy mud	21	Predominately mud with minor to significant fractions of sand. May contain minor fractions of or gravel	Low reflectivity			
Muddy sand	13	Predominately sand with significant fractions of mud and muddy sand. May contain minor fractions of or gravel	Low to medium reflectivity			
Sand	12	Predominately sand and. May contain minor fractions of mud and/or gravel	Medium reflectivity			

Geological interpretation	Colour and code	Sediment interpretation	Acoustic Description (Backscatter)	MBES image	Backscatter image	LF SSS image
Gravel and coarse sand	11	Mixed sediment. Predominately gravel and sand. May contain mud.	Medium to High reflectivity. Patches of high reflectivity interspersed in areas of low to medium reflectivity			
Till/diamicton	41	Mixed sediment. Constituents range between mud and boulders.	Low to High reflectivity. Patches of high reflectivity interspersed with areas of low to medium reflectivity. Usually, positive relief in MBES data			

Bathymetric data aided the interpretation mainly in outlining of possible outcrops and the boulder field delineation.

The resultant seabed surface geology has been correlated to the soil description of the surficial grab samples and the onshore laboratory results. For the grab sample analysis, the definition of the particle sizes followed the Wentworth scale (Figure 37).

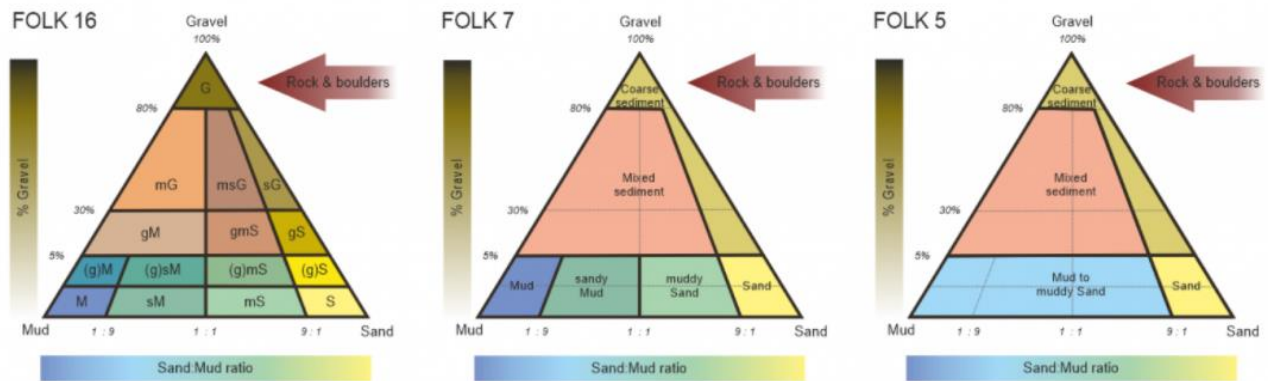
Major Grade	Phi (Φ) limits		Wentworth size class
	Lower	Upper	
gravel	<-8	-8	boulder
	-8	-6	cobble
	-6	-2	pebble
	-2	-1	granule
sand	-1	0	very coarse sand
	0	1	coarse sand
	1	2	medium sand
	2	3	fine sand
	3	4	very fine sand
mud	4	5	coarse silt
	5	6	medium silt
	6	7	fine silt
	7	8	very fine silt
	8	>8	clay

Scale by Wentworth (1922) classifying sediment particles according to the diameter expressed in units of N (phi, the negative log 2 of the diameter in millimeters).

Figure 37: Wentworth Scale – classifying sediment particles

Therefore, for the needs of correlation, the results have been further processed and reclassified, according to the Folk 7 classification system (Figure 38). For sand, muddy sand, and mud and muddy sand seafloor sediment classes, there is a direct correlation to the Folk 7 classification. Gravel and coarse sand, and Till/diamicton sediment classes have been correlated to mixed sediment grab samples and for their separation, reflectivity, relief and sub-surficial geology have been considered.

EMODnet Folk substrate classification



FOLK, 16 classes	FOLK, 7 classes	FOLK, 5 classes
Rock & Boulders	Rock & Boulders	Rock & Boulders
Gravel - G sandy Gravel - sG gravelly Sand - gS	Coarse sediment	Coarse sediment (Gravel >= 80% or (Gravel >= 5% and Sand >=90%))
muddy Gravel - mG muddy sandy Gravel - msG gravelly Mud - gM gravelly muddy Sand - gmS	Mixed sediment	Mixed sediment (Mud 95-10%; Sand < 90%; Gravel >= 5%)
(gravelly) Mud - (g)M Mud - M	Mud (Mud >= 90%; Sand < 10%; Gravel < 5%)	Mud to muddy Sand (Mud 100-10%; Sand < 90%; Gravel < 5%)
(gravelly) sandy Mud - (g)sM sandy Mud - sM	sandy Mud (Mud 50-90%; Sand 10-50%; Gravel < 5%)	
(gravelly) muddy Sand - (g)mS muddy Sand - mS	muddy Sand (Mud 10-50%; Sand 50-90%; Gravel < 5%)	
(gravelly) Sand - (g)S Sand	Sand (Mud < 10%; Sand >= 90%; Gravel < 5%)	Sand

Figure 38: EMODNET Folk substrate classification

Finally, seafloor sediment classification has been integrated to the sub-seabed geology data. The seabed geology across the Kattegat II area is presented in Figure 39.



Figure 39: Seabed surface geology classification

The surface geology across the Kattegat II area is relatively complex, with extensive, irregular areas of Till/Diamicton covering much of the northern/north-eastern half of the site (Figure 40), partially covered by areas of sands and/or areas of gravels and coarse sands, with finer grained, muddy sands (silty/clayey sands) becoming more prevalent towards the south and west. Muddy sand is predominant in Kattegat II. A curved area of outcropping Quaternary clay and silt is present within the eastern section of the meandering channel feature, which runs across much of the northern section of the site.

The seabed across the central, western section of the site (Figure 41) comprises mainly of an expanse of muddy sands (silty/clayey sands), with occasional, irregular areas of sands and/or areas of gravels and coarse sands.

Smaller, less extensive areas of Till/Diamicton are also present in the southern/south-western section of the site (Figure 42), together with several small areas of sands and a larger, irregular area of gravels and coarse sands.

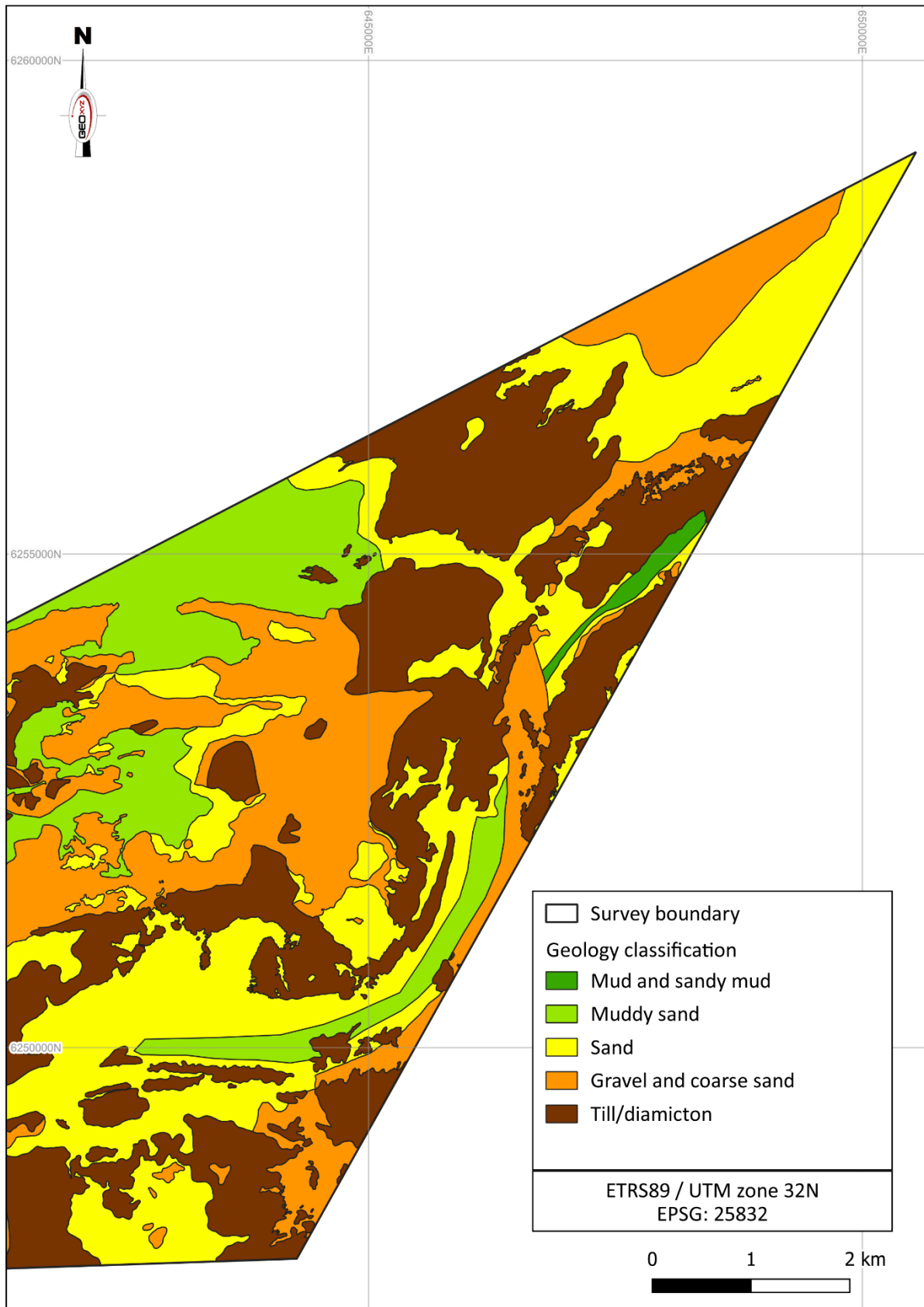


Figure 40: Seabed surface classification: Seabed geology across the northern/north-eastern section of Kattegat II

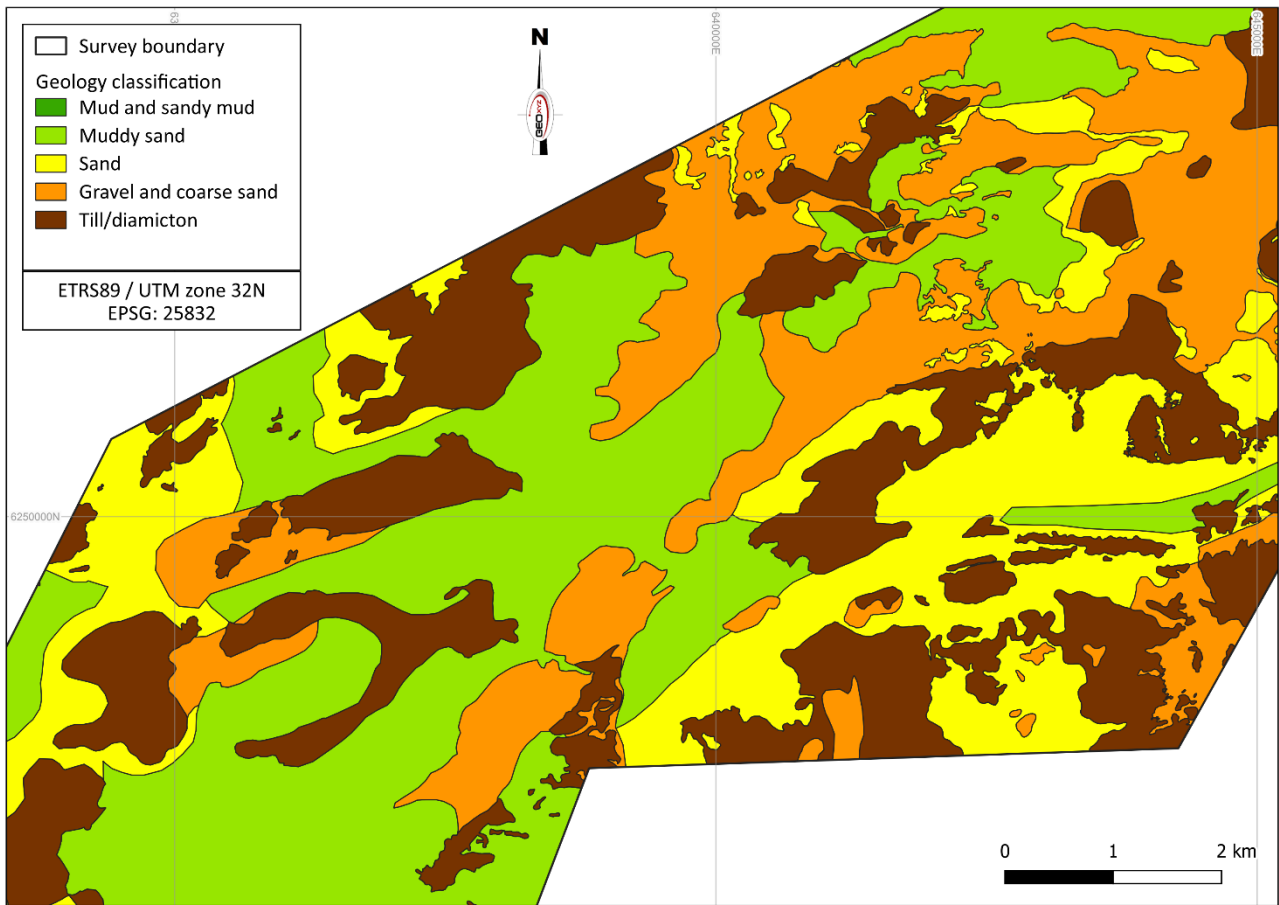


Figure 41: Seabed surface classification: Seabed geology across central section of Kattegat II

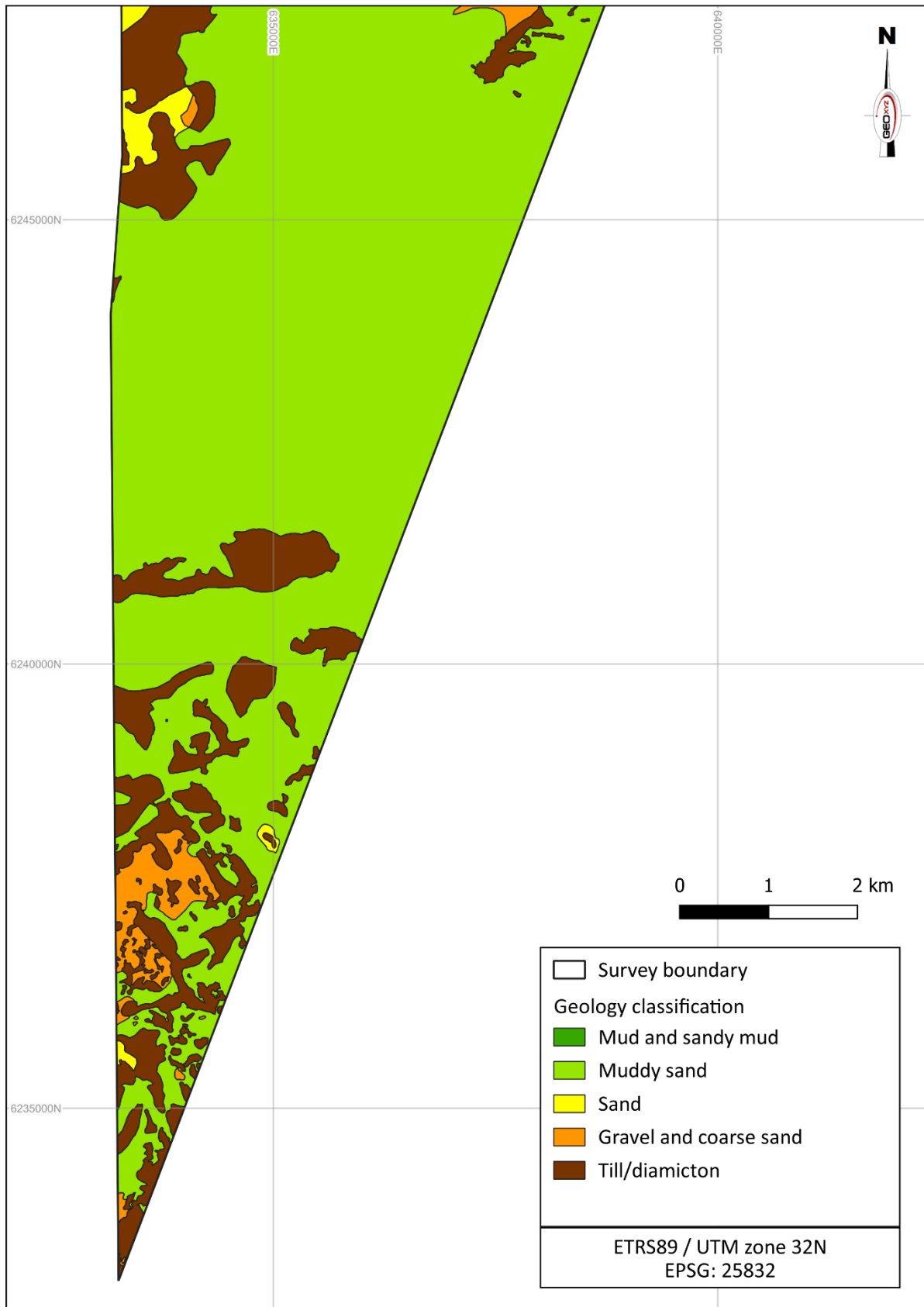
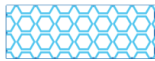
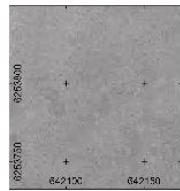
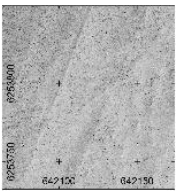
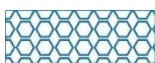
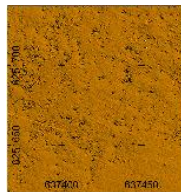
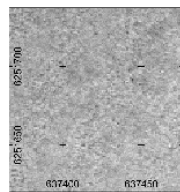
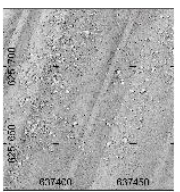
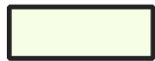
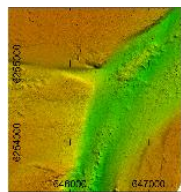
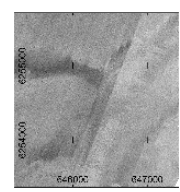
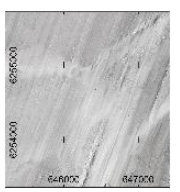
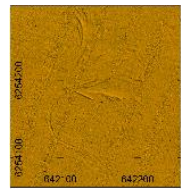
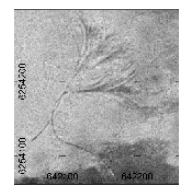
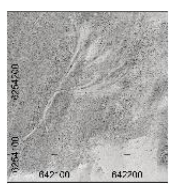
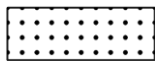
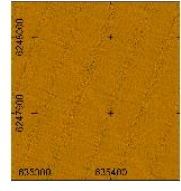
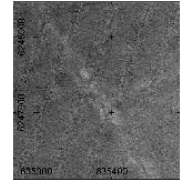
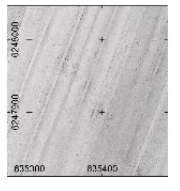
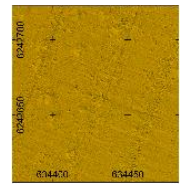
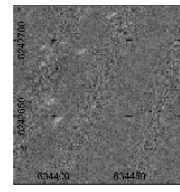
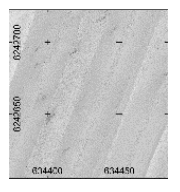


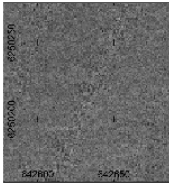
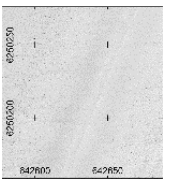
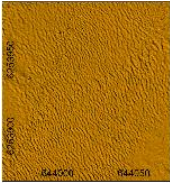
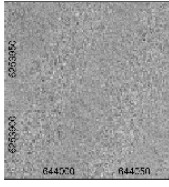
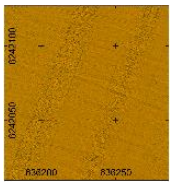
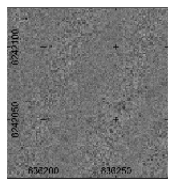
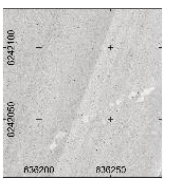
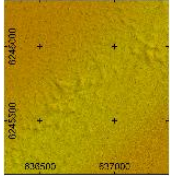
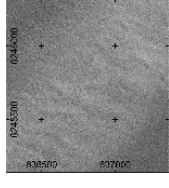
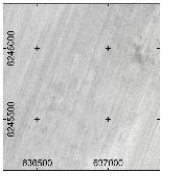
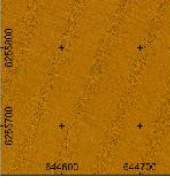
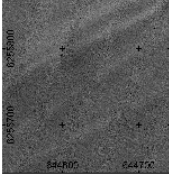
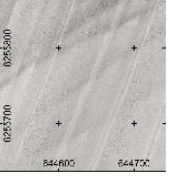
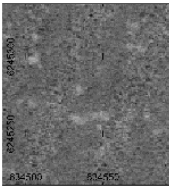
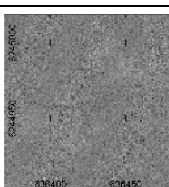
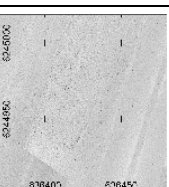
Figure 42: Seabed surface classification: Seabed geology across southern section of Kattegat II

8.4 SEABED SURFACE CLASSIFICATION: MORPHOLOGY

Seafloor morphology and seabed feature descriptions were based on the interpretation of SSS, BKS and MBES datasets, whereas the results from the SBP have been considered. The acoustic characteristics of the interpreted seabed features across the Kattegat II site are summarized in Table 46. Various morphological seabed features of different dimensions were identified in the Kattegat II site seafloor. Some of them are the result of a variable geological environment and past and present hydrodynamic conditions within the regime of sea level fluctuations (e.g. Areas of boulders, Ripples, etc.), whereas others have anthropogenic origin (e.g. Trawl marks).

Table 44: Morphological interpretation

Seabed Feature	Symbology	Description	MBES image	Backscatter image	SSS image
Boulder Field – intermediate density (Class 1)		High reflectivity contacts of intermediate density (40 to 80 boulders in a 100x100 box), visible in MBES			
Boulder Field – high density (Class 2)		High reflectivity contacts of high density (more than 80 boulders in a 100x100 box), visible in MBES			
Channel		Low to medium reflectivity, distinguishable in BKS, visible in MBES			
Other – Scour pattern		Low to medium reflectivity linear scars forming a pattern, visible in MBES			
Other – Seabed scars		Low to medium reflectivity linear scars, visible in MBES. (Mapped as polygons, as well as linear features)			
Other – Possible depressions		Medium to high reflectivity circular objects, visible in MBES			

Seabed Feature	Symbology	Description	MBES image	Backscatter image	SSS image
Trawl marks		Low to medium reflectivity linear features, visible in MBES			
Ripples		Low to high reflectivity alternating areas. Not clear in MBES. Wavelength (0.5 – 2.0 m) is the primary classifier			
Unknown – Patches of low reflectivity		Low reflectivity irregular patches, distinguishable only in SSS.			
Unknown – Possible bedforms		Low to medium reflectivity alternating areas, visible in MBES			
Unknown – Possible bedforms or possible erosional features		Low to medium reflectivity alternating areas, hardly visible in MBES			
Unknown – Possible coarse grain sediment accumulation OR benthic habitat		High reflectivity irregular patches, visible in MBES			
Unknown – Possibly three linearly aligned small seabed mounds		Low to medium reflectivity circular objects, unclear in SSS, visible in MBES			

The resulting seabed surface morphology interpretation is presented in Figure 43. A detailed overview of the northern part of the area is shown in Figure 44; the central part of the survey area in Figure 45, and the southern part of the area, in Figure 46.

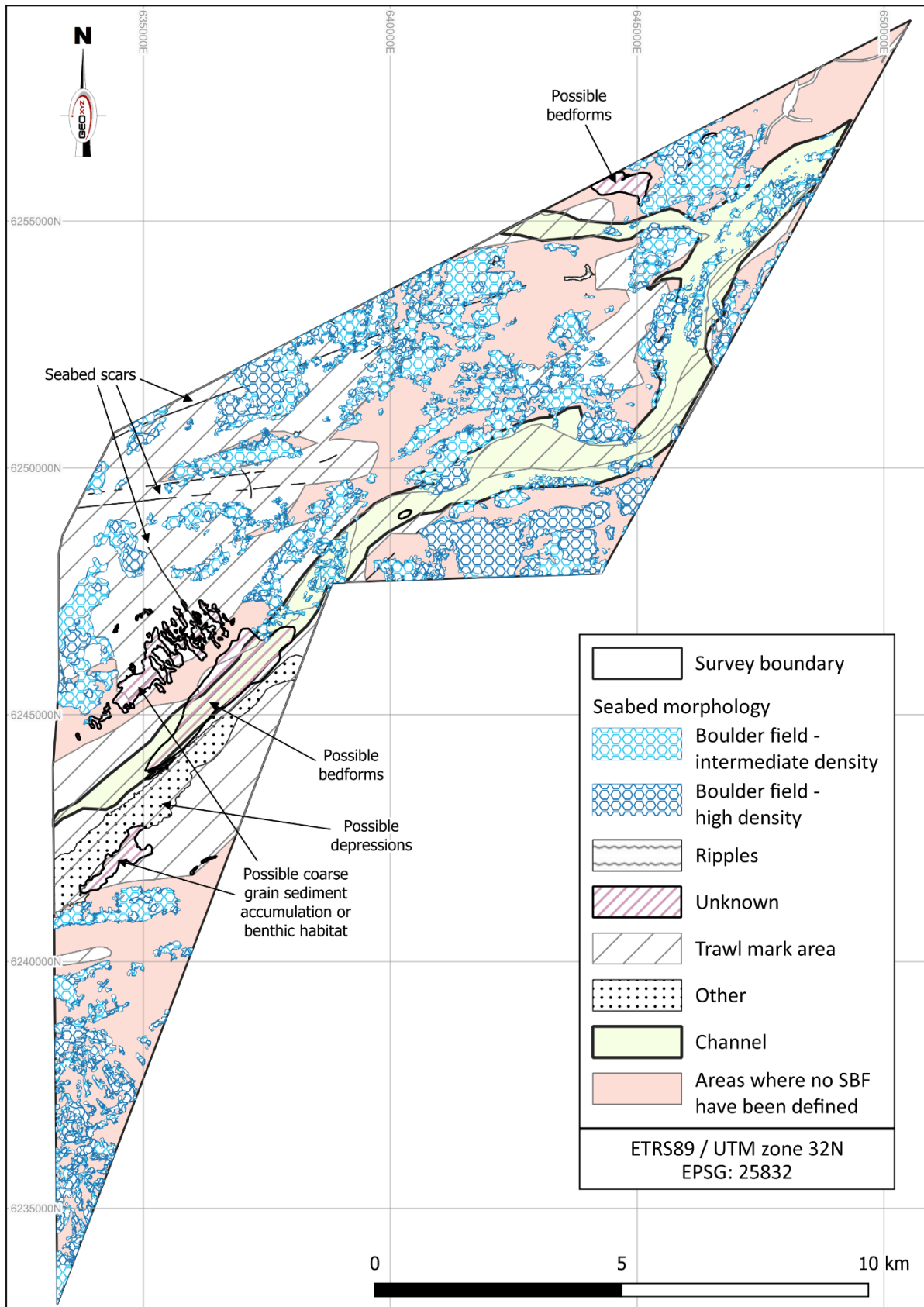


Figure 43: Seabed morphology classification

A meandering, 750 – 1650 m wide channel feature crosses much of the site (Figure 44 to Figure 46). This feature runs approximately north-east to south-west across most of the northern and central sections. In the northern section, the channel is deep and distinct, whereas it gets shallower and less clear in the southern section. The channel feature is bounded to the north-west and south-east, by frequent boulder fields, with extensive trawls scarring also noted. Some localised areas of indistinct bedforms are present. Scattered trawl marks of different orientations can also be noted in the central and northern part of the survey area (Figure 44 and Figure 45).

Alternating zones of low to medium reflectivity are present on the SSS data set, centred within a small part of the channel and more extensively in the southern section of the site. These are clearly visible in the backscatter data, as well as in the MBES data, where they show positive relief, generally less than 1 m, with a tentative NW -SE direction. They may be interpreted as bedforms, possibly related to channel bottom currents. Alternatively, the Holocene (Unit I) thickness in parts of those areas, suggests sub-cropping/outcropping of Unit II (Figure 58). The surficial sediment is 'Muddy sand' in the extended southern area, cross-correlated to the adjacent grab samples (KG_II_008_GR and KG_II_007_GR) and 'Gravel and coarse sand' in the smaller northern part. The interpretation of those features is uncertain.

Four seabed scour patterns are present in the northern and eastern parts of the site (Figure 43). These possibly relate to the dragging of a large object. During the survey, no such object was identified. They are possibly related to fishing activities.

Seabed scars are also noted, mainly in the north-western as well as in the central part of the site. These scars are orientated in SW-NE, NW-SE and SW-NE directions. The most extended one is found in the north-western part of the site, crossing more than half of the area, with a length of approximately 9000 m (Figure 44).

In the northern part of the site, three elongated areas of alternating low to medium reflectivity are seen, over a sandy substrate, near or within the Till/diamicton sediment (Figure 43). They have approximately 0.1 m difference in elevation and they show predominately SW-NE orientation. They could be interpreted as possible bedforms, although their external geometry is rather straight to be current-related. Alternatively, they could be interpreted as possible ice-related erosional features and a seabed expression of the H05 erosional surface, considering that the Unit I - Holocene sediments are very thin or absent in those parts. The interpretation of those features is uncertain.

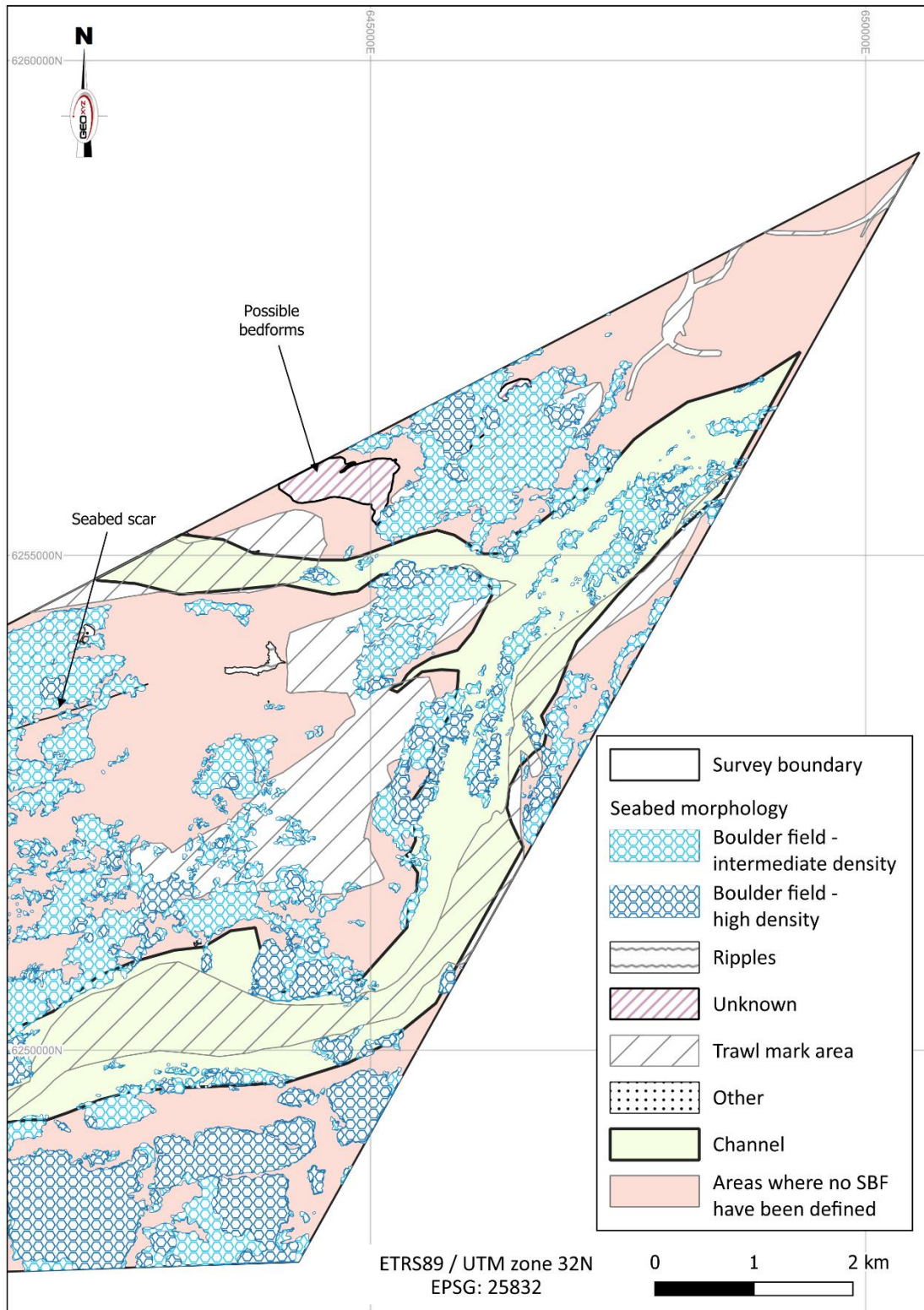


Figure 44: Seabed morphology classification: Morphology across northern section of Kattegat II

A smaller, associated channel feature spurs off towards the west. This feature runs approximately east to west and is between 1000 m and 1400 m wide. It is bounded to the north and south by areas of boulder fields, with numerous trawl scars noted.

A minor area of ripples is present in the north-eastern part of the site (Figure 44). Their wavelengths vary between 0.5 and 2.0 m.

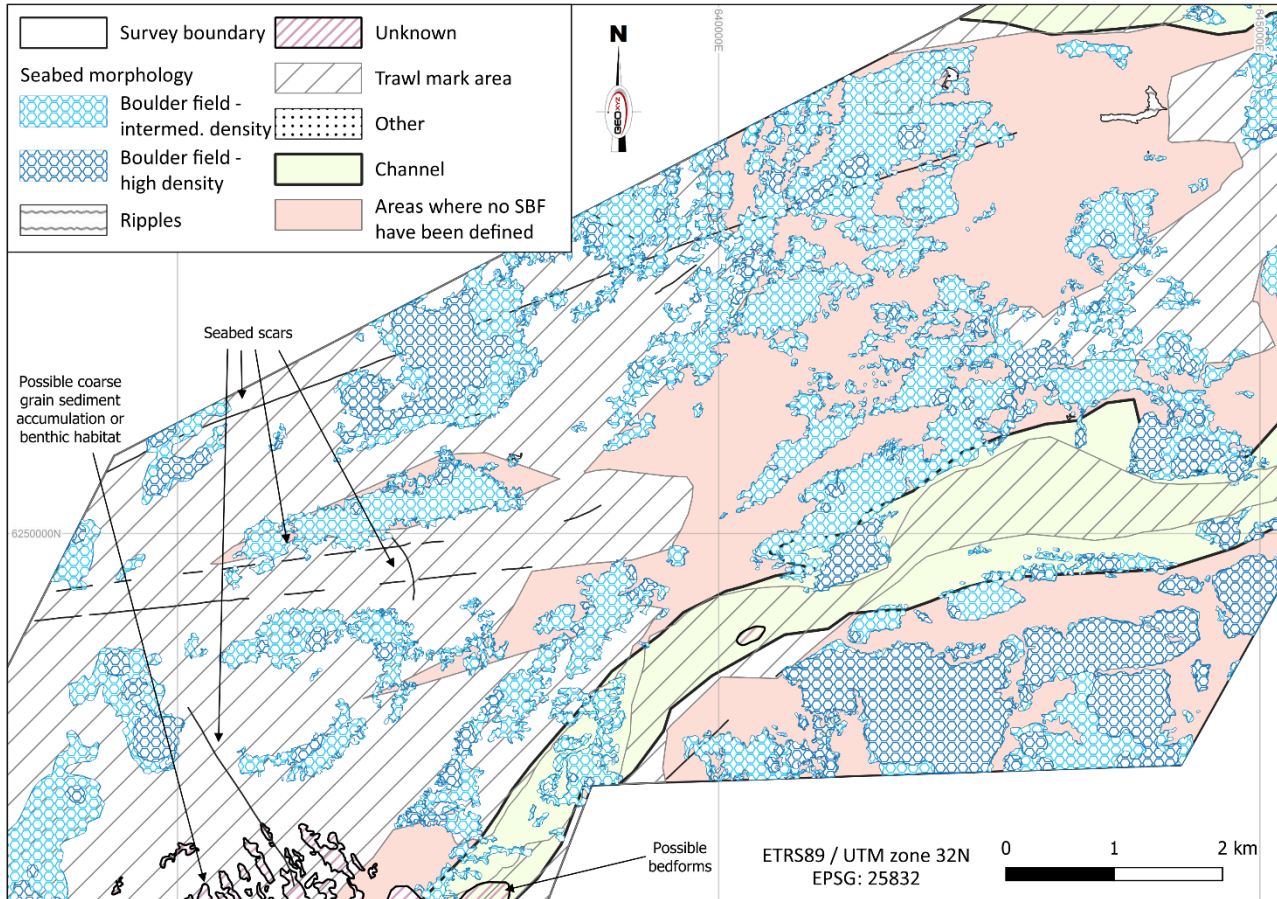


Figure 45: Seabed morphology classification: Morphology across central section of Kattegat II

In the central-southern part of the site (Figure 45 and Figure 46), high reflectivity scattered patches have been outlined, covering approximately 1.8 km². Those patches are found on a seabed classed as muddy sand. They could be interpreted as bedform-related, coarse grained sediment accumulations. Alternatively, their acoustic character and shape, together with the presence of known shells in the grab samples (KG_II_010_GR and KG_II_035_GR) may result in their interpretation as a benthic habitat. The interpretation of those features is uncertain.

A NE-SW orientated area of minor seabed depression features is present, running parallel with, and to the south of the channel feature. This area has a minimum size of 200 m to a maximum of 7000 m in width and length. A general localized depression was observed over these areas and measures between 0.1 and 0.4 m.

Two elongated areas, covering approximately 20 km², are present in the south-eastern section of the site. These outline irregular, scattered patches of low reflectivity (Figure 46). Those patches are identifiable on the SSS data, on more than one overlapping line, but are not visible in the MBES records. They could be the result of seabed effects related to gas, which is imaged close to seabed in those lines, although no bubbles were detected in the SSS water column. The origin of those features is uncertain at this point.

Trawl scars are extensive over the northern part of this southern section, before disappearing to the south, where localised, irregular areas of boulder fields are noted.

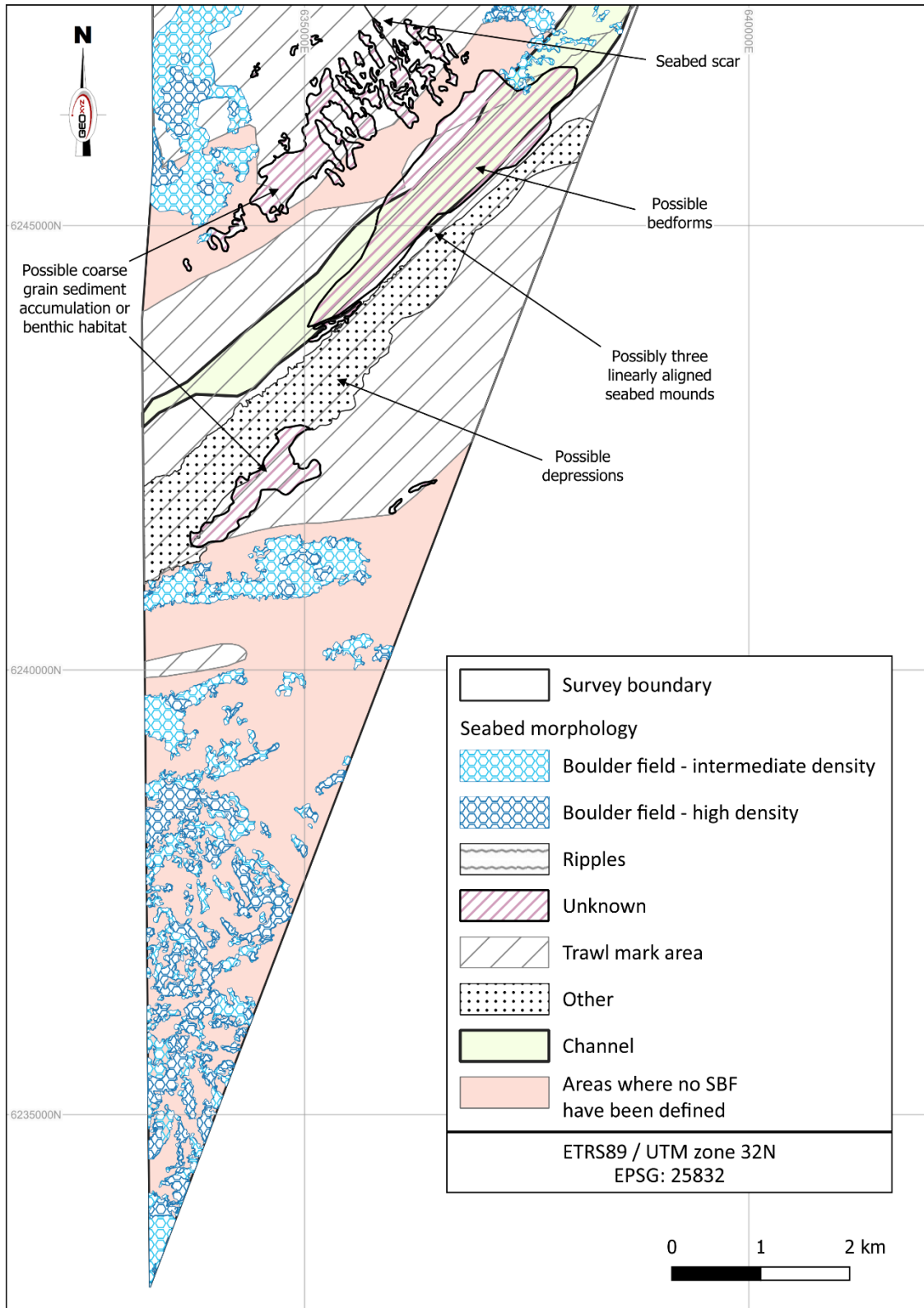


Figure 46: Seabed morphology classification: Morphology across southern section of Kattegat II

Finally, three circular, linearly aligned features were outlined in the south-eastern part of the site (Figure 46). They have low to medium reflectivity and are clearly visible in the MBES data. Their width is approximately 2.5 m with heights of around 0.2 m. They are interpreted as possible seabed mounds. The interpretation of those features is uncertain.

8.4.1 Boulder field identification criteria

The boulder field identification criteria for the survey are outlined in Technical Query TQ-009. Seabed objects, including boulders > 0.5 m in any direction were interpreted and classified. Areas with high boulder densities were provided as POL delineated from the SW projects and classified as per Table 45 below. Individual boulders within the boulder fields were picked using the automatic boulder picking algorithm, as outlined in the Processing Report. Debris objects larger than 0.5 m in any direction within the boulder fields were isolated from the auto-picked boulder fields and further investigated.

Table 45: Boulder field classification

Boulder density	Classification	Description
Intermediate	Class 1	Concentration of 40 – 80 boulders within an area of 100 x 100 m
High density	Class 2	Concentration of > 80 boulders within an area of 100 x 100 m

8.5 SEABED SURFACE CLASSIFICATION: MAN-MADE FEATURES

Seabed surface objects which are determined to be man-made objects (MMO) are outlined in Table 46. A total of 983 objects were identified through the interpretation of the MBES, SSS, and MAG datasets. It should be noted that some MMOs could be classified into more than one feature type (e.g., two objects have been classified as both metallic objects and sonar contacts). Therefore, the sum of the amounts found in Table 46 does not amount to the total number of objects.

Table 46: Summary of man-made objects

Feature type	Total amount	Comment
Wrecks	1	One unknown shipwreck.
Metallic	569	569 metallic contacts found within a 5 m radius of a magnetic anomaly.
Anchor	2	Two anchors were found within the site.
Ropes	10	Ten contacts related to possible soft rope item.
Other contacts	401	401 sonar contacts are identified to be related to either a cluster of contacts or a single contact item.
Cable/pipeline	0	No cable nor pipeline infrastructure was identified.

A total of 211 sonar contacts were observed within the survey area. Of these, there are 152 sonar contacts noted within 10 m radius of a magnetic contact which has a low possibility of being a ferrous object. The rest of the sonar contacts show high reflectivity, but are not interpreted as debris.

8.5.1 Archaeological findings

GEOxyz is not specialized in providing archaeological services. As such, the findings in this report are based on an interpretation of the data, which is a matter of opinion on which professionals may differ.

8.5.2 Wrecks

One wreck was identified in the Kattegat II area. Its details are presented in Table 47. It has been identified as an unknown shipwreck. It appears to be resting on the seabed and is well preserved.

Table 47: Wrecks within Kattegat II survey area

Wreck No	MMO ID	Wreck Name	Easting (m)	Northing (m)	Length (m)	Width (m)	Max. Height (m)	Water Depth (m)	Comments
1	972	unknown	645001.3	6250788.9	44.0	9.0	3.0	27.0	Largely intact. Large magnetic signature

The feature is located in the north-western part of the Kattegat II site, in approximately 27 m WD (Figure 47).

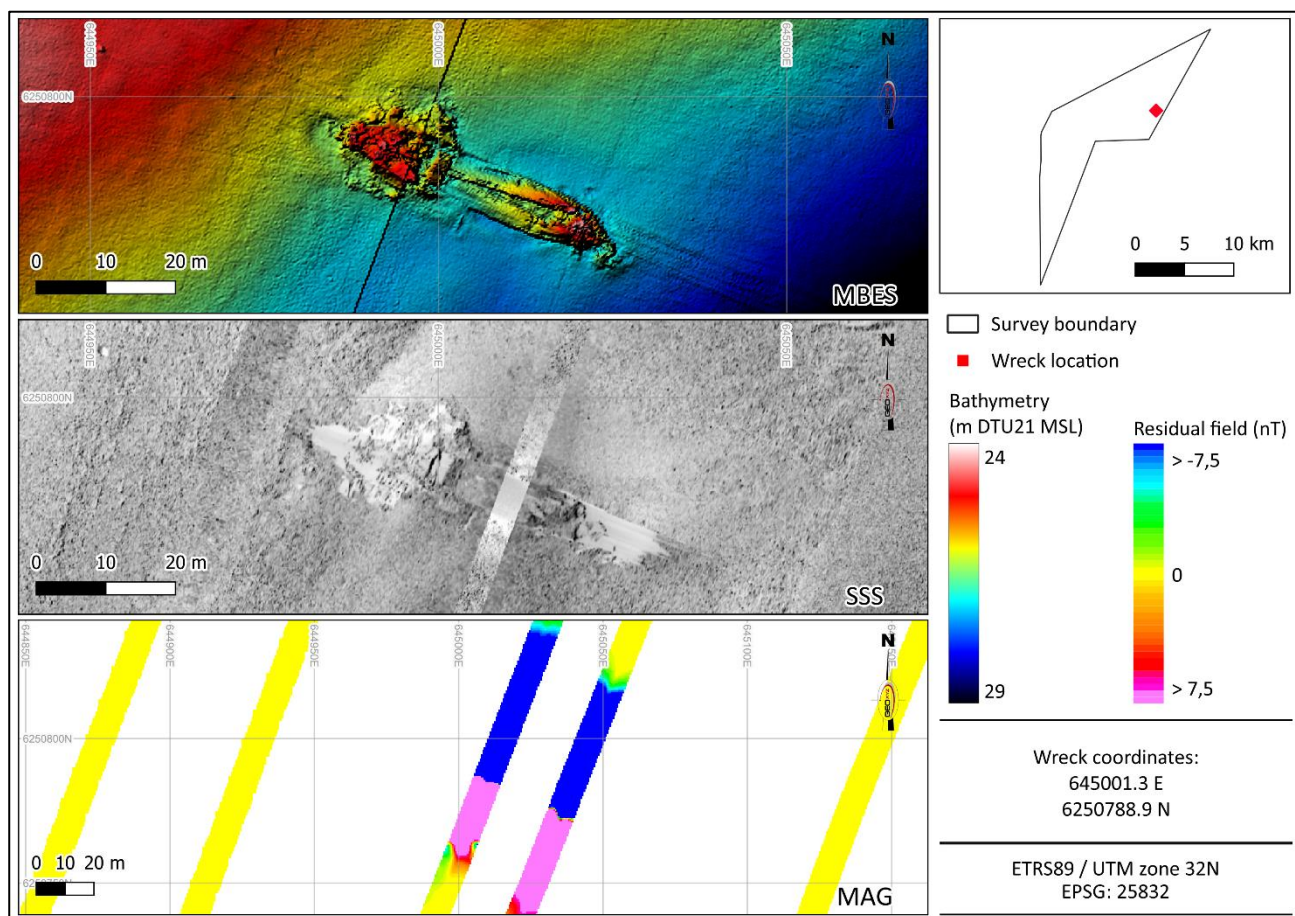


Figure 47: Overview of wreck

Its measurements are 44 m x 9 m x 3 m (L x W x H), where 3 m is the approximately maximum height above the surrounding seabed. The long axis of the object is oriented WNW-ESE.

8.5.3 Cables, wires and ropes

No infrastructure or communication related cables were identified within the Kattegat II site.

A total of 19 linear man-made objects (MMO) were identified across the Kattegat II OWF site. These features range in length from 4.4 m to 66.6 m (Figure 48).

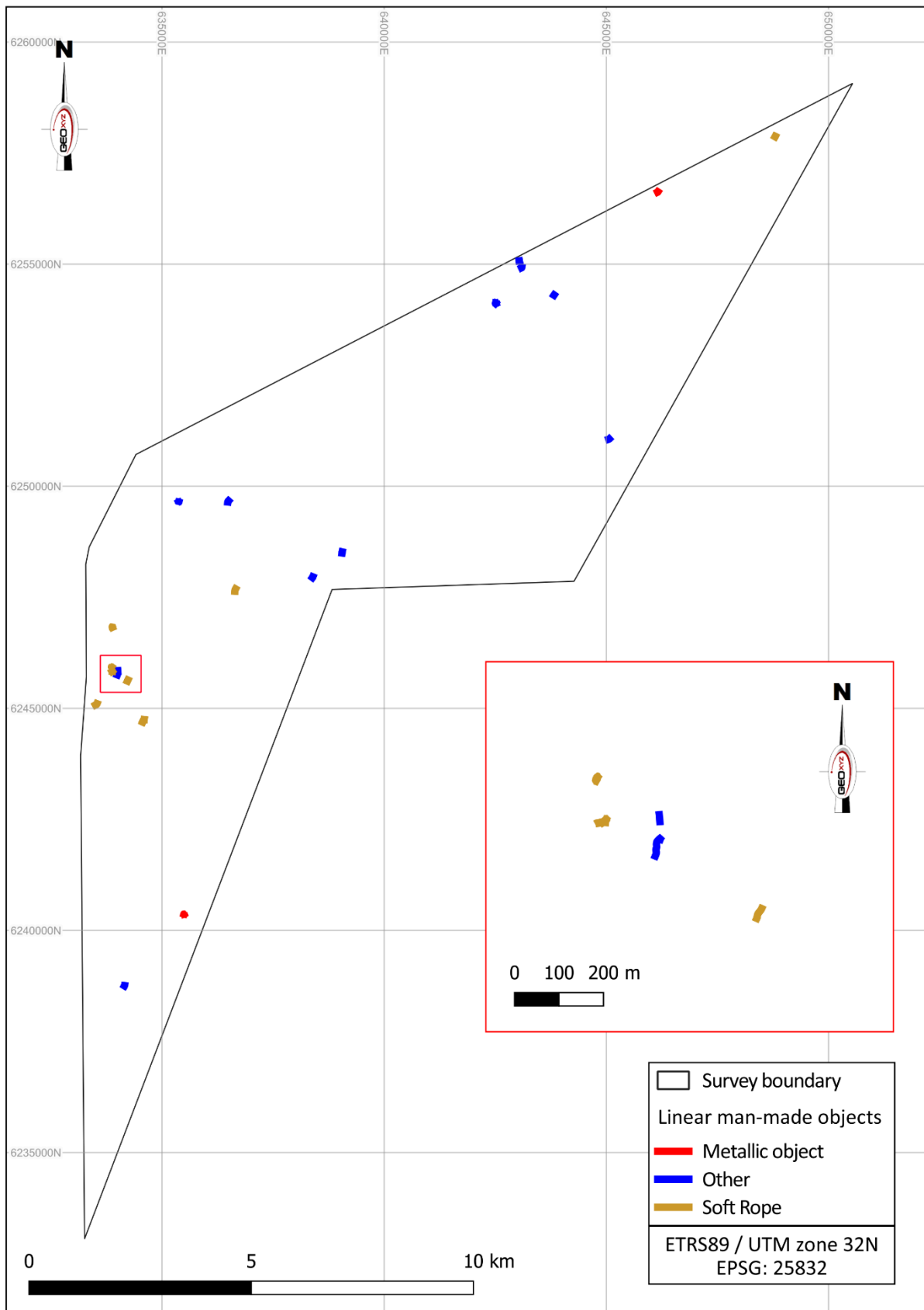


Figure 48: Overview of linear MMO found within the survey site

Two linear objects (MMO ID 742 and 747) were identified within the Kattegat II survey area (Figure 49). For these, no discernible linear magnetic response was detected. Both objects displayed a strong and sharp shadow in the SSS dataset, which indicates a possible man-made object, with significant height.

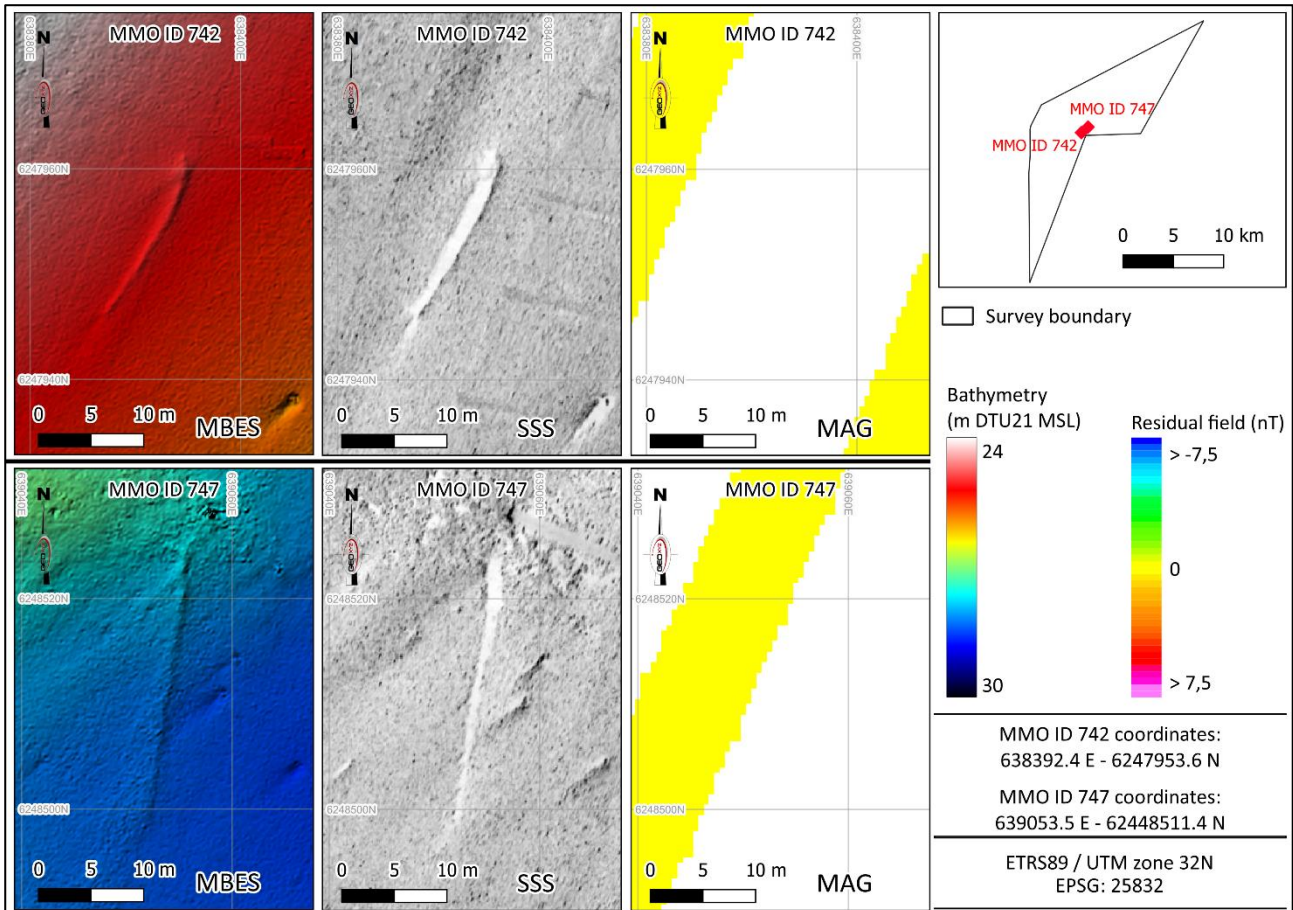


Figure 49: Possible linear objects (MMO ID 742 & 747)

A total of 10 objects (MMO IDs 32, 100, 102, 103, 395, 396, 416, 417, 533 & 965) of low to medium sonar reflectivity observed in the SSS data, are interpreted as soft rope or possible soft rope (top chartlets in Figure 50). All the objects show no discernible linear magnetic response. Among all the soft ropes, MMO ID 32 and 533 have a significant height that allow the MBES to identify both objects.

A total of six possible rope/wire/cable fragments were identified within the survey area. For these targets, no discernible linear magnetic response was detected. The fragments (MMO IDs 401, 434, 462, 512, 770 & 822) are interpreted as a possible non-ferrous rope/cable/wire fragments due to their subtle to prominent appearance in the SSS data. One of the targets (MMO ID 401) is shown in the bottom chartlets in Figure 50.

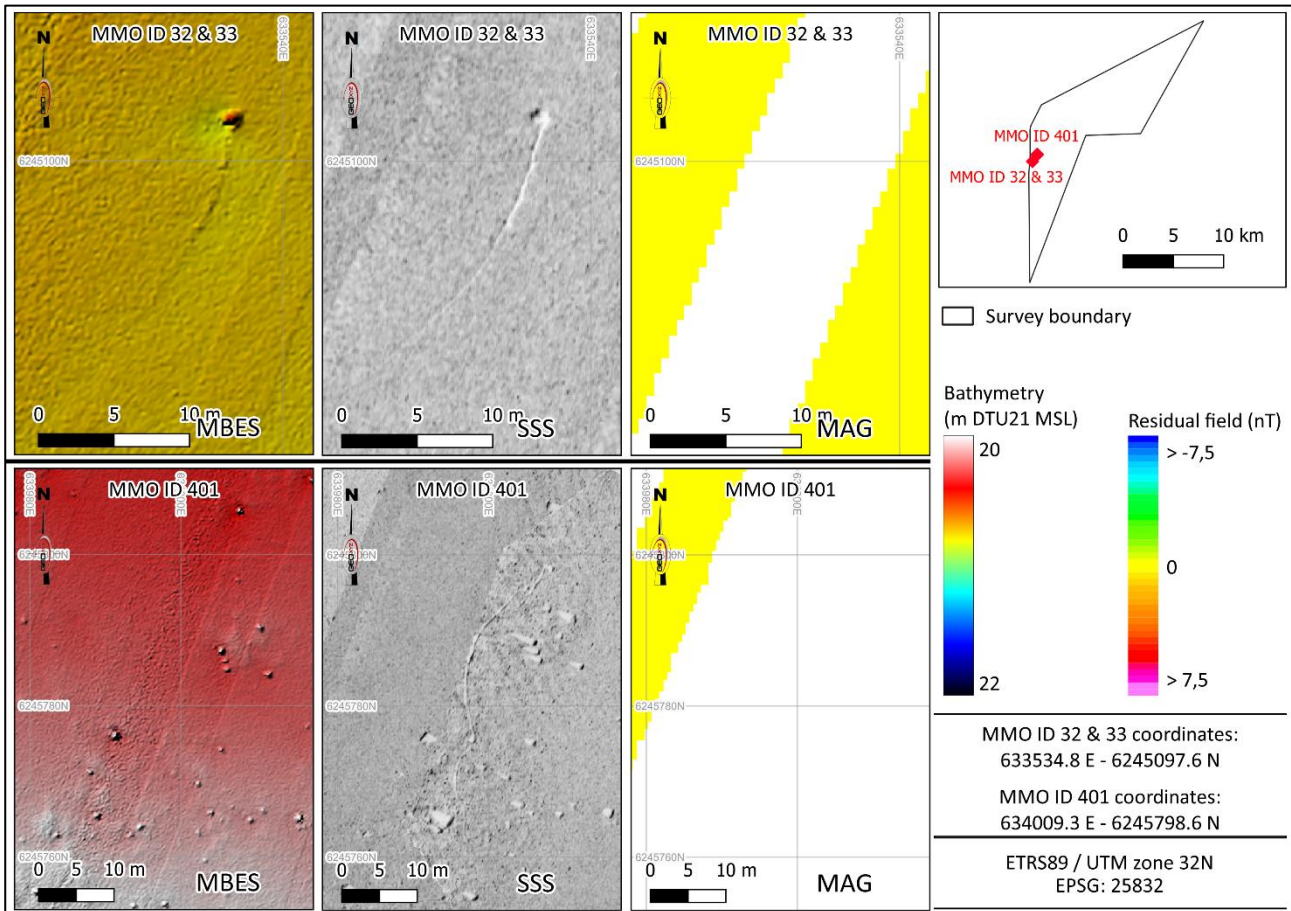


Figure 50: Possible soft rope (MMO ID 32) which appears to be attached to a debris item (MMO ID 33) at top, and possible rope/wire/cable fragment (MMO ID 401) at bottom

8.5.4 Pipelines

No pipelines were identified within the Kattegat II OWF site.

8.5.5 Debris

Two possible anchors (MMO ID 413 and 613) were observed within the Kattegat II survey area (Figure 51). In general, anchor is a ferrous metal object, however, the magnetometer survey does not identify both anchors as a magnetic anomaly. This is likely due to the anchor locations being too far off from the survey lines. Both anchors are clearly noted in the SSS and MBES datasets.

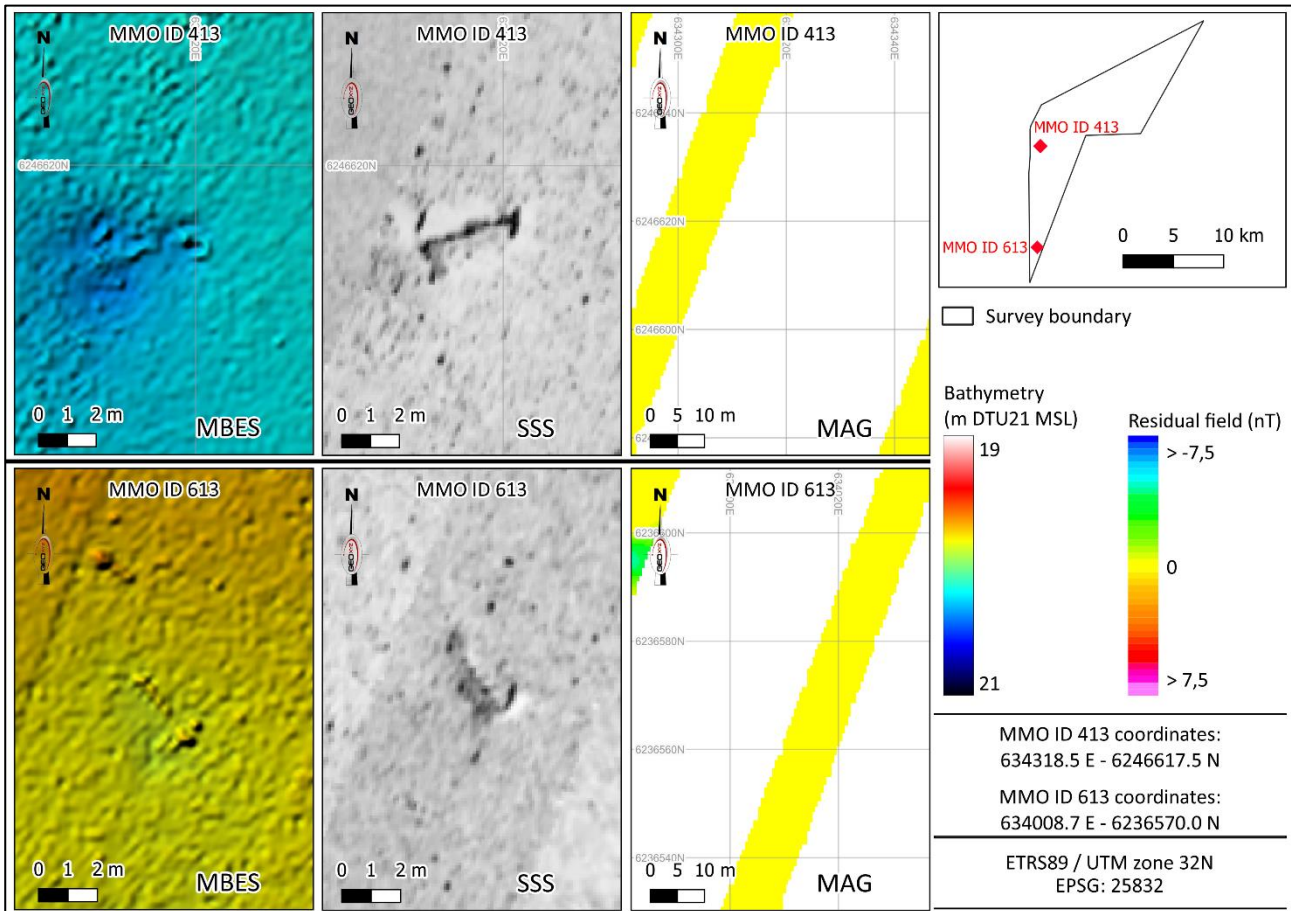


Figure 51: Possible anchors MMO ID 413 and 613

An object that has been confirmed located within a 5 m radius of a magnetic anomaly is classified as a metallic object. A total of 569 metallic objects were found within the Kattegat site. These metallic objects were identified either as single objects, or as a cluster of objects (example in Figure 52).

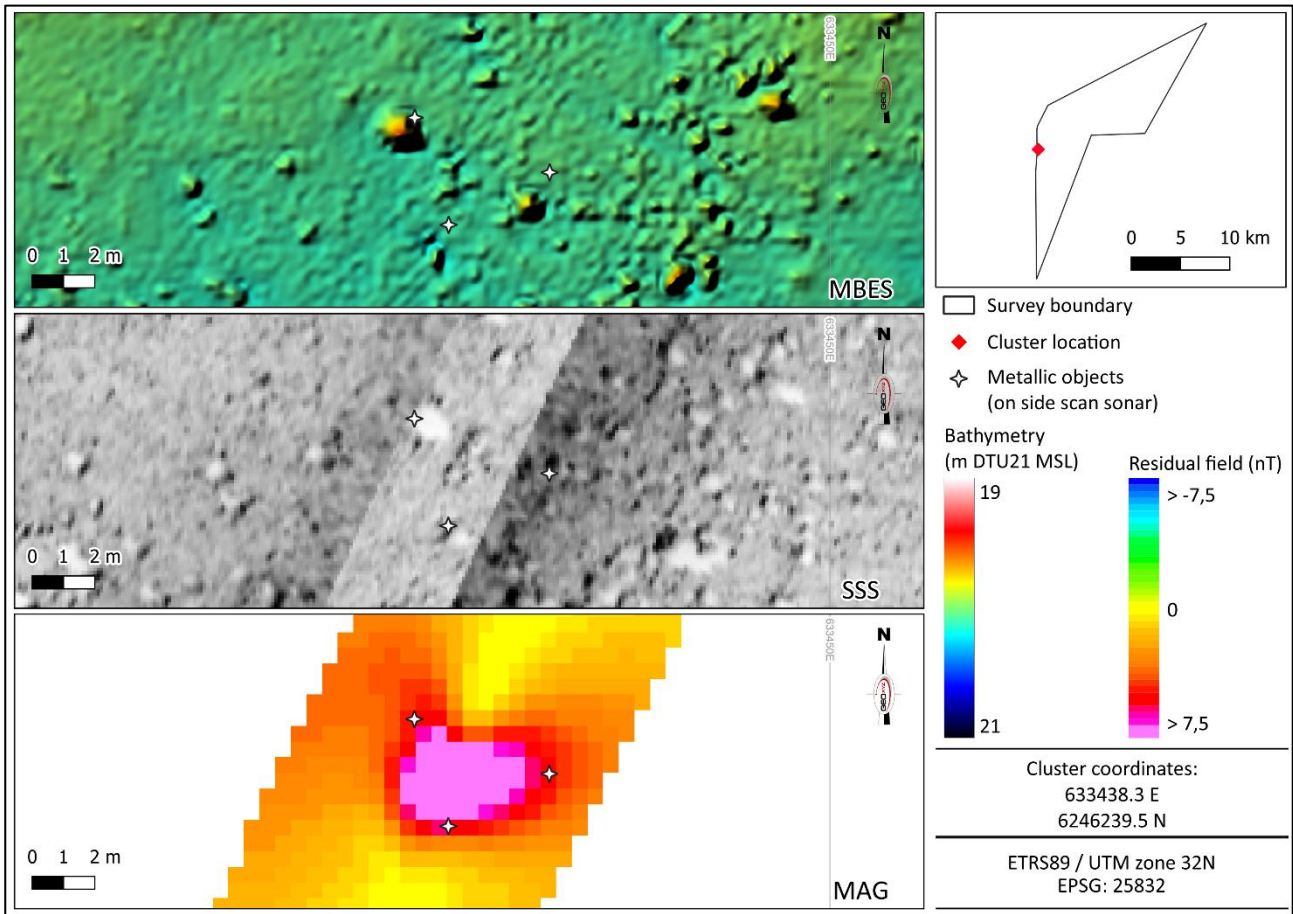


Figure 52: Cluster of metallic objects (MMO IDs 21, 22 and 24)

A total of 182 items of debris were observed within the site (Figure 53). All of these were interpreted as non-ferrous objects.

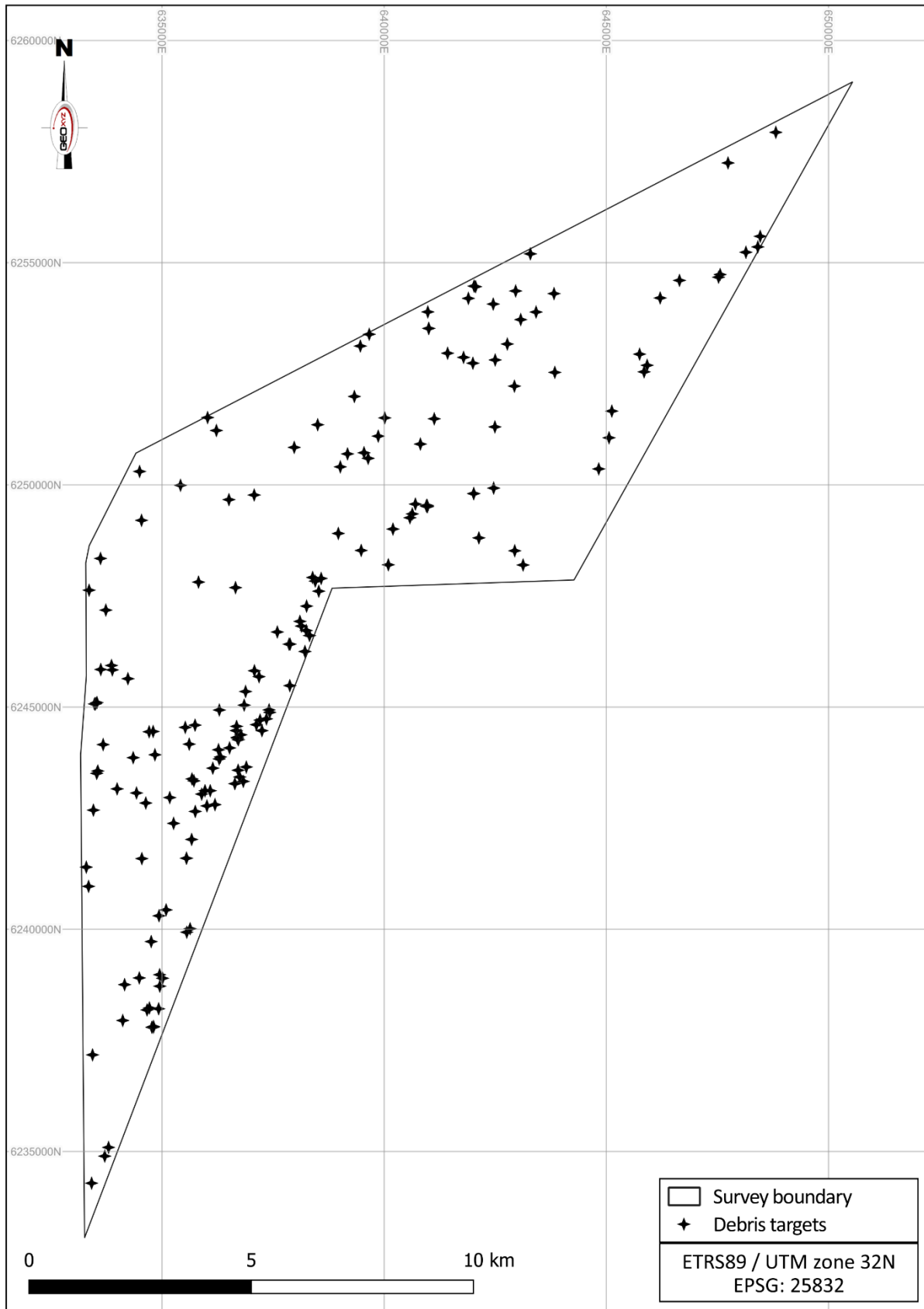


Figure 53: Overview of debris items within the survey site



8.5.6 Items related to fishing activity and seabed disturbance

All trawl marks, ropes and wires identified within the Kattegat II OWF site are highly likely related to fishing activities.

9 SUB-SURFACE GEOLOGY

9.1 REGIONAL GEOLOGICAL HISTORY

9.1.1 Pre-Quaternary Geology

The Kattegat II site is located near the south-western boundary of the Baltic shield between the southern part of Sweden, the Kattegat and the northern part of Jutland. In the late Cretaceous – early Paleogene, the previous subsiding depocenter became inverted, primarily along pre-existing faults, due to a change in the regional stress orientation, dominated by compression associated with the Alpine Orogeny and the opening of the north Atlantic. The bedrock of the Kattegat II OWF is expected to consist of Jurassic to Lower Cretaceous mudstone or siltstone and Precambrian crystalline rocks may be found in the northern part.

9.1.2 Quaternary Geology

During the Quaternary period, several glacial events have been identified in the northern Danish area. The different glacial events are separated by interglacial or interstadial marine or glaciolacustrine conditions. Till from the Last Weichselian glaciation is found south of Anholt, along with late glacial and Holocene deposits. The Scandinavian Ice Sheet reached its maximum extent in Denmark about 22 ka BP, followed by a stepwise retreat. Around 18 ka BP, the sea began to inundate northern Denmark, which led to rapid deglaciation. At ca. 17 ka BP, the ice margin had retreated to the Halland coastal moraines along the Swedish west coast.

In the Danish area, the ice cap steadily retreated, which caused the opening of the Kattegat depression and transgression of the area. A glaciomarine environment was established, where the glacier was in direct contact to the sea. Therefore, discharge of meltwater-borne sediments could be dispersed from the glacier to the sea and drop stones, rafted by calving icebergs, should be expected. Thick glaciomarine deposits, related to late glacial, are reported from the area.

The interplay between eustatic sea-level rise, caused by global melting of icecaps and glacio-isostatic rebound (regional reaction to the relief of the glacier burden), causes the sea-level to fluctuate in the late glacial and Holocene. In the early Holocene, the sea level dropped and may have caused the area to become terrestrial for a short time, before a new transgression, from which marine conditions continued through the rest of the Holocene.

9.1.3 Late Glacial and Holocene

In the period after the deglaciation, the southern Kattegat area was characterised by high-stand sea-level conditions, followed by a continuous moderate regression, until the eustatic sea-level rise surpassed the glacio-isostatic rebound in the early Holocene.

Late Weichselian subaqueous sediments occur typically as basin infill in the area north of the anticlinorium, or in local depressions elsewhere.

In the early Holocene, the relative sea level began to rise, as the eustatic sea-level rise surpassed the isostatic uplift of the crust. Mörner (1969, 1983) made comprehensive pioneer studies of the relative sea-level changes in the Younger Dryas–Holocene Kattegat, while later studies have resulted in more detailed

palaeogeographic reconstructions, based on sequence stratigraphical studies (Bennike et al. 2000; Jensen et al. 2002; Bendixen et al. 2015, 2017).

The Kattegat II OWF area has been submerged most of the time after the last deglaciation, but in the lowstand period around 10.5 ka BP only partly, and lowstand sediments must be expected. Already in the initial phase of the Holocene transgression the Kattegat II OWF area was fully submerged, while the cable corridor area has a longer transgression history.

9.2 SOIL UNIT INTERPRETATION

9.2.1 Shallow Geological Overview

The geological foundation zone extends to ~70 m below seabed. The rocks and sediments within this interval have been interpreted, with reference to the supplied GEUS desk study. This desk study applies a stratigraphic model developed by Jensen et al (2002), in conjunction with archive seismic data and limited ground truthing information. There is generally a good correlation between the shallow geology imaged in this project's sub-seabed data and the desk study. This project's unit names are equivalent to those in the desk study (for example Glacial deposits, GL, in this report are equivalent to glacial deposits, GL, within the desk study). The result is that it will be easier for future workers to use these survey reports, in conjunction with the desk study.

In general, the area has a glacial to post-glacial sequence of relatively recent sediments, overlying much older bedrock. The recent sediments are generally 40-50 m thick, although locally, these recent sediments are interpreted to be much thicker.

9.2.2 Stratigraphy and general arrangement of units

Figure 54 below displays the arrangement of units within Kattegat II. Table 48 presents the basic characteristics of the stratigraphic units. Key surfaces are the top of Unit III (H20/H05/seabed), which is the top of potentially overconsolidated deposits, and H30, which presents the top of the bedrock.

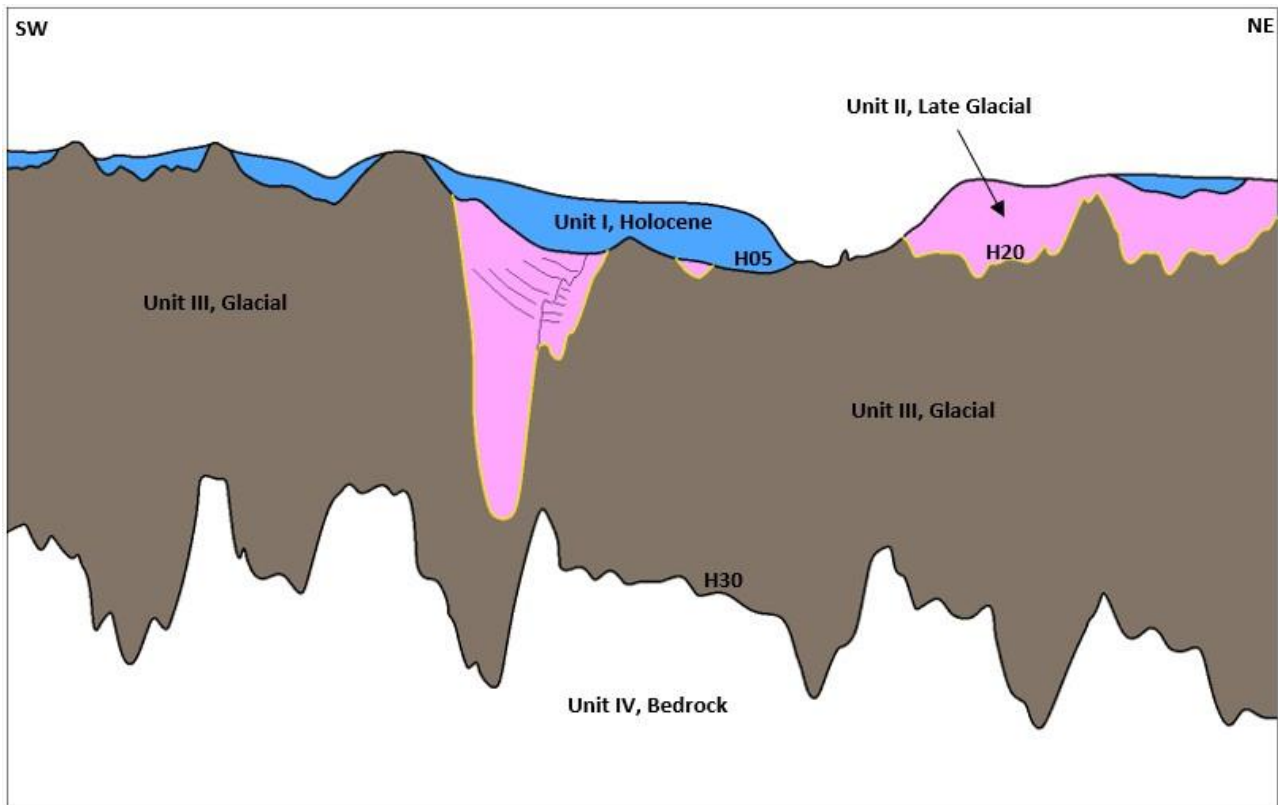


Figure 54: Geological schematic overview and general arrangement of seismic units

Table 48: Shallow geological units

Unit	Upper surface	Lower surface	Main Soil Description	Depositional Environment
I, H, Holocene	Seabed	H05	Silty, sandy CLAY with thin veneer of SAND at seabed	Post-glacial marine
II, GL, Late Glacial	Seabed/H05	H20	Variable, includes intervals of laminated CLAY, SAND-prone packages	Periglacial, glaciomarine
III, GL, Glacial	H05	H30	Variable, CLAY-prone, locally overconsolidated	Glacial with localised direct ice contact
IV, BR, Bedrock	H20/H30	-	Various carbonates and clastics. Possible crystalline basement	

9.2.3 Quaternary Deglaciation History

The following stratigraphic units, largely derived from information in the GEUS desk study, have been linked to the changing paleoenvironments:

- In Denmark, the Scandinavian Ice Sheet reached its maximum extent about 22 000 years BP, followed by retreat, with evidence for short-lived advances over the following four thousand years. The deposition of Unit III was associated to changes in this ice sheet.
- Marine transgression began around 18 000 years BP, leading to rapid deglaciation and the establishment of glaciomarine conditions. An isostatic regression occurred shortly after 18 000 years

BP. This was followed by a renewed marine transgression, related to the wasting of the Baltic Ice Stream. Over the course of this complex period, Unit II was deposited.

- After deglaciation, the area generally experienced high-stand conditions, though glacio-isostatic rebound outstripped background sea level rise around 10 000 - 11 000 years ago, driving a local regression. The Holocene deposits (Unit I) were deposited in this marine environment.

Unit I Holocene Deposits

The Holocene deposits are a package of post-glacial silty, sandy CLAY which is less than 1.5 m thick over large parts of the site. The interval includes a thin veneer of sandier seabed sediments, though these are interpreted to be very thin and are seldom resolved in the SBP data (Figure 55 and Figure 56). The Holocene sediments are widely distributed over the study area (Figure 58). The Holocene is very thin or absent (unmapped) over the centre/north of the area and in the far south, where till is close to the seabed. Small pockets of Holocene may occur in these areas and a <0.2 m thick seabed veneer may still be present.

The Holocene deposits are thickest over a south-west to north-east trending ~1 km wide zone crossing the area. Here, the deposits partially infill a channel which is still apparent at the seabed. The thickness of these deposits goes up to 9.5 m and is generally over 3 m thick. The sediments are best developed on the eastern side of the axis of the channel and subdue the complex morphology at the base of the Holocene. In the south of the area, the Holocene deposits on the east flank of the channel are quite mounded. As a bathymetric feature, the channel is as much a product of Holocene depositional patterns as it is a glaciomarine drainage system (Figure 55). The channel appears to have originated during the preceding late glacial/glaciomarine period but is located over a broad low in the bedrock. Here, some of the bedded deposits included within Unit II (the Late Glacial division) may correspond with the earliest Holocene, the first ~2000 years prior to a short regression caused by glacio-isostatic rebound.

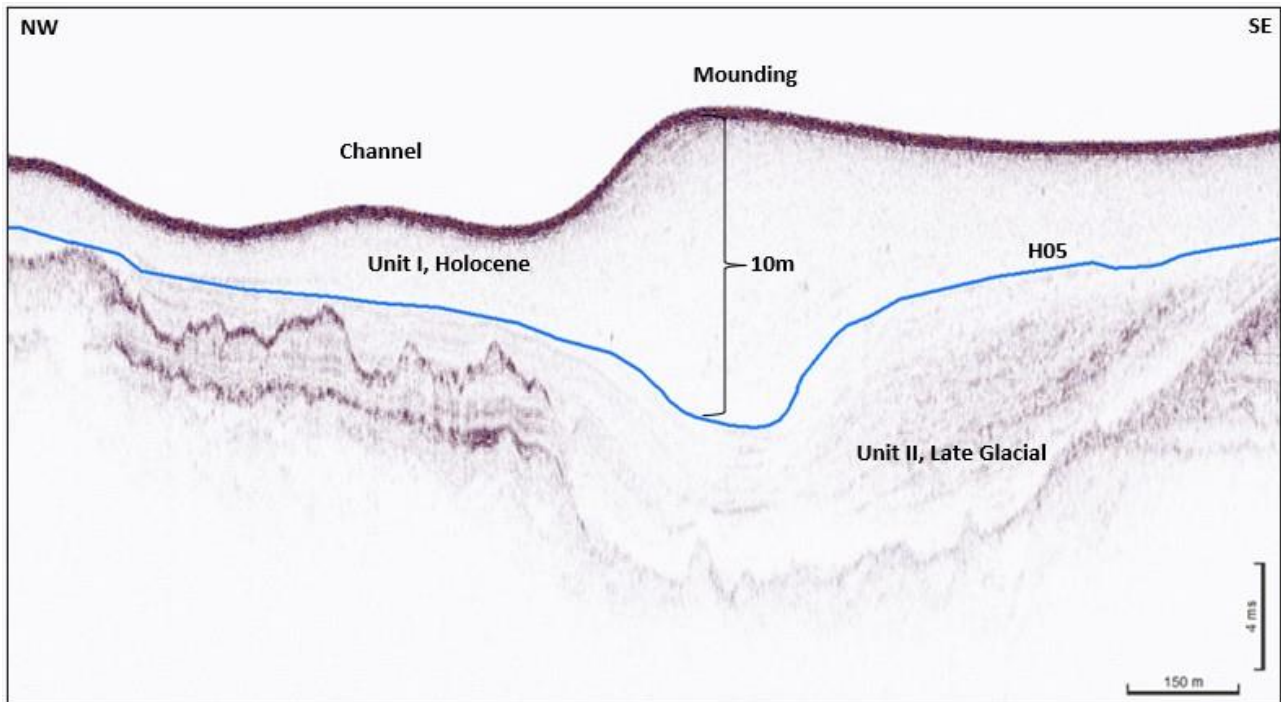


Figure 55: SBP data example, line X10 (location presented in Figure 58), Holocene deposits, mounded

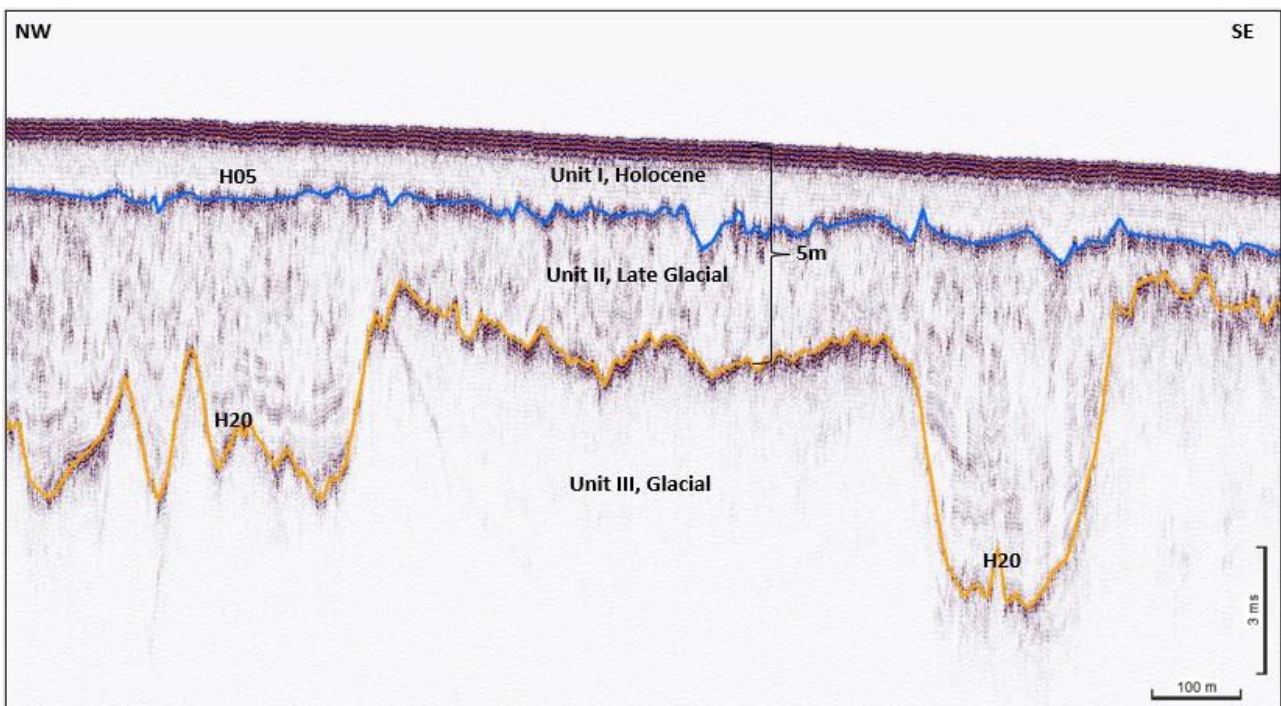


Figure 56: SBP data example, line X13 (location presented in Figure 58), Holocene deposits, thin

Acoustically the interval is almost featureless, with very low amplitude, concordant internal reflections. Locally there are very subtle unconformities. These may represent sea level variations related to the interplay of isostatic rebound and background sea level rise.

The base Holocene is mapped as H05. Over broad areas, where the Holocene is thin, it is interpreted to be a mild erosion surface where thickness variations are due to relief at this surface and a degree of mounding at the seabed (Figure 56 and Figure 57). The erosion at H05 may be related to the final regression of the area ~10 000 years ago when sea level dropped, potentially allowing storm erosion of the contemporary seabed. The erosion does not plane off the soft pre-existing sediments, as might be expected if the area became sub-aerially exposed.

The Holocene (Unit I) deposits have seismic characteristics which indicate that it is extremely soft/weak. There were instances of seabed equipment sinking into these sediments during geotechnical work.

There are very occasional bright spots which may possibly be organic material or, more likely, dropstones melted out of floating icebergs.

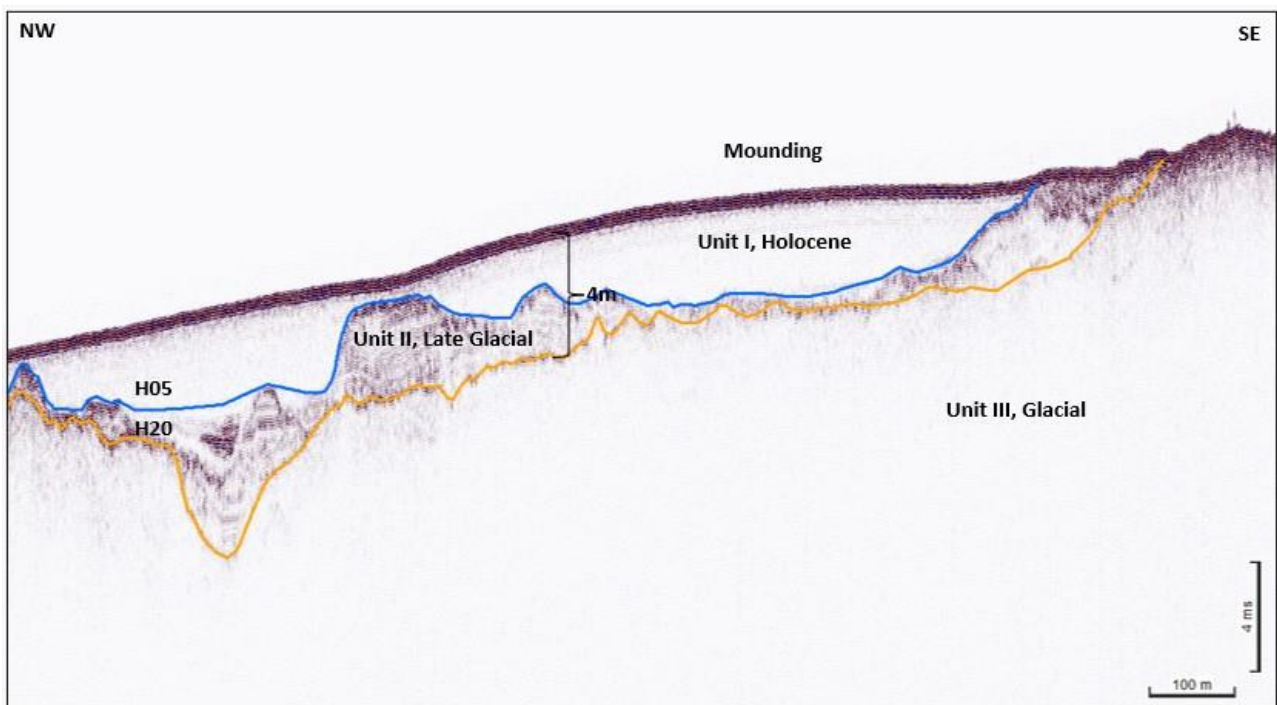


Figure 57: SBP data example, line X24 (location presented in Figure 55)

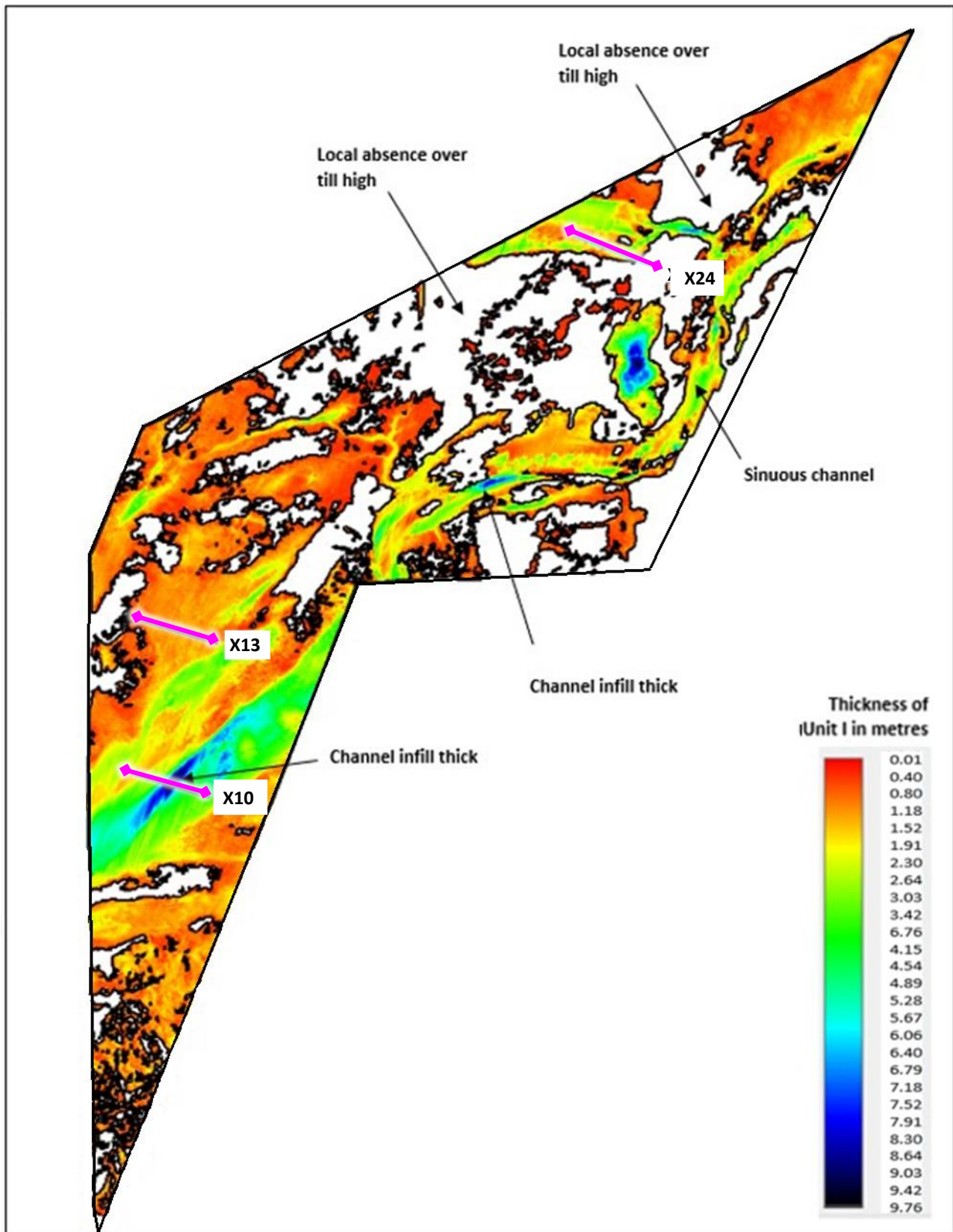


Figure 58: Thickness and distribution of Holocene deposits

Unit II Late Glacial Deposits

This interval is very complex due to the area's range of environmental conditions during the Late Weichselian and earliest Holocene. Some intervals show laminations indicative of clays and silts, others may represent sandy beach-type deposits. The unit is mapped with H20 at its base. This is generally at the top of deposits, which show clear signs of ice contact, true glacial deposits. The relief at this basal surface strongly influences the thickness and distribution of the Unit II Late Glacial sediments. Figure 59 and Figure 60 show Unit II deposits downlapping into lows in the till.

In the extreme south, and over many parts of the central and northern regions of the area, the Unit II glaciomarine sediments pinch out over ridges and highs comprised of the subcropping Unit III tills. As a result, the distribution pattern of Unit II is fragmentary and complex and closely linked to morphology at the top till surface (Figure 61).

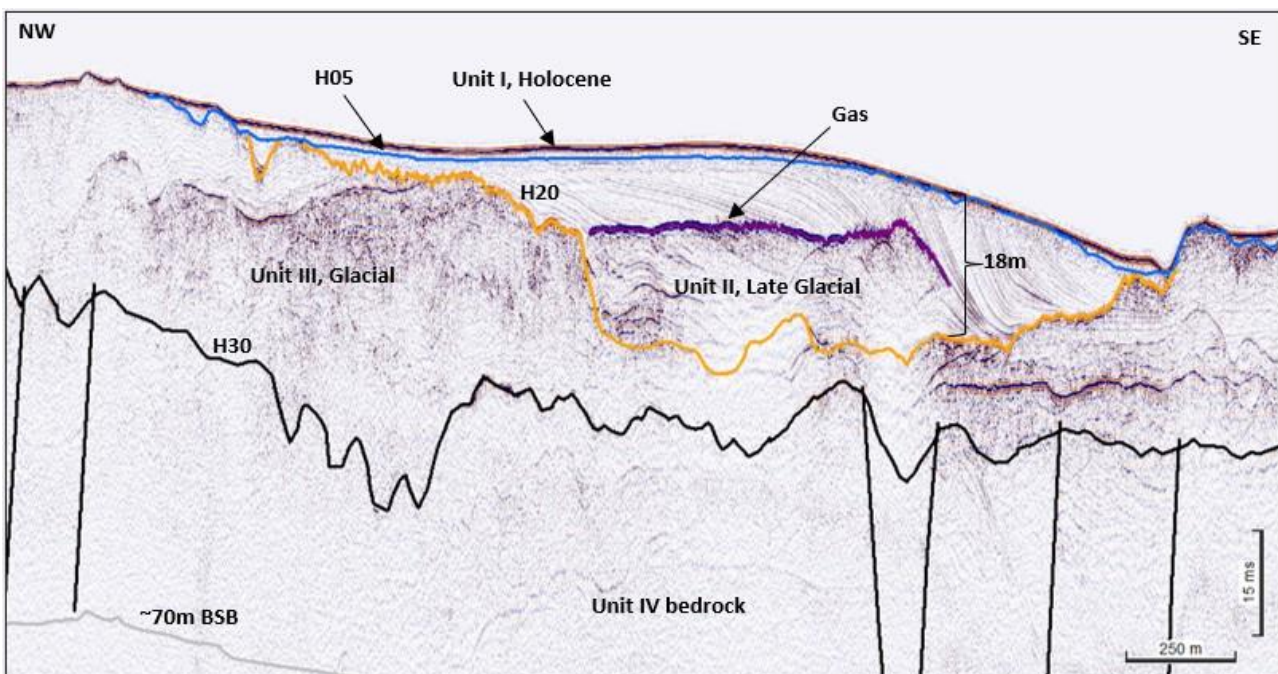


Figure 59: UHR data example, line X20 (location presented in Figure 58), downlapping Unit II

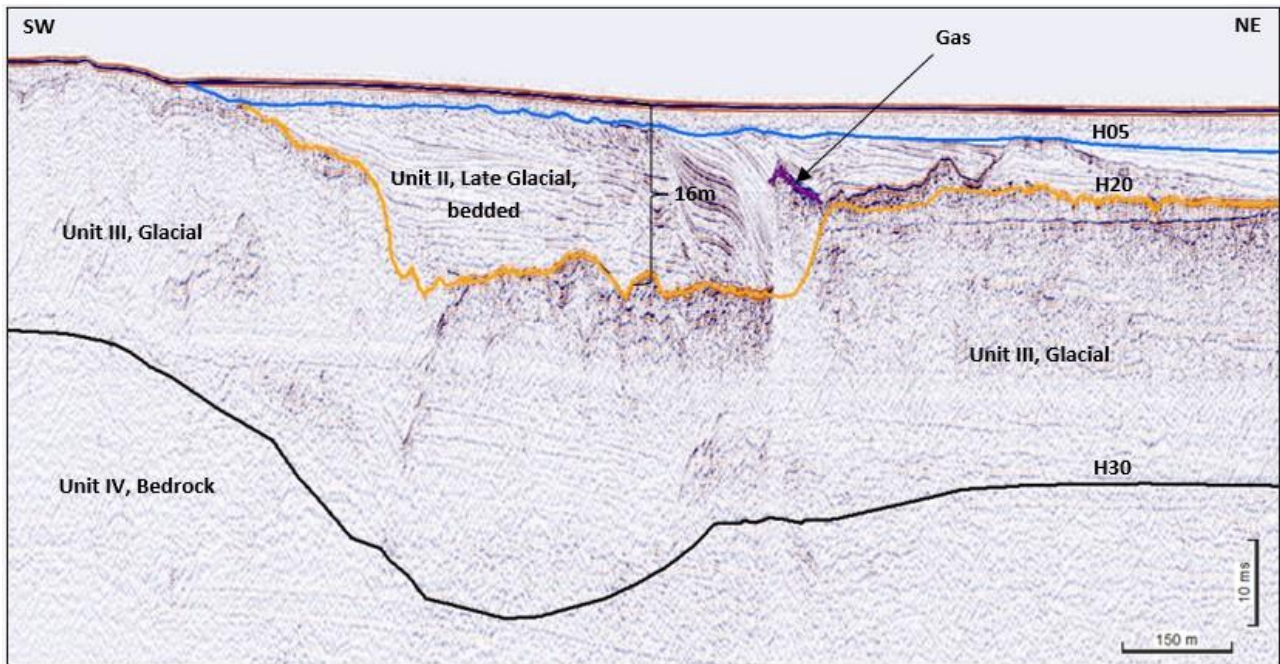


Figure 60: UHR data example, line X16A (location presented in Figure 58), downlapping Unit II

The desk study divides the late glacial sequence into earlier and later parts. Once geotechnical data are available, this sequence can be further subdivided using the existing geophysical database.

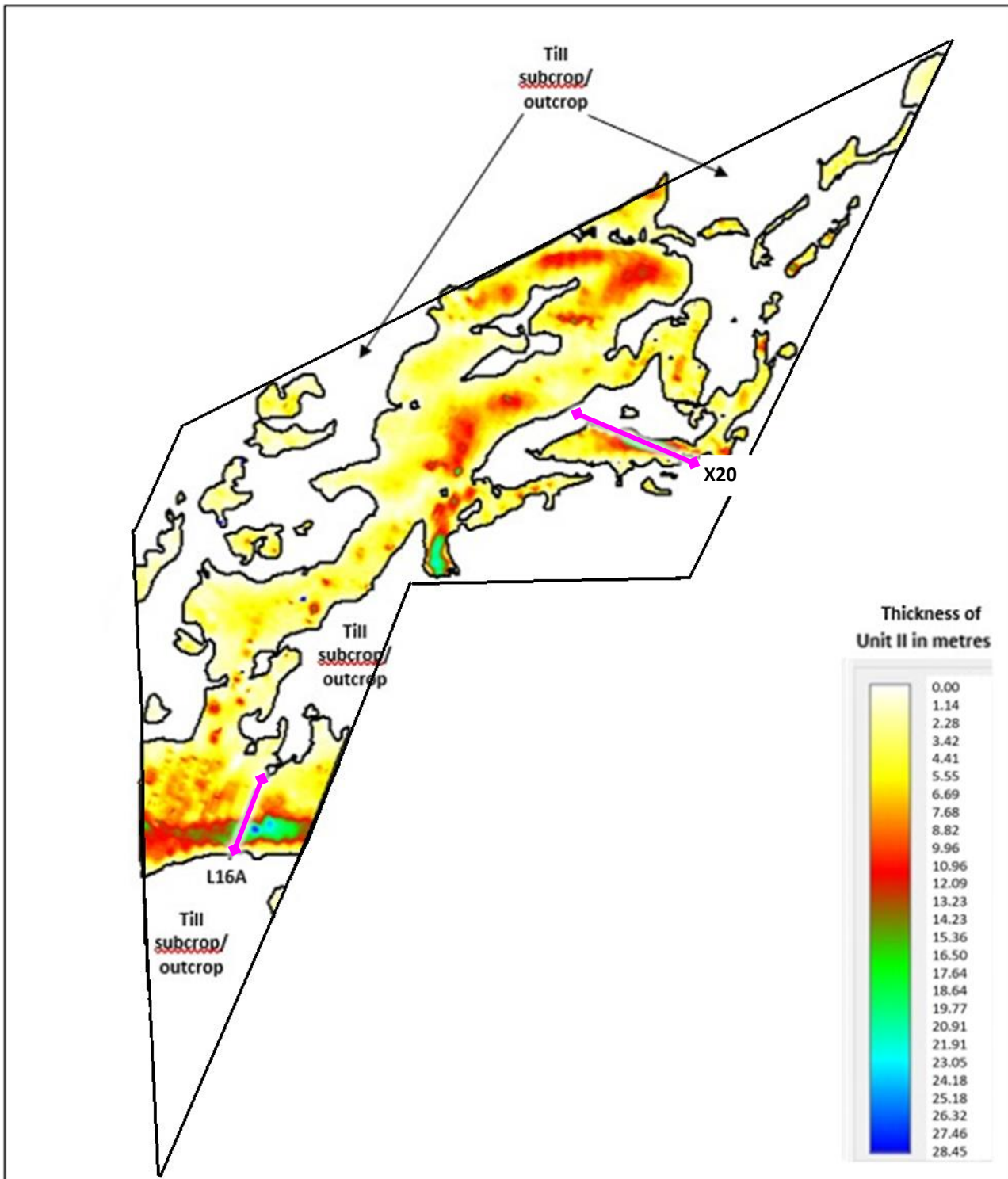


Figure 61: Thickness and distribution of Unit II Late Glacial Deposits

Unit III Glacial Deposits

Unit III deposits occur throughout the entire study area (Figure 62). Unit III is interpreted to be a till deposited in association with the last major ice advance over the area, approximately 22 000 years ago. The till forms a relatively thick blanket over the site, with variations due to bedrock highs, patterns of primary deposition

and possible erosion at the later onset of glaciomarine conditions. Unit III is typically 25 to 40 m thick, but can range locally from 2 to 90 m. The GEUS desk study provides an explanation for this and shows that the area is at a confluence of ice marginal ridges, which have amalgamated to generate a great volume of tills.

The till of Unit III is at or close to outcrop over the southern 5 km of the area and over a significant proportion of the central and northern parts of the site, west of the seabed channel.

Unit III is generally a glacial till which has been subjected to direct ice contact, though the unit contains other facies which may have been deposited in ice-marginal environments during oscillations of the ice front. The ice-contact facies may comprise a clay-prone diamicton which is likely to contain subordinate silt, sand, gravel, cobbles and boulders and will be overconsolidated. Consolidation levels may significantly vary over short distances. Seismically, the ice contact facies are structureless with a very irregular upper surface, which probably forms a series of ridges.

Unit III might be further sub-divided, perhaps separating the ice contact facies from the ice-marginal glaciomarine packages. It should be noted that even the glaciomarine intervals will have undergone some level of overconsolidation during the area's last ice advance. The complexity of Unit III can be seen in examples shown in Figure 63 and Figure 64.

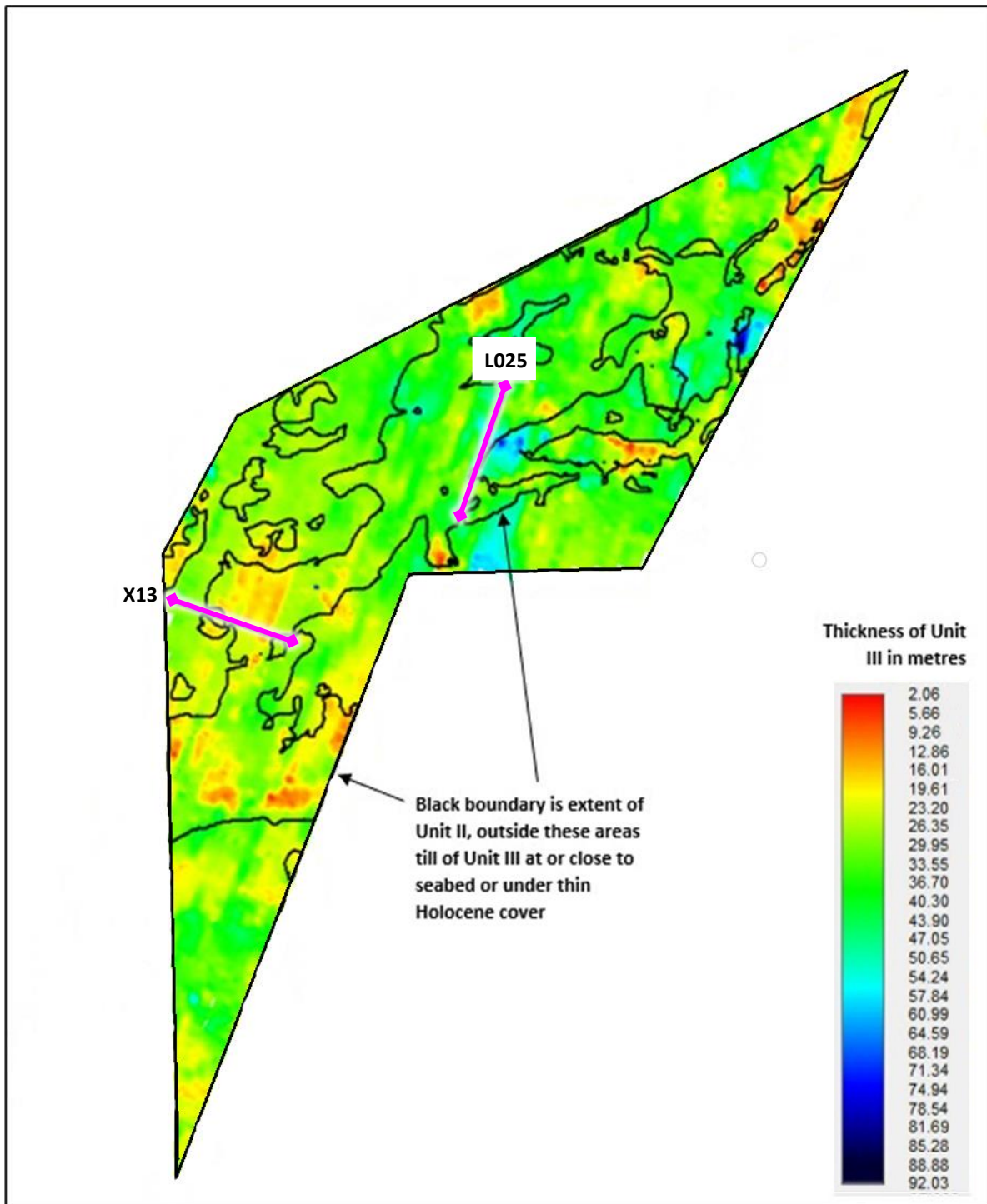


Figure 62: Thickness and distribution of Unit III Glacial Deposits

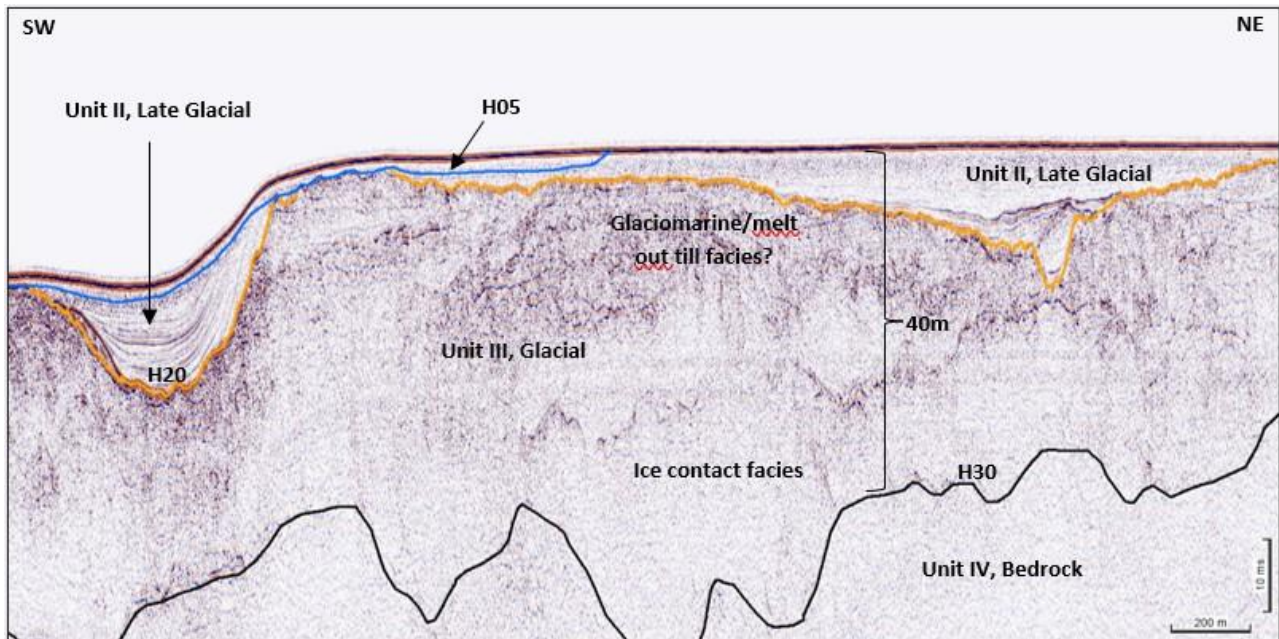


Figure 63: UHR data example, line L025 (location shown in Figure 62), Unit III, till

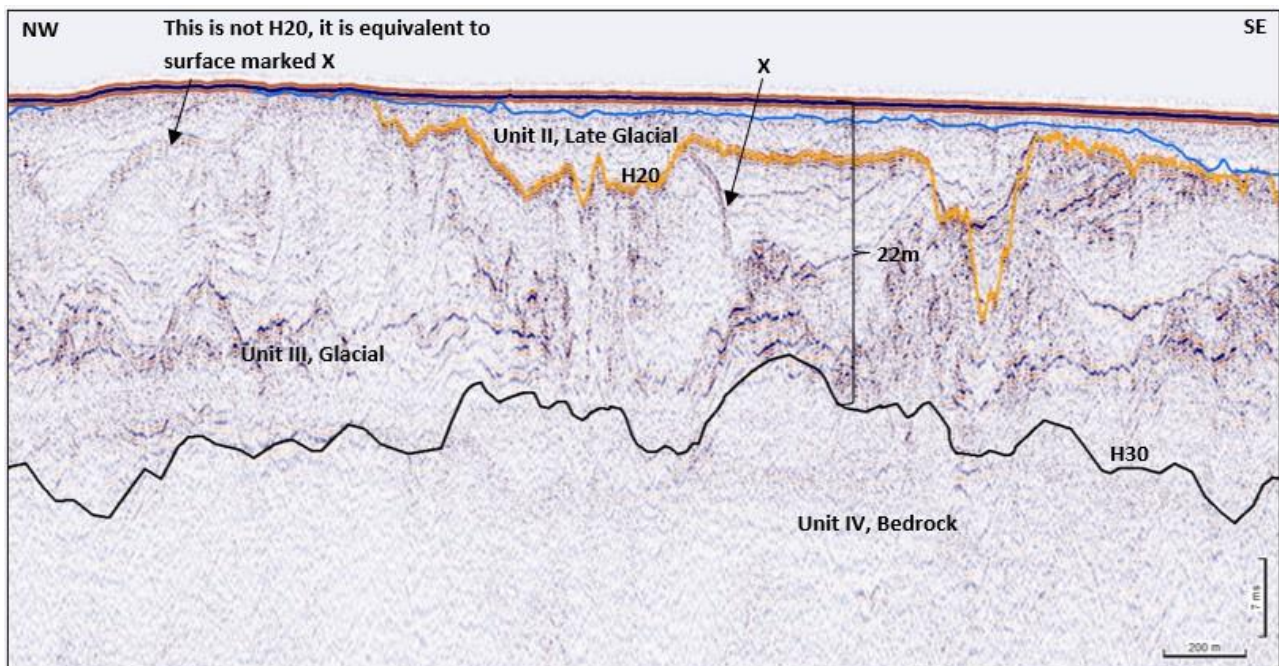


Figure 64: UHR data example, line X13 (location presented in Figure 62), Unit III, till

Unit IV Bedrock

The GEUS desk study shows that the Grenå-Helsingborg Fault runs west-north-west to east-south-east through the centre of the area. Bedrock faults are almost certainly present. These ancient faults were reactivated during the Jurassic/Cretaceous and, in this area, generated subsidence.

The desk study indicates that the bedrock will likely comprise Cretaceous carbonates and/or Jurassic clastics.

The top of the bedrock is generally 30-50 m below seabed (BSB), exceeding 60 m over small parts of the centre of the area. The latter may be related to displacements on the Grenå-Helsingborg Fault.

The upper surface of the bedrock is a truncation surface, with an angular unconformity between the Mesozoic rocks and their much younger overburden. Figure 65 shows the depth of the bedrock below seabed. The bedrock may have been subjected to numerous phases of erosion during early glaciations.

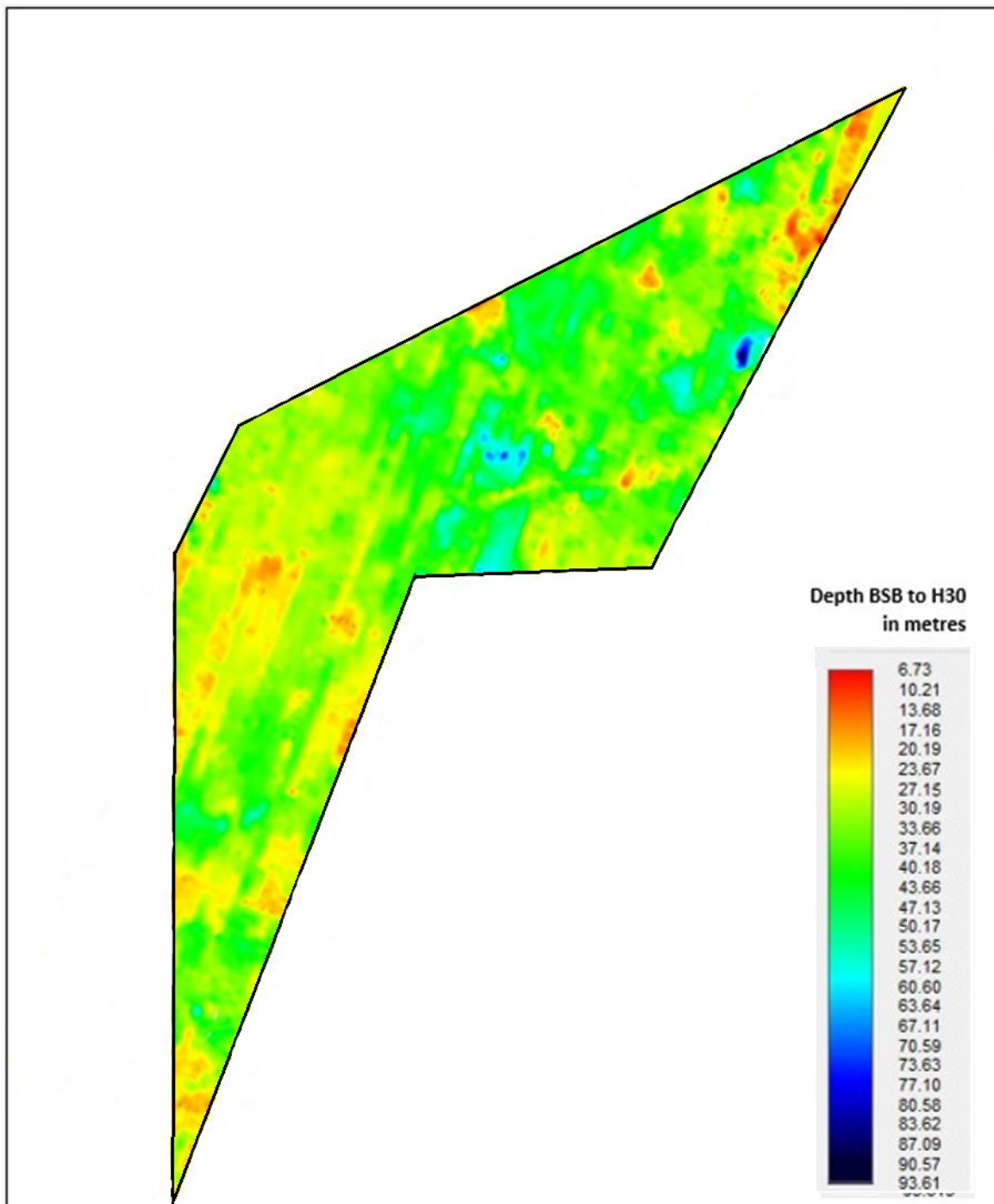


Figure 65: Depth BSB to H30 (Bedrock)

9.2.4 Shallow geological installation constraints

The following considerations could be made regarding installation constraints based on assessment made from the geophysical dataset:

- Holocene (Unit I) sediments are very weak/soft. Their bearing capacity will be negligible and could cause retrieval difficulties related to settlement of seabed frames etc.
- The Holocene unit and Unit II contain diffuse gas.
- Unit III may have variable levels of overconsolidation.
- Unit III may contain numerous cobbles and boulders.
- Unit IV may have strength variations.
- Unit IV may be weathered at the upper truncation surface.
- Unit IV may locally be weakened by faulting and micro fractures.

Cobbles and Boulders

There are occasional indications of boulders within the sub-bottom profiler data (Figure 66). These data have been optimized to resolve the shallow stratigraphy and do not readily generate diffraction hyperbola, which are the usual seismic indication of point contacts in the sub-surface. A further complication is that the units II and III, which most likely to contain boulders, have been deformed and compressed by ice confusing any returns from individual point contacts.

These circumstances, and the great volume of data, make line-by-line assessment of point contacts impractical and potentially inaccurate.

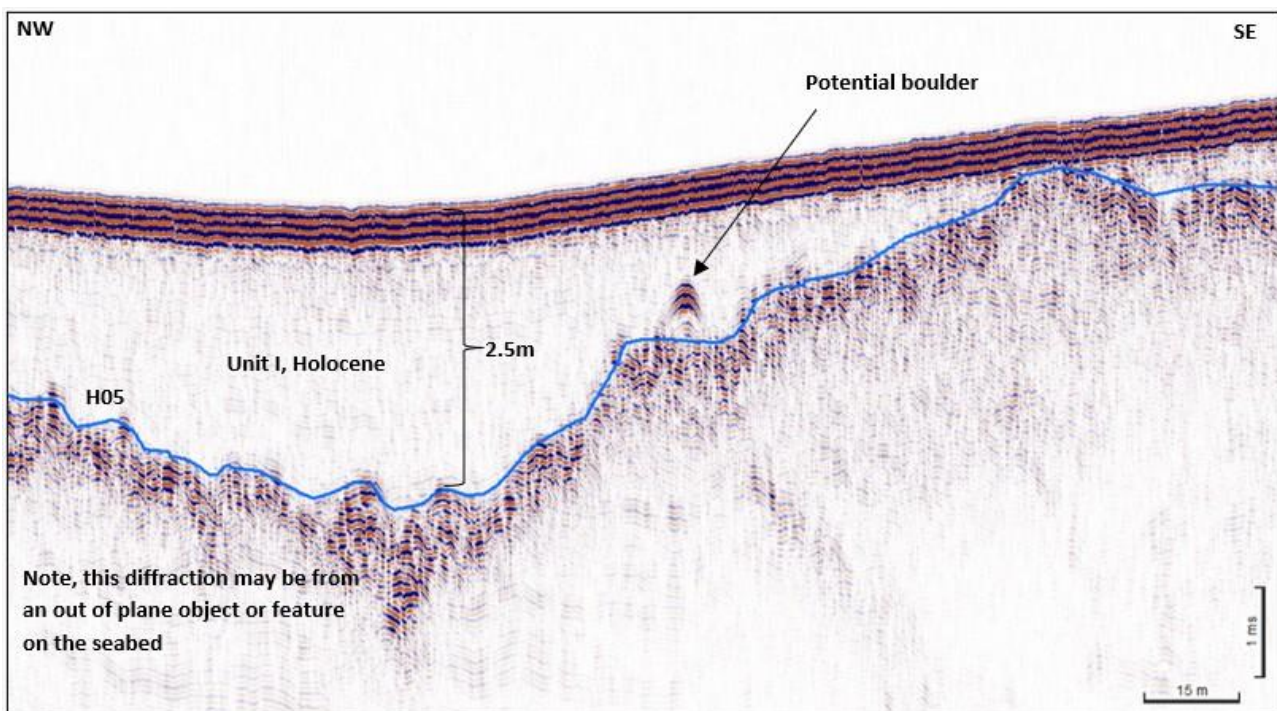


Figure 66: SBP data example, line X004, Holocene deposits (Holocene unit), rare point diffraction

A probability (Boulder Factor) grid has been generated to indicate where boulders are more or less likely to be encountered (Figure 67). This is based on the thicknesses of Units I, II and III:

- The thickness of the post-glacial Holocene unit (Unit I) is multiplied by 1: There are rare indications of boulders, which may have derived from the melting of floating ice.
- The thickness of glaciomarine Unit II is multiplied by 3: There are occasional indications of point diffractions and a greater influence of ice. There are indications of diffractions at seabed where it crops out.
- The thickness of Unit III is multiplied by 8: Though this unit has few direct point diffractions, it contains what are interpreted to be ice contact tills. This type of facies are most likely to contain erratics. The overall probability of encountering boulders is driven by the presence and thickness of the Unit III tills.

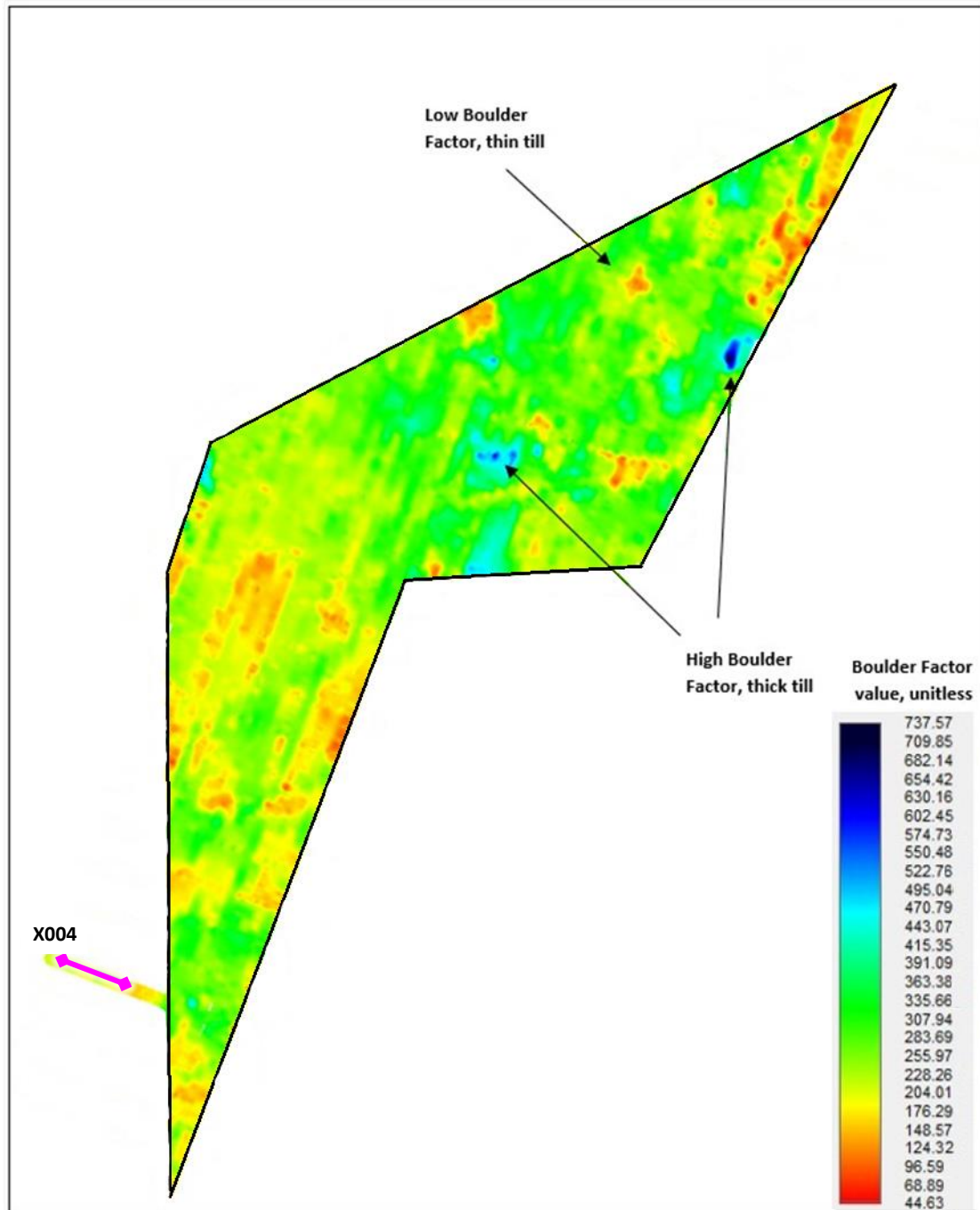


Figure 67: Boulder Factor, Quaternary

The resulting grid is a unitless value, which has been generated as depth, and is a product of the total thickness of the Quaternary sequence. A similar grid could be depth limited to the top 5 or 10 metres. Such a grid would show a strong response where the Unit III tills are close to the seabed.

Gas

Diffuse gas blanks the sub-bottom profiler data over three small areas (Figure 68 and Figure 69). It also influences the UHR data, producing high amplitude reflections and a range of imaging problems such as

blinking and internal multiples (Figure 70). A boundary has been drawn around the coherent areas of gas, based on the SBP data. The gas grids are from the BSB depth to the top of the gas.

The gas appears to inhabit the bedded facies of Unit II, occasionally extending into Holocene (Unit I), and is likely to be decomposition gas from the decay of in-situ organic matter.

The consequences of the gas include:

- Blanking of seismic data
- Possible alteration of geotechnical properties of host sediments
- Safety impact on invasive operations
- Uncertainty over long term soil behaviour around any installations

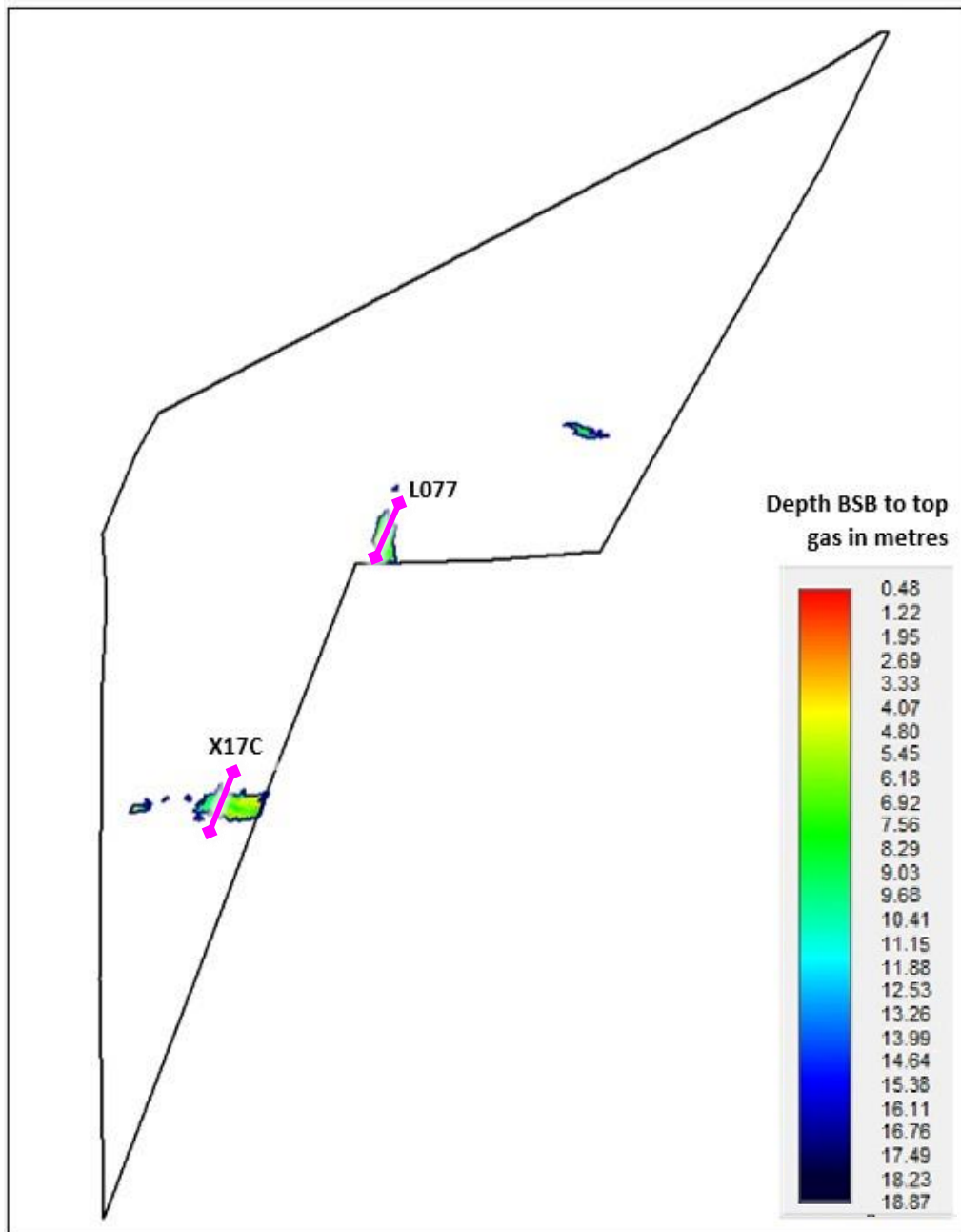


Figure 68: Depth BSB, Gas

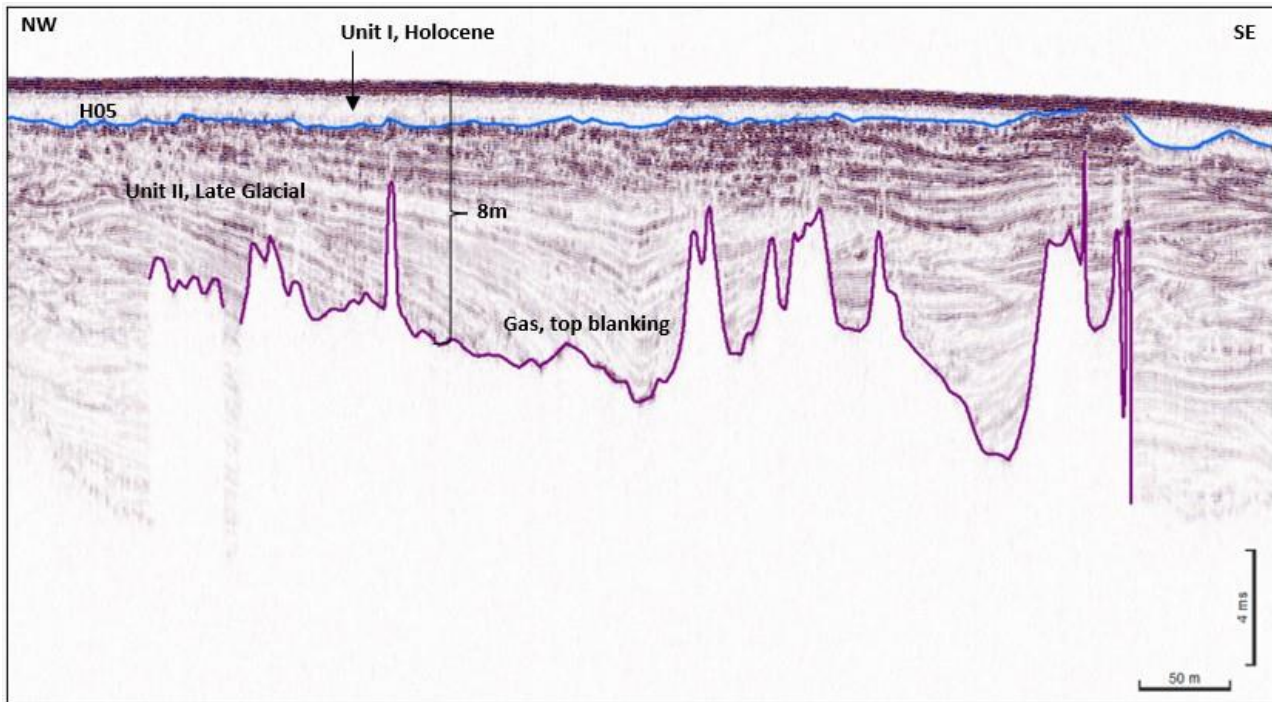


Figure 69: SBP data example, line L077 (location presented in Figure 68), gas in Unit II

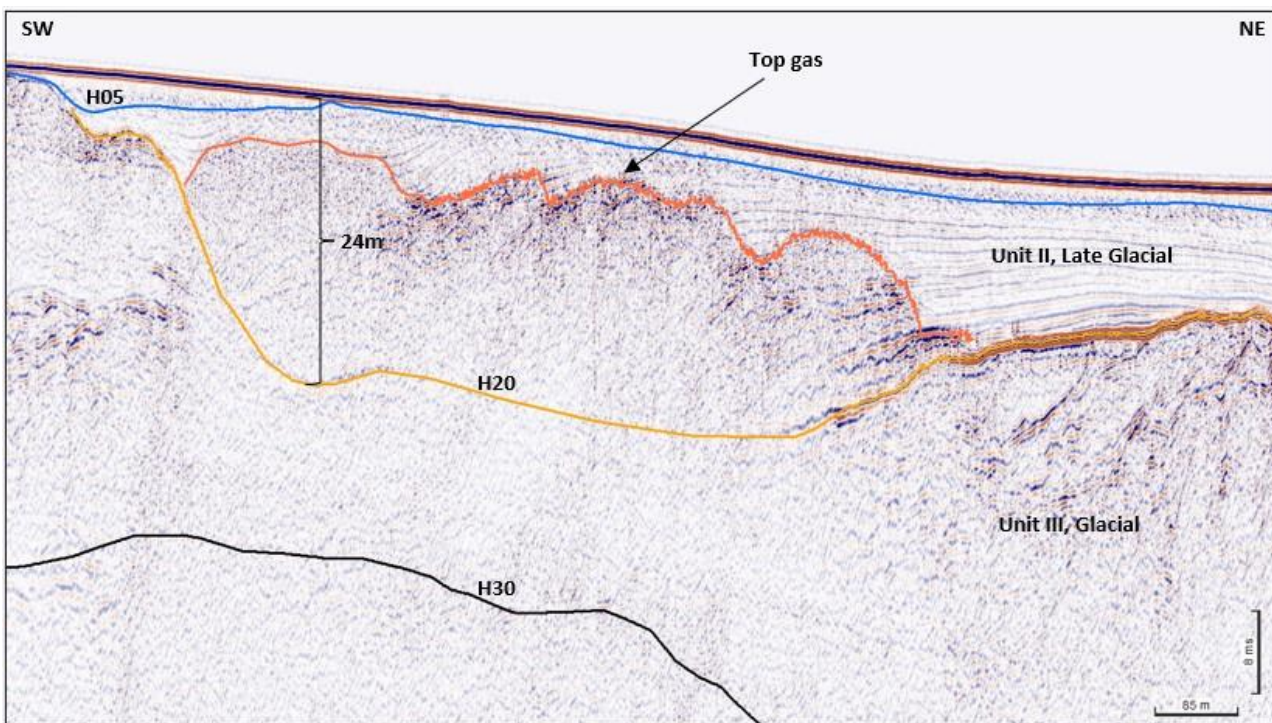


Figure 70: UHR data example, line X17C (location presented in Figure 68), gas in Unit II

9.2.5 Sub-surface acoustic velocity model

SBP depth data

The SBP depth data are based on the final time segy files. The water column and recorder delay are depth converted at the water velocity. This velocity interval extends from the top of the record to a point just above the picked water bottom. This small offset ensures that the seabed return signal is not distorted by the transition from one interval velocity to another.

The remainder of the record is converted at an assumed velocity of 1600 m/s. This is because these shallow penetrating data only image normally consolidated, uncompacted, sediments and there are no associated processing velocities to consider.

This sub-seabed interval velocity was also applied to the thickness conversion of the interpretation of the upper two units: the depth SBP data match the supplied thickness/depth grids for units I and II.

UHR depth data

The UHR depth data have been built using an iterative approach. The limited range of acquisition offsets mean that there is little moveout in the raw data beyond 20-30 milliseconds below seabed. In turn, this means that the data are not especially sensitive to variations in velocity picking. This diminishes the consistency and strength of the relationship between velocity picks and the depth of primary reflections.

The time versions of the data have been depth converted with reference to a time grid of the base of the Quaternary sequence, based on interpretation of the final time data versions. This surface is the transition from relatively young sediments to relatively ancient rocks. The surface has been used to apply and control an interval velocity ramp from lower velocities, above, and higher velocities in the deeper bedrock.

There may be small miss ties at the intersection of depth segy lines which are not present in the parent time versions of the lines. This is due to differences in depth conversion velocities which, in time, only influence signal characteristics rather than vertical position.

Deployment of depth versions

The depth segy lines are loaded into the Kingdom projects as multiversions of the parent time lines. All interpretation is of the time data. These time interpretations have been thickness and depth converted and can be displayed on the depth lines as grids. There may be minor mis-ties between these depth grids and events in the depth segy, especially with the UHR data, as the two depth products have been generated by separate workflows.

10 COMPARISON BETWEEN SEABED AND SUB-SEABED FINDINGS

In the final stage of interpretation, surficial geology has been correlated to the SBP results. It is evident that there is not an absolute match; however, seabed geology boundaries tie in very well with the top of H05 - Holocene (Unit I) thickness grid and the top of H20 -Unit II thickness grid. In general, where the surficial sediment has been interpreted as 'Gravel and coarse sand' (Figure 39), The Holocene deposits (Unit I) are absent and Unit II subcrops/outcrops (Figure 58 and Figure 61). The 'Till/diamicton' interpreted regions correlate well to the absence of both Holocene (Unit I) and Unit II. There are areas interpreted as 'Sand' (based on the reflectivity and relief) (e.g., in the south-eastern part of the site – southern part of Block 06), where there is an absence of Holocene deposits (Unit I) and Unit II in the SBP grids. In such cases the different interpretation is justified, considering a veneer (<20 cm) of sand that cannot be resolved in the SBP profiles.

11 CONCLUSIONS

Seabed levels across the Kattegat II site range from a minimum of 15.5 m MSL, in the central, eastern of the site, to a maximum of 48.6 m MSL, within the central section of a channel feature, which runs from north-east to south-west across much of the area.

A meandering, 750 – 1650 m wide channel feature crosses much of the site, approximately delineated by the 23.0 m MSL contours. This feature runs approximately north-east to south-west. Seabed levels within this channel feature range from approximately 23.0 m MSL to depths of up to 48.6 m MSL, within the central, northern section of the Kattegat II site. Steep side slopes, with localised slope gradients of between 5.0° and 20.0°, are present along the northern and southern slopes of the channel feature. Within its northern part, the seabed is very uneven, with a series of narrower channels separated by narrow ridges of sediments, which stand up to 9.0 m high. A smaller, associated channel feature spurs off towards the west, in the northern section of the site. This feature runs approximately east to west and is between 1000 m and 1400 m wide, with depths of up to 29.0 m MSL. Maximum side slopes of up to 3.0° are present.

Elsewhere across the site, to the north-west of the major channel feature, seabed levels are relatively flat, lying between 19.0 m MSL and 24.0 m MSL.

In the northern part of the site, the channel is deep and distinct, becoming shallower and less clear in the southern half. The channel feature is bounded, to the north-west and south-east, by frequent boulder fields, with extensive trawls scarring noted. Some localised areas of indistinct bedforms are present. Scattered trawl marks of different orientations can also be noted in the central and northern part of the survey area. A smaller, associated channel feature spurs off towards the west. This feature runs approximately east to west and is bounded to the north and south by areas of boulder fields, with numerous trawl scars again noted.

Alternating zones of low to medium reflectivity are present within parts of the channel and more extensively in the southern part of the site. These are generally less than 1 m in height, with a tentative NW -SE orientation. They are interpreted as bedforms, possibly related to channel bottom currents. Alternatively, the thicknesses of the Holocene (Unit I) sediments in those areas suggests subcropping/outcropping of Unit II sediments. The surficial sediment is classed as 'Muddy sand' in the extended southern area, cross-correlated to the adjacent grab samples (KG_II_008_GR and KG_II_007_GR) and as 'Gravel and coarse sand' in the smaller, northern part.

Four seabed scour patterns are present in the northern and eastern parts of the site, possibly related to fishing activities. Seabed scars are also noted, mainly in the north-western, as well as in the central part of the site. These scars are orientated in SW-NE, NW-SE and SW-NE directions. The longest of these is found in the north-western part of the site, with a length of approximately 9000 m.

In the northern part of the site, three elongated areas of alternating low to medium reflectivity are seen, over a sandy substrate, near or within the Till/diamicton sediment. These differ by ~0.1 m difference in elevation and exhibit predominately SW-NE orientations. They may be interpreted as bedforms, or possible ice-related erosional features and a seabed expression of the H05 erosional surface, noting that the Holocene (Unit I) sediments are very thin or absent in those parts.

An area of unknown features is present in the northern part of the site. They may be interpreted as possible sandwaves or erosional features/ice-sculpted areas and a seabed expression of the H05 erosional surface, in

an area where Unit II – periglacial-glaciomarine sediments are covered by a thin layer of Holocene (Unit I) sediments.

In the central-southern part of the site, scattered patches of high reflectivity are outlined, within a total area of approximately 1.8 km². These are present across areas classed as muddy sand. They may be interpreted as bedform-related accumulations of coarse-grained sediments, or possibly as benthic habitat.

A NE-SW orientated area of minor seabed depression features is present, running parallel with, and to the south of the channel feature. This area has a minimum size of 200 m to a maximum of 7000 m in width and length.

Two elongated areas, covering approximately 20 km², are present in the south-eastern section of the site. These outline irregular, scattered patches of low reflectivity. They may be the result of seabed effects, related to gas. Trawl scars are extensive over the northern part of this southern section of the site, before disappearing to the south, where irregular, localised areas of boulder fields are present.

Finally, three linearly aligned, roughly circular features are present in the south-eastern part of the site. They have low to medium reflectivity. Their width is approximately 2.5 m, with heights of around 0.2 m. They are interpreted as possible seabed mounds.

One wreck was found within the survey area.

A total of 569 metallic features were identified within the survey area. These all lie within 5 m of magnetic anomalies. Two anchors were identified within the survey area, although these features do not have associated magnetic anomalies. A total of 401 items were classified as other contacts. Ten items, identified as varying lengths of soft rope, are present within the survey area. These do not appear to be associated with any magnetic anomalies. Two other linear objects were also noted. 182 items of debris are present within the survey area. A total of 211 other sonar contacts were seen, with 152 of these noted to lie within 10 m of magnetic anomalies.

No subsea cables or pipelines are present within the Kattegat II site.

The geological foundation zone extends to ~70 m below seabed. The rocks and sediments within this interval have been interpreted, with reference to the supplied GEUS desk study. This desk study applies a stratigraphic model developed by Jensen et al (2002), in conjunction with archive seismic data and limited ground truthing information. There is generally a good correlation between the shallow geology imaged in this project's sub-seabed data and the desk study. In general, the area has a glacial to post-glacial sequence of relatively recent sediments (Units I, II and III), overlying much older bedrock. The recent sediments are generally 40-50 m thick, although locally, these recent sediments are interpreted to be much thicker.

The Holocene unit (Unit I) is a package of Holocene deposits, comprising post-glacial silty, sandy CLAY, which is less than 1.5 m thick over large parts of the site. The interval includes a thin veneer of sandier seabed sediments, though these are interpreted to be very thin. The Holocene sediments are widely distributed over the study area. The Holocene is very thin or absent (unmapped) over the centre/north of the area and in the far south, where till is close to the seabed. Small pockets of Holocene may occur in these areas and a <0.2 m thick seabed veneer may still be present.

The Holocene deposits are thickest over a south-west to north-east trending, ~1 km wide zone, crossing the area. Here, the deposits partially infill a channel which is still apparent at the seabed. The thickness of these deposits increases to 9.5 m and is generally over 3 m thick. The sediments are best developed on the eastern side of the axis of the channel and subdue the complex morphology at the base of the Holocene. In the south of the area, the Holocene deposits on the east flank of the channel are quite mounded. As a bathymetric feature, the channel is as much a product of Holocene depositional patterns, as it is a glaciomarine drainage system. The channel appears to have originated during the preceding late glacial/glaciomarine period, but is located over a broad low in the bedrock. Here, some of the bedded deposits included within Unit II (the Late Glacial division) may correspond with the earliest Holocene, the first ~2 000 years, prior to a short regression caused by glacio-isostatic rebound.

Locally, there are very subtle unconformities. These may represent sea level variations related to the interplay of isostatic rebound and background sea level rise.

The base Holocene is mapped as horizon H05. Over broad areas, where the Holocene is thin, it is interpreted to be a mild erosion surface, where thickness variations are due to relief at this surface and a degree of mounding at the seabed. The erosion at H05 may be related to the final regression of the area ~10 000 years ago, when sea level dropped, potentially allowing storm erosion of the contemporary seabed. The erosion does not plane off the soft pre-existing sediments, as might be expected if the area became sub-aerially exposed.

The Holocene (Unit I) sediments have seismic characteristics indicating that they are extremely soft/weak. There were instances of seabed equipment sinking into these sediments during geotechnical work. There are also very occasional bright spots, which may possibly be organic material or, more likely, dropstones melted out of floating icebergs.

The Late Glacial deposits of **Unit II** are very complex, due to the area's range of environmental conditions during the Late Weichselian and earliest Holocene. Some intervals show laminations, indicative of clays and silts, others may represent sandy beach-type deposits. The unit is mapped with horizon H20 at its base. This is generally at the top of deposits, which show clear signs of ice contact - true glacial deposits. The relief at this basal surface strongly influences the thickness and distribution of the Unit II Late Glacial sediments.

In the extreme south, and over many parts of the central and northern regions of the area, the Unit II glaciomarine sediments pinch out over ridges and highs, comprised of the subcropping Unit III tills. As a result, the distribution pattern of Unit II is fragmentary and complex and closely linked to the morphology at the top till surface.

Unit III (glacial deposits) occur throughout the entire study area. Unit III is interpreted to be a till, deposited in association with the last major ice advance over the area, approximately 22 000 years ago. The till forms a relatively thick blanket over the site, with variations due to bedrock highs, patterns of primary deposition and possible erosion at the later onset of glaciomarine conditions. Unit III is typically 25 to 40 m thick, but can range locally from 2 to 90 m. The GEUS desk study provides an explanation for this and shows that the area is at a confluence of ice marginal ridges, which have amalgamated to generate a great volume of tills.

The till of Unit III is at, or close to, outcrop over the southern 5 km of the area and over a significant proportion of the central and northern parts of the site, west of the seabed channel.

Unit III is generally a glacial till, which has been subjected to direct ice contact, though the unit contains other facies, which may have been deposited in ice-marginal environments, during oscillations of the ice front. The ice-contact facies may comprise a clay-prone diamicton, which is likely to contain subordinate silt, sand, gravel, cobbles and boulders, and will be overconsolidated. Consolidation levels may vary significantly over short distances. Seismically, the ice contact facies are structureless, with a very irregular upper surface, which probably forms a series of ridges. Unit III might be further sub-divided, possibly separating the ice contact facies from the ice-marginal glaciomarine packages. It should be noted that, even the glaciomarine intervals will have undergone some level of overconsolidation during the area's last ice advance.

The GEUS desk study shows that the Grenå-Helsingborg Fault runs west-north-west to east-south-east through the centre of the Kattegat II site. Bedrock faults are almost certainly present. These ancient faults were reactivated during the Jurassic/Cretaceous and, in this area, generated subsidence.

The desk study indicates that the bedrock (**Unit IV**) will likely comprise Cretaceous carbonates and/or Jurassic clastics. The top of the bedrock is generally 30-50 m below seabed (BSB), exceeding 60 m over small parts of the centre of the site. The latter may be related to displacements on the Grenå-Helsingborg Fault.

The upper surface of the bedrock is a truncation surface, with an angular unconformity between the Mesozoic rocks and their much younger overburden. The bedrock may have been subjected to numerous phases of erosion during early glaciations.

The presence of gas and cobbles and/or boulders may constrain installation. Holocene (Unit I) and Unit II sediments contain diffuse gas, while numerous cobbles and boulders may be present within Unit III.

12 OVERVIEW OF THE DIGITAL DELIVERABLES

12.1 GEOLOGICAL SURVEY

Table 49: Overview digital deliverables Work Package A

Deliverable	Format	Data Location
All sensors		
Trackplots (line)	Shapefile	SN2023_002_F_ETRS89_UTM32N
Man-made objects (point)	Shapefile	SN2023_002_F_ETRS89_UTM32N
Man-made objects (line)	Shapefile	SN2023_002_F_ETRS89_UTM32N
Man-made objects (polygon)	Shapefile	SN2023_002_F_ETRS89_UTM32N
Seabed features (point)	Shapefile	SN2023_002_F_ETRS89_UTM32N
Seabed features (line)	Shapefile	SN2023_002_F_ETRS89_UTM32N
Seabed features (polygon)	Shapefile	SN2023_002_F_ETRS89_UTM32N
Seabed geology (polygon)	Shapefile	SN2023_002_F_ETRS89_UTM32N
Catalogue of Seabed objects	PDF	108_GEOPHYSICAL_REPORT - WPA&C
SVP		
SVP logfiles	Raw and excel	101_MBES - WPA&C
SBP and UHRS		
Processed SBP data and UHRS recordings (Depth and Time)	SEGY	104_SBP_2D_URHS - WPA
SBP and UHRS instrument tracks	Shapefile	SN2023_002_F_ETRS89_UTM32N
Boulder Factor	Encoded TIF	SN2023_002_R_ETRS89_UTM32N
Interpretation of post-processed seismic data	ASCII	104_SBP_2D_URHS - WPA
Horizon interpretation depth BSL gridded surface	ASCII	104_SBP_2D_URHS - WPA
	Encoded TIF	SN2023_002_R_ETRS89_UTM32N
Horizon interpretation depth below seabed gridded surface	ASCII	104_SBP_2D_URHS - WPA
	Encoded TIF	SN2023_002_R_ETRS89_UTM32N
Isochore gridded surface	ASCII	104_SBP_2D_URHS - WPA
	Encoded TIF	SN2023_002_R_ETRS89_UTM32N
Processing Project	Kingdom Project Files	104_SBP_2D_URHS - WPA
Reports		
Mob and Cal Report	PDF	Energinet SharePoint
Operations Report	PDF	Energinet SharePoint
Technical Report	PDF	Energinet SharePoint
Charts		
Overview	PDF	108_GEOPHYSICAL_REPORT - WPA&C
Trackplots	PDF	108_GEOPHYSICAL_REPORT - WPA&C

Deliverable	Format	Data Location
Sub-seabed Geology	PDF	108_GEOPHYSICAL_REPORT - WPA&C
GIS		
Trackplots (all sensors)	Shapefile	SN2023_002_F_ETRS89_UTM32N
Boulder Factor	Encoded TIF	SN2023_002_R_ETRS89_UTM32N
SBP Horizon BSL Grids H05	Encoded TIF	SN2023_002_R_ETRS89_UTM32N
SBP Horizon BSL Grids H20	Encoded TIF	SN2023_002_R_ETRS89_UTM32N
SBP Horizon BSL Grids H35 and H50	Encoded TIF	SN2023_002_R_ETRS89_UTM32N
SBP Horizon DBS Grids H05	Encoded TIF	SN2023_002_R_ETRS89_UTM32N
SBP Horizon DBS Grids H20	Encoded TIF	SN2023_002_R_ETRS89_UTM32N
SBP Horizon DBS Grids H35	Encoded TIF	SN2023_002_R_ETRS89_UTM32N
SBP Isochore Grids	Encoded TIF	SN2023_002_R_ETRS89_UTM32N

12.2 GEOPHYSICAL SURVEY

Table 50: Overview digital deliverables Work Package C

Deliverable	Format	Data Location
All sensors		
Trackplots (line)	Shapefile	SN2023_002_F_ETRS89_UTM32N
Man-made objects (point)	Shapefile	SN2023_002_F_ETRS89_UTM32N
Man-made objects (line)	Shapefile	SN2023_002_F_ETRS89_UTM32N
Man-made objects (polygon)	Shapefile	SN2023_002_F_ETRS89_UTM32N
Seabed features (point)	Shapefile	SN2023_002_F_ETRS89_UTM32N
Seabed features (line)	Shapefile	SN2023_002_F_ETRS89_UTM32N
Seabed features (polygon)	Shapefile	SN2023_002_F_ETRS89_UTM32N
Seabed geology (polygon)	Shapefile	SN2023_002_F_ETRS89_UTM32N
Catalogue of Seabed objects	PDF	108_GEOPHYSICAL_REPORT - WPA&C
MBES		
Despiked, motion and tidal corrected point clouds	ASCII	101_MBES - WPA&C
Bathymetric average values gridded surface 0.25m, 1m and 5m	ASCII	101_MBES - WPA&C
	Encoded TIF	SN2023_002_R_ETRS89_UTM32N
Bathymetry Total Vertical Uncertainty values gridded surface 1m	ASCII	101_MBES - WPA&C
	Encoded TIF	SN2023_002_R_ETRS89_UTM32N
Bathymetry Contours 0.5m	Shapefile	SN2023_002_F_ETRS89_UTM32N
MBES Anomaly Points	Shapefile	SN2023_002_F_ETRS89_UTM32N
Vessel Tracks	Shapefile	SN2023_002_F_ETRS89_UTM32N
SVP		

Deliverable	Format	Data Location
SVP logfiles	Raw and excel	101_MBES - WPA&C
Backscatter		
Gridded 1m	Encoded TIF	SN2023_002_R_ETRS89_UTM32N
	ASCII	101_MBES - WPA&C
SSS		
Processed SSS data	HF XTF	102_SSS – WPC
	LF XTF	102_SSS – WPC
Navigation Files	ASCII	102_SSS – WPC
SSS mosaics HF	Single band TIF	SN2023_002_R_ETRS89_UTM32N
SSS mosaics LF	Single band TIF	SN2023_002_R_ETRS89_UTM32N
SonarWiz 7 Project	SonarWiz Project Files	102_SSS – WPC
Target Images	Single band TIF	SN2023_002_R_ETRS89_UTM32N
SSS Anomaly Points	Shapefile	SN2023_002_F_ETRS89_UTM32N
Magnetometer		
Processed Magnetometric Data	ASCII	103_MAG - WPC
Mag Anomaly Points	Shapefile	SN2023_002_F_ETRS89_UTM32N
Total Field Grid	Encoded TIF	SN2023_002_R_ETRS89_UTM32N
Residual Signal Grid	Encoded TIF	SN2023_002_R_ETRS89_UTM32N
Analytical Signal Grid	Encoded TIF	SN2023_002_R_ETRS89_UTM32N
Altitude Grid	Encoded TIF	SN2023_002_R_ETRS89_UTM32N
Oasis Montaj Project	Oasis Montaj Project	103_MAG - WPC
SBP and UHRS		
Processed SBP data and UHRS recordings (Depth and Time)	SEGY	104_SBP_2D_URHS - WPA
SBP and UHRS instrument tracks	Shapefile	SN2023_002_F_ETRS89_UTM32N
Boulder Factor	Encoded TIF	SN2023_002_R_ETRS89_UTM32N
Interpretation of post-processed seismic data	ASCII	104_SBP_2D_URHS - WPA
Horizon interpretation depth BSL gridded surface	ASCII	104_SBP_2D_URHS - WPA
	Encoded TIF	SN2023_002_R_ETRS89_UTM32N
Horizon interpretation depth below seabed gridded surface	ASCII	104_SBP_2D_URHS - WPA
	Encoded TIF	SN2023_002_R_ETRS89_UTM32N
Isochore gridded surface	ASCII	104_SBP_2D_URHS - WPA
	Encoded TIF	SN2023_002_R_ETRS89_UTM32N
Processing Project	Kingdom Project Files	104_SBP_2D_URHS - WPA
Grab Sampling		
Grab Sample Positions	Shapefile	SN2023_002_F_ETRS89_UTM32N
Grab Sample Classifications	Excel Doc	108_GEOPHYSICAL_REPORT - WPA&C
Grab Sample Lab Analysis	Excel Doc	108_GEOPHYSICAL_REPORT - WPA&C

Deliverable	Format	Data Location
Onboard 48h deliverables		
MBES coverage	Shapefile	Onboard
Bathymetric average values gridded surface	ASCII	Onboard
Bathymetric density values gridded surface	ASCII	Onboard
Bathymetric standard deviation values gridded surface	ASCII	Onboard
MBES track	Shapefile	Onboard
SSS coverage	Shapefile	Onboard
SSS mosaic merged HF and LF	Single band TIF	Onboard
SSS mosaic per line HF and LF	Single band TIF	Onboard
SSS track processed	Shapefile	Onboard
MBES targetlist	ASCII	Onboard
SSS targetlist	ASCII	Onboard
Reports		
Mob and Cal Report	PDF	Energinet SharePoint
Operations Report	PDF	Energinet SharePoint
Technical Report	PDF	Energinet SharePoint
GIS		
Trackplots (all sensors)	Shapefile	SN2023_002_F_ETRS89_UTM32N
MBES Contours	Shapefile	SN2023_002_F_ETRS89_UTM32N
MBES Anomalies	Shapefile	SN2023_002_F_ETRS89_UTM32N
MBES Grid 0.25m, 1.0m and 5.0m	Shapefiles	SN2023_002_F_ETRS89_UTM32N
MBES THU Grid 1.0m	Shapefile	SN2023_002_F_ETRS89_UTM32N
MBES TVU Grid 1.0m	Shapefile	SN2023_002_F_ETRS89_UTM32N
Backscatter Grid 1.0m	Shapefile	SN2023_002_F_ETRS89_UTM32N
Boulder factor	Encoded TIF	SN2023_002_R_ETRS89_UTM32N
SBP Horizon BSL Grids H05	Encoded TIF	SN2023_002_R_ETRS89_UTM32N
SBP Horizon BSL Grids H20	Encoded TIF	SN2023_002_R_ETRS89_UTM32N
SBP Horizon BSL Grids H30	Encoded TIF	SN2023_002_R_ETRS89_UTM32N
SBP Gas BSL Grids	Encoded TIF	SN2023_002_R_ETRS89_UTM32N
SBP Horizon DBS Grids H05	Encoded TIF	SN2023_002_R_ETRS89_UTM32N
SBP Horizon DBS Grids H20	Encoded TIF	SN2023_002_R_ETRS89_UTM32N
SBP Horizon DBS Grids H30	Encoded TIF	SN2023_002_R_ETRS89_UTM32N
SBP Gas DBS Grids	Encoded TIF	SN2023_002_R_ETRS89_UTM32N
SBP Isochore Grids	Encoded TIF	SN2023_002_R_ETRS89_UTM32N
Charting		
Trackplots and sampling locations	PDF	108_GEOPHYSICAL_REPORT - WPA&C



Deliverable	Format	Data Location
Bathymetry	PDF	108_GEOPHYSICAL_REPORT - WPA&C
Backscatter	PDF	108_GEOPHYSICAL_REPORT - WPA&C
Seabed Surface Classification	PDF	108_GEOPHYSICAL_REPORT - WPA&C
Seabed Objects	PDF	108_GEOPHYSICAL_REPORT - WPA&C
Seabed Features	PDF	108_GEOPHYSICAL_REPORT - WPA&C
Sub-seabed Geology	PDF	108_GEOPHYSICAL_REPORT - WPA&C

REFERENCES

- Huuse, M. and Lykke-Andersen, H., 2000: Buried valleys in the North Sea and in Southern Jutland. Geological News 5/00
- Jensen et al. 2011: Mapping of raw materials and habitats in the Danish sector of the North Sea. Geological survey of Denmark and Greenland bulletin 23, pp. 33-36.
- Jensen, J.B., Borre, S., Nørgaard-Pedersen, N. & Leth, J.O., 1999: Model for potential sand and gravel deposits for Danish waters. The sub-areas Kattegat South and the Baltic Sea West'. GEUS report 2010/99.
- Leth, J.O., 2003: The North Sea after the ice age – the exploration of the Jyske Rev. Geo-logy – News from GEUS, No. 3, 2003.
- Leth, J.O., Anthony, D., Larsen, B., Andersen, L.T. and Jensen, J.B., 2001: Geological mapping of the West Coast. Combined results of the regional geological mapping of the coastal zone between Lodbjerg and Blåvandshuk. GEUS report 2001/111.
- Lomholdt, S., Leth, J.O., and Skar, S., 2013: Marine resource mapping in the North Sea 2012. Geological survey of Denmark and Greenland report 2013/5.
- Nielsen et al. 2007: *Base Quaternary in the Danish parts of the North Sea and Skagerrak*. Geological survey of Denmark and Greenland bulletin.
- National drilling database (Jupiter database), GEUS. Borings DGU 550711.12, DGU 550711.18, DGU 560722.3 <https://data.geus.dk/Jupiter-WWW/index.jsp>
- Jensen, J. B., Bennike, O., 2020; General geology of the southern Kattegat, Desk Study. Report for Energinet Eltransmission A/S. GEUS.
- Jensen, J. B., Petersen, K. S., Konradi, P., Kuijpers, A., Bennike, O., Lemke, W. & Endler, R. 2002: Neotectonics, sea-level changes and biological evolution in the Fennoscandian Border Zone of the southern Kattegat Sea. *Boreas*, Vol. 31, pp. 133–150. Oslo.
- Bendixen, C., Jensen, J.B. Boldreel, L. O., Claousen, O. R., Seidenkrantz, M.-S., Nyberg, J., Hübscher, C. 2015 - The Holocene Great Belt connection to the southern Kattegat, Scandinavia: Ancyclus Lake drainage and Early Littorina Sea transgression. *Boreas* 10.1111/bor.12154.
- Lykke-Andersen, H, Seidenkrantz, M.-S. & Knudsen, K. L. 1993. Quaternary sequences and their relations to the pre-Quaternary in the vicinity of Anholt, Kattegat, Scandinavia. *Boreas*, bind 22, nr. 4, s. 291-298
- Jensen, P., Aagaard, I., Burke, R. A., Dando, P. R., Jørgensen, N. O., Kuijpers, A., Laier, T., O'Hara, S. C. M., Schmaljohann, R. 1992. 'Bubbling reefs' in the Kattegat: submarine landscapes of carbonate cemented rocks support a diverse ecosystem at methane seeps. *Marine Ecology Progress Series* Vol. 83 pp. 103-112
- Chester K. Wentworth. A Scale of Grade and Class Terms for Clastic Sediments: University of Iowa, 1922
- Robert L. Volk. The distinction between Grain Size and Mineral Composition in Sedimentary-Rock Nomenclature; *Journal of Geology*, Vol 62, Number 4, July 1954



APPENDIX A. KATTEGAT II – UHR SEISMIC PROCESSING REPORT



APPENDIX B. SURFICIAL GEOTECHNICAL GROUND-TRUTHING REPORT